

12

TECHNICAL REPORT RD-CR 82-25

AD A120115



AN INVESTIGATION FOR MODELING JET PLUME EFFECTS ON MISSILE AERODYNAMICS

by:
James H. Henderson
New Technology, Inc.
4811 Bradford Dr.
Huntsville, AL 35805

for:
Systems Simulation and Development Directorate
US Army Missile Laboratory
US Army Missile Command

JULY 1982



U.S. ARMY MISSILE COMMAND
Redstone Arsenal, Alabama 35809

Approved for public release; distribution unlimited.

DTIC FILE COPY

DTIC
ELECTE
S OCT 12 1982 D
B

82 10 12 115

BLANK PAGE

FOREWORD

The Army is currently engaged in a program to investigate air as a medium for modeling propulsive jet plume interference effects on missile aerodynamics. Past research of plume effects on stability characteristics has indicated the presence of a beneficial effect for free rockets. The large stable transonic pitching moment usually associated with free rockets is undesirable because of its effect on free rocket sensitivity to low level winds during the boost phase of flight (Refs. 1 through 3). Plume interference can be utilized to reduce stability (or destabilize the rocket) at transonic, low supersonic speeds while maintaining stability at the desired supersonic speeds. Other techniques for tailoring the variation of static margin with Mach number are discussed in Refs. 1 and 4. Several rocket systems being developed by the Army would benefit by this scheme of tailoring the stability characteristics. However, at the present time the estimate of plume effects on longitudinal stability cannot be made with the required precision.

Korst (Refs. 5 and 6) has proposed a modeling concept based on matching the plume shape of the rocket (prototype) and the model. He imposes the additional condition that jet plume surface Mach number be adjusted for the model to account for the different specific heat ratio of the prototype. A more detailed description of this modeling concept is presented in Ref. 7.

The purpose of this investigation is to experimentally contribute to verifying the plume modeling concepts proposed by Korst and thereby improve prediction of simulated plume effects. The investigation consisted of two parts: (1) investigate the plume effects of four separate nozzles with matching plume shapes (when tested at the proper jet total pressure ratio) but with different plume surface Mach numbers, and (2) test nozzles modeled to match data obtained from sled tests of a rocket configuration using a ZAP motor. In addition, a solid plume matching the four air plumes was tested. A normal jet simulator similar to ones used in longitudinal stability tests was also tested. Wind tunnel tests were conducted using air

to supply the jets. The tests were conducted at the Calspan 8-ft transonic wind tunnel at Mach numbers of 0.4 to 1.25 and at the NASA Langley Research Center unitary wind tunnel at Mach numbers of 1.6 to 2.5. All tests were made at an angle of attack of zero with the exception of two configurations where data were obtained at an angle of attack of -5 degrees. Some preliminary results of the transonic tests are discussed in Ref. 8.

TABLE OF CONTENTS

	<u>Page</u>
FOREWORD	ii
LIST OF ILLUSTRATIONS	vii
LIST OF TABLES	ix
LIST OF SYMBOLS	xi
1.0 BACKGROUND	1
2.0 ANALYTICAL BACKGROUND	3
3.0 TEST CONCEPT	5
4.0 APPARATUS AND TESTS	9
4.1 Wind Tunnels	9
4.2 Model	9
4.3 Tests	12
5.0 MODEL NOMENCLATURE	21
6.0 RESULTS AND DISCUSSION	23
7.0 CONCLUDING REMARKS	59
8.0 REFERENCES	61
APPENDIX A: DATA BASE	65



Accession For	
NTIS GRA&I	<input checked="" type="checkbox"/>
DTIC TAB	<input type="checkbox"/>
Unannounced	<input type="checkbox"/>
Justification	
By _____	
Distribution/	
Availability Codes	
Dist	Avail and/or Special
A	

BLANK PAGE

LIST OF ILLUSTRATIONS

<u>Figure</u>		<u>Page</u>
1	Effect of Being Off Design Point on Initial Plume Geometry	6
2	Installation Drawing of Model in the Calspan 8-ft Transonic Wind Tunnel	10
3	Photograph of the Model in the NASA Langley Research Center Unitary Plan Wind Tunnel	11
4	Configuration Description	13
5	Comparison of Pressure Distributions of the Four Nozzles at the Design Pressure Ratio and a Solid Plume	24
6	Comparison of Measured Nozzle Pressures with Computed Distribution	34
7	Variation of Initial Plume Angle with Jet Total Pressure Ratio for ZAP Nozzle and ZAP Model Nozzle	38
8	Comparison of Jet-On and Jet-Off Base and Afterbody Pressures Between the 6.12-in Sled Configuration and Wind Tunnel Configuration (1.76-3.95-.8)	39
9	Comparison of Wind Tunnel Model (1.76-3.95-.93) Pressures Related to Sled P_c/P_b at $M=1.65$ to 7-in Diameter Sled Base Pressures at $M=1.63$	41
10	Variation of Base Pressure with Thrust Coefficient for the Four Nozzles with Same "Design: Plume Shape	42
11	Effect of D_N/D_B on Variation of Base Pressure with Thrust Coefficient	49
12	Variation of Base Pressure with Radial Thrust Coefficient for the Normal Jet Plume Effects	54
13	Ratio of Radial Thrust to Axial Thrust Required for the Same Plume Effect	57

BLANK PAGE

LIST OF TABLES

<u>Table</u>		<u>Page</u>
1	Plume Geometry and Nozzle Characteristics	5
2	Orifice Locations (X/D Forward of Base)	18
3	Model Nomenclature	21

BLANK PAGE

LIST OF SYMBOLS

A_B	Base area
A_j	Nozzle exit area
C_{RT}	Radial thrust coefficient
C_T	Thrust coefficient
D_N/D_B	Nozzle exit to base diameter ratio
M, M_∞	Freestream Mach number
M_F	Plume surface Mach number
M_{FM}	Model plume surface Mach number
M_{FP}	Prototype plume surface Mach number
M_j	Nozzle exit Mach number
P_∞	Freestream static pressure
P_j	Nozzle exit static pressure
P_b/P_∞	Base pressure ratio
$P_C/P_b, PC/PB$	Jet total pressure ratio
P_C/p	Jet total to local nozzle static pressure ratio
PL/P	Local to freestream static pressure ratio
q_∞	Freestream dynamic pressure
R/R_B	Local to base radius ratio
R_R	Radius of plume curvature in nozzle exit radii
γ_m	Specific heat ratio, model plume
γ_p	Specific heat ratio, prototype plume
γ_j	Specific heat ratio, jet exit
γ_∞	Specific heat ratio, freestream
θ_i	Initial plume angle
θ_n	Nozzle exit angle

BLANK PAGE

1.0 BACKGROUND

The Army has been interested in jet plume effects on missile aerodynamics for the past 15 years. The primary interest has been the adverse effects on longitudinal stability and control effectiveness. These effects can significantly influence the flight behavior of free rockets and missiles having simplified guidance and control systems.

A research program (Ref. 9) was started for the purpose of obtaining an understanding which would enable the avoidance or alleviation of adverse effects. The general objectives of the program were: (1) prediction of flight conditions where plume effects would occur, (2) development of wind tunnel test techniques which would adequately simulate plume effects on longitudinal stability, and (3) development of design techniques for avoiding problem areas and where not possible, find means of alleviating undesirable aerodynamic effects.

During this program a strut-mounted model with an axial jet and a sting-mounted force model with a normal jet plume simulator were used. Effects of nozzle geometry, afterbody geometry, body length, fin shape and size, and the longitudinal distance of the fins from the base of the model were investigated. The sting-supported model was tested at Mach numbers of 0.2 to 2.3 (Refs. 10 through 14) and the strut-supported model was tested at Mach numbers of 0.4 to 2.87 (Refs 15 through 18). Results of these tests showed base pressure to be a good indicator of the degree of plume effects present. Comparisons of base and body pressure distributions with the axial jet and the normal jet simulator were made to determine the level of plume effects that each was simulating. It was apparent from stability tests on various configurations that normal force and pitching moment coefficients varied smoothly with increased normal jet simulator chamber pressure (increased simulated plume effects) and that these characteristics were repeatable. It became apparent that design control of the variation of pitching moment with Mach number could be used to advantage in reducing the highly stable transonic pitching moments in a manner which would reduce the wind sensitivity of free rockets.

The severity of plume effects vary with missile acceleration. Plume effects are first noticed at subsonic-transonic speeds for moderate accelerations and extend to higher Mach numbers as acceleration is increased. For a constant acceleration the region of plume influence on the missile recedes with increasing Mach number with only a small region at the base influenced at the highest Mach number. By placing fins forward of the base (on the order of 0.5 to 2.0 missile diameters) it is possible for the fins to become fully effective at the desired supersonic Mach number while the body surface near the base is still under the influence of the plume. By proper sizing and location of the fins it is possible to have some design control over the pitching moment characteristics.

In addition to wind tunnel tests, a series of sled tests were made with a ZAP rocket firing during the sled run in an attempt to verify plume effects during flight (Refs. 19 and 20). It was planned to make both force and pressure measurements during the tests. The force tests were unsuccessful but sufficient pressure data were obtained to verify the presence of jet plume effects. Most of the pressure data were influenced by sled interference but some interference free data were obtained for Mach numbers of about 1.4 to 1.6.

At the present time, tailoring the pitching moment for free rockets cannot be done as precisely as required for the optimum reduction in wind errors during boost. For improved tailoring it is necessary to know how well the actual rocket plume is being simulated in the wind tunnel. A comparison can be made between the normal jet simulator and various cold air nozzle axial jets. The remaining problem is knowing the difference between the effects of cold air axial jet (or other unheated fluid) and the actual rocket plume.

2.0 ANALYTICAL BACKGROUND

The analysis of axially symmetric supersonic flow near the center of expansion as developed by Johannesen and Meyer (Ref. 21) has been used by Korst (Refs. 5 and 6) to form the basis for plume modeling involving gases with dissimilar specific heat ratios. This analysis allows the rapid calculation of plume shapes which are approximated by a circular arc defined by the initial slope of the jet boundary (θ_i) and the radius of curvature (R_R). The first requirement of Korst's modeling technique is the geometric matching of the plume to be modeled (prototype) with the model plume. The assumption of locally conical source flow near the exit of the nozzle leads to a direct correspondence of nozzle shapes producing the same plume geometry. Thus, modeling requirements are reduced to determining the nozzle exit Mach number (M_j) and nozzle exit angle (θ_n).

Korst sets another condition in addition to the geometric matching of the plumes: the proper modeling of the closure condition for the wake is necessary. Korst suggests for consideration a choice of four specifying conditions for the wake closure of the modeling law in Ref. 5. These conditions are matching the wake recompression of the Chapman-Korst flow model, matching momentum at the corresponding plume boundaries, matching mass flux at the corresponding plume boundaries, and matching the supersonic inviscid streamline deflection-pressure rise relation on the basis of local linearization. In Ref. 7, Korst and Deep recommend the final specifying condition which requires that

$$\frac{\gamma_M M_{F_M}^2}{(M_{F_M}^2 - 1)^{1/2}} = \frac{\gamma_P M_{F_P}^2}{(M_{F_P}^2 - 1)^{1/2}} \quad (1)$$

where γ is specific heat ratio, M_F is the plume surface Mach number, and the subscripts M and P represent the model and prototype, respectively.

Although the circular arc approximation starts to diverge from the actual plume shape after about one nozzle radius, the analysis of Ref. 21 provides the second-order initial conditions necessary for the calculation of the plume boundary by the method of characteristics (Ref. 22). Thus, it is possible to obtain accurate plume matching well beyond the validity of the circular arc approximation. (See the plume comparisons of Ref. 5.)

3.0 TEST CONCEPT

The purpose of the tests was to verify the plume modeling concepts proposed by Korst. By using the simplified method for rapid determination of plume shape, it was possible to determine families of nozzles which produce identical plume shapes when operating at the proper jet total pressure (P_c/P_b). Since the plume surface Mach number (M_F) would differ for each nozzle, the validity of wake closure conditions could be investigated with the use of only one jet gas. With the specific heat ratio constant, the direct effect of plume surface Mach number on afterbody flow could be investigated. An investigation to verify the plume modeling concept using dissimilar propellant gases is now in progress in Sweden (Ref. 23).

The exit geometry of four nozzles were determined which would give matching plume shapes at the desired (design) pressure ratio. An initial plume angle of 42 deg was selected to insure a plume having characteristics which would cause flow interference. The matching plume geometry and the characteristics of the four nozzles are given in Table 1.

Table 1 Plume Geometry and Nozzle Characteristics

M_J	θ_n	DESIGN P_c/P_b	M_F	R_R
1.7	9.1	39.6	3.05	3.734
2.0	13.6	55.14	3.274	3.739
2.4	19.35	82.44	3.555	3.739
2.7	23.3	108.2	3.750	3.734

The plumes of the four nozzles match only at the proper value of chamber to base pressure ratio. With a change of chamber pressure from the "design point," the radius of curvature changes slightly for matching values of initial plume angle (Fig. 1). Comparisons of plumes with matching initial angles several degrees off of the design value should be valid.

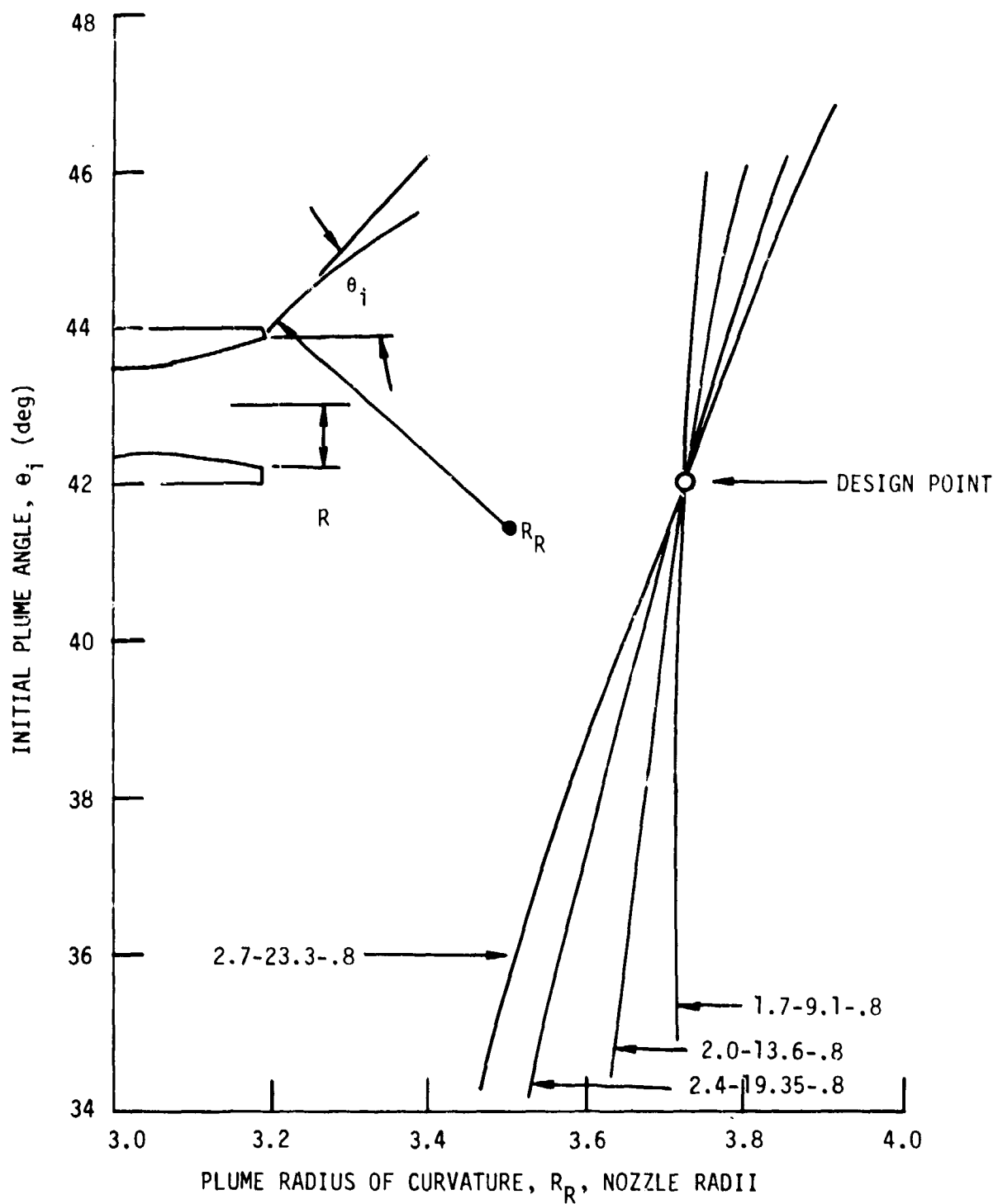


Fig. 1 Effect of Being Off Design Point on Initial Plume Geometry

In addition to the four nozzles a solid plume was investigated. The plume shape was determined by the method of characteristics and matched the plume shape produced by the four nozzles at the "design point." By comparing the effects of the solid plume on afterbody pressures with the effects of the four nozzles, a measure of plume flexibility may be determined. The solid plume represents a plume with infinite stiffness (Ref. 8).

The second part of the investigation of plume modeling techniques consisted of an attempt to model the plume effects of the ZAP rocket motor. The Army Missile Command has recently been involved in sled tests where ZAP motors were fired. The sled was accelerated to low supersonic Mach numbers with the rocket being ignited at various sled velocities. The sled test configuration had an ogive nose and was strut mounted on the sled with a boundary layer plate between the sled and the model. The first series of tests used the same rocket diameter as the ZAP vehicle (6.13 in). The second series of tests had diameters of 7 in. Both afterbody and base pressure measurements were made. An unsuccessful attempt was made to also measure aerodynamic forces on the 7-in model. A complete description of the sled test is given in Refs. 19 and 20.

In order to model the ZAP plume effects it was necessary to determine nozzle exit conditions. The Solid Propellant Equilibrium Chemistry Program utilized for this purpose gave an exit Mach number of 2.53 and a ratio of specific heats at a nozzle exit of 1.235. ZAP nozzle has an exit cone angle of 10.36 deg. The measurable thrust obtained during the sled tests varied between about 10,000 to 27,000 lb. For plume modeling purposes a thrust of about 19,000 lb was chosen. At this thrust the ZAP (prototype) has a plume Mach number (M_p) of 3.35, an initial plume angle of 32.31 deg, an initial plume radius of curvature of 5.427, and a chamber to base pressure ratio of 83.1. Using the streamline deflection closure condition [Eq. (1)], a plume Mach number for the ZAP model was determined to be 2.906. It was determined that the model (air) nozzle would have an exit Mach number of 1.76 and an exit angle of 3.95 deg, and would match the prototype plume when the chamber to base pressure ratio was 39.1. Model nozzles were fabricated to match both the 6.13-in and 7.0-in diameter sled vehicles having nozzle to base diameter ratios (D_N/D_B) of 0.8 and 0.93, respectively.

Since the nozzles of this investigation have short divergent sections, the supersonic flow can be significantly affected by throat geometry. A program was written by Korst (Ref. 24) where throat curvature could be determined which would give flow conditions approaching the nozzle lip that were close to ideal conical source flow. This program uses transonic flow field solutions near the throat, suggested by a combination of the Oswattitch-Rothstein (Ref. 25) and Sauer (Ref. 26) analysis followed by the method of characteristics.

A normal jet plume effects simulator has been utilized by the Army Missile Command to obtain stability characteristics on several missile and free rocket configurations (e.g., Refs. 10 through 14). The normal jet simulator is advantageous because of the comparatively low mass flow required to simulate jet effects and because of the absence of unintended interference with the model flow field. A normal jet simulator was tested so that its relationship with the modeled plumes could be investigated.

4.0 APPARATUS AND TESTS

4.1 WIND TUNNELS

Tests were conducted in the Calspan Corporation 8-ft transonic wind tunnel and the NASA Langley Research Center unitary plan facility.

The Calspan 8-ft transonic wind tunnel is a continuous flow, variable density facility. The maximum clear tunnel Mach number is 1.30. The tunnel may be operated at stagnation pressures from 0.10 to 3.25 atmospheres to provide a variation of Reynolds number independent of Mach number. A detailed description of the tunnel is presented in Ref. 27.

The supersonic tests were conducted in the low-speed circuit of the unitary plan wind tunnel. This facility is a continuous circuit wind tunnel with a 4 x 4 ft test section capable of operating at stagnation pressures up to 60 psia and at Mach numbers of 1.50 to 2.87. A detailed description of the facility is given in Ref. 28.

4.2 MODEL

The model was a 2.5-in diameter body of revolution having a four-caliber tangent ogive nose followed by a cylinder. The model was 32.5-in long with the aft 8.55 in of the cylinder consisting of interchangeable afterbodies. A strut support was used to mount the model to the wind tunnel support system. The strut was ducted internally to supply high pressure air to the model chamber. Pressure instrumentation was also routed through the strut.

A drawing of the model installed in the Calspan 8-ft transonic wind tunnel is shown in Fig. 2. A photograph of the model in the Langley Research Center unitary plan facility is shown in Fig. 3. In the Langley facility the model was arranged in the test section so that the support strut was 30 deg above the horizontal. The sting support system was offset to the right side of the model center line.

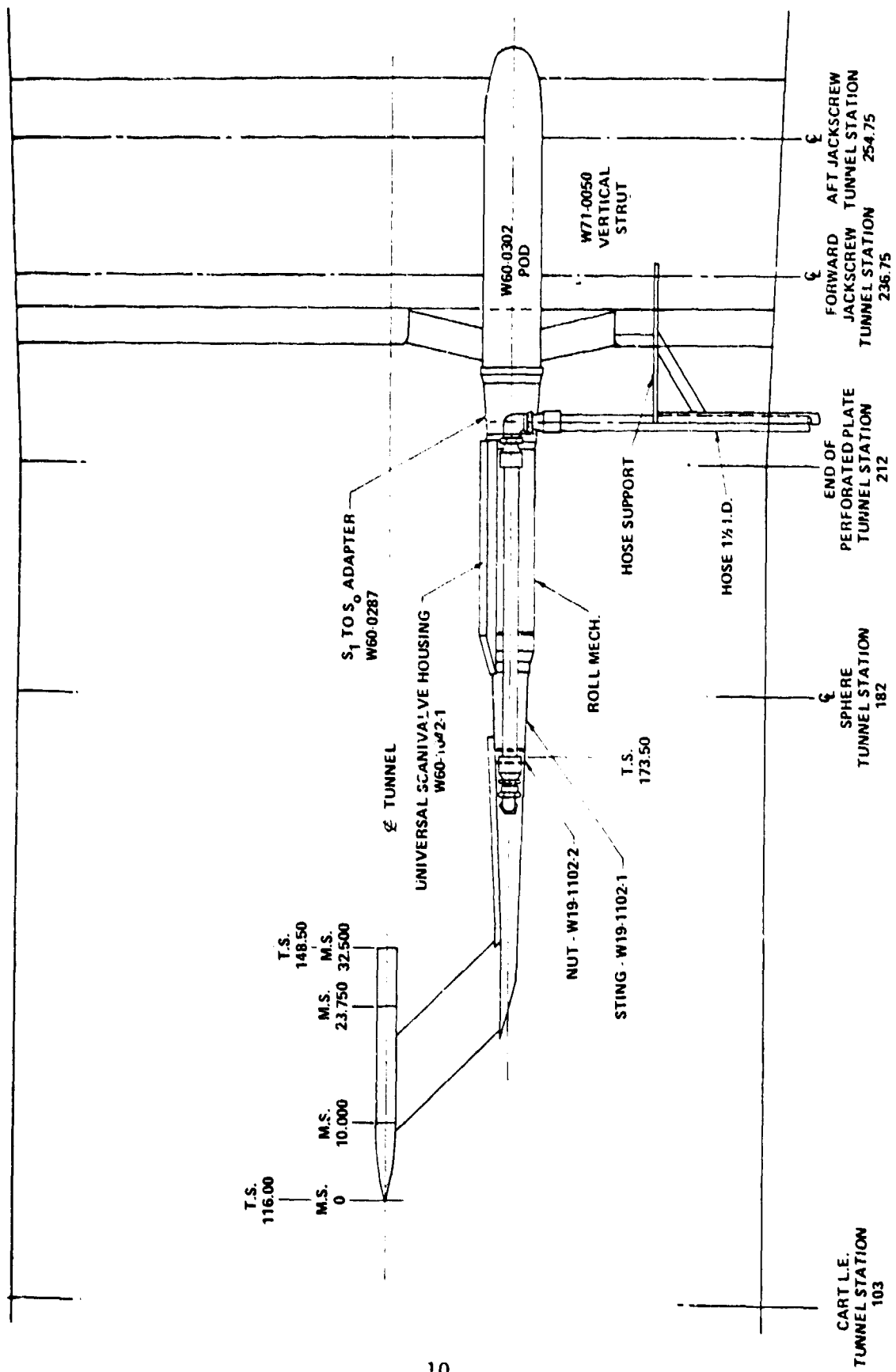


Fig. 2 Installation Drawing of Model in The Calspan 8-ft Transonic Wind Tunnel

NASA
1-9 62-9

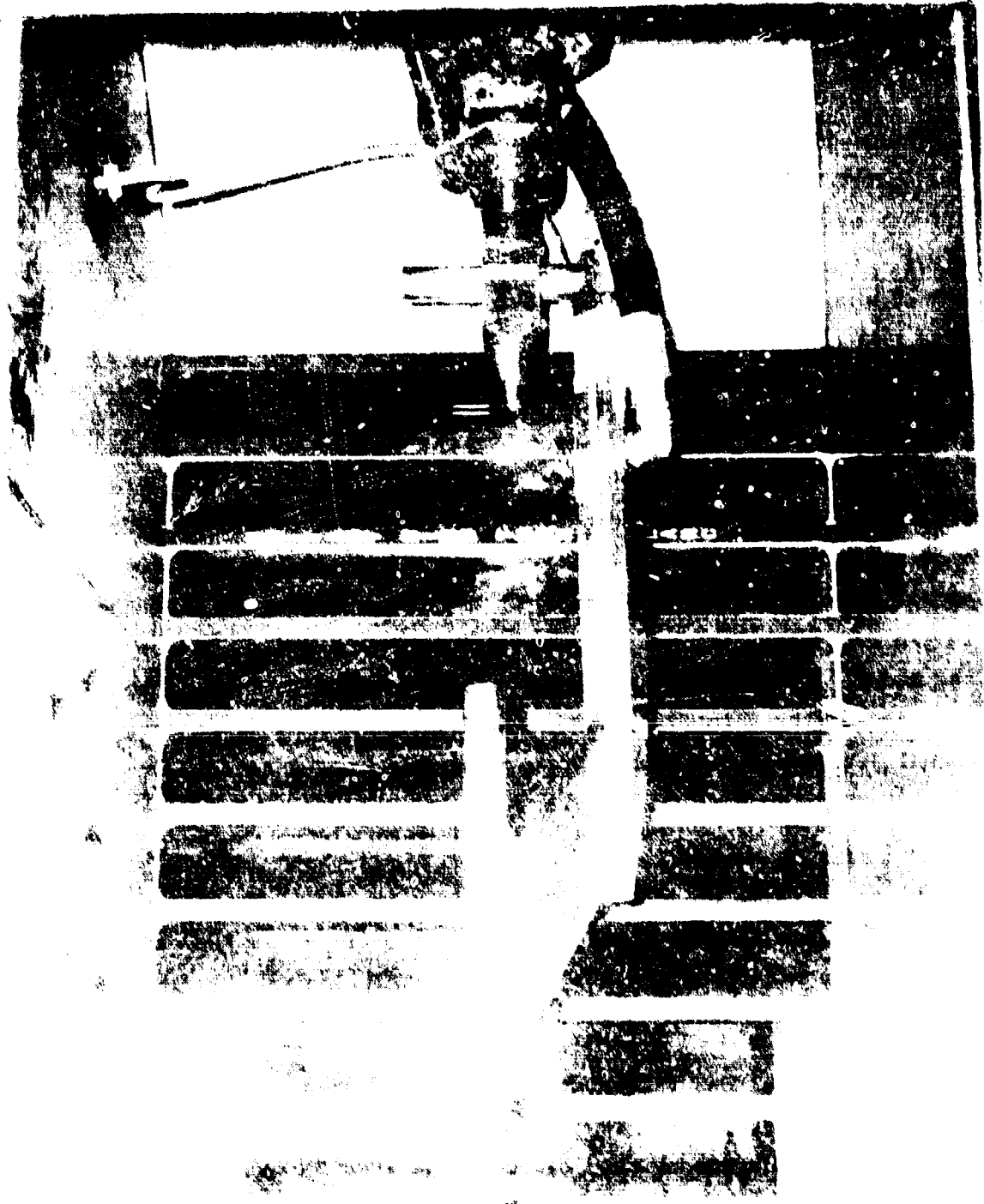


Fig. 3 Photograph of the Model in the NASA Langley Research Center Unitary Plan Wind Tunnel

Seven afterbodies were built by Calspan for the present tests. On each afterbody 10 external static pressure orifices were installed in a single row 180 deg from the strut. A manifold of three base pressure orifices was installed in the upper quadrant of each afterbody.

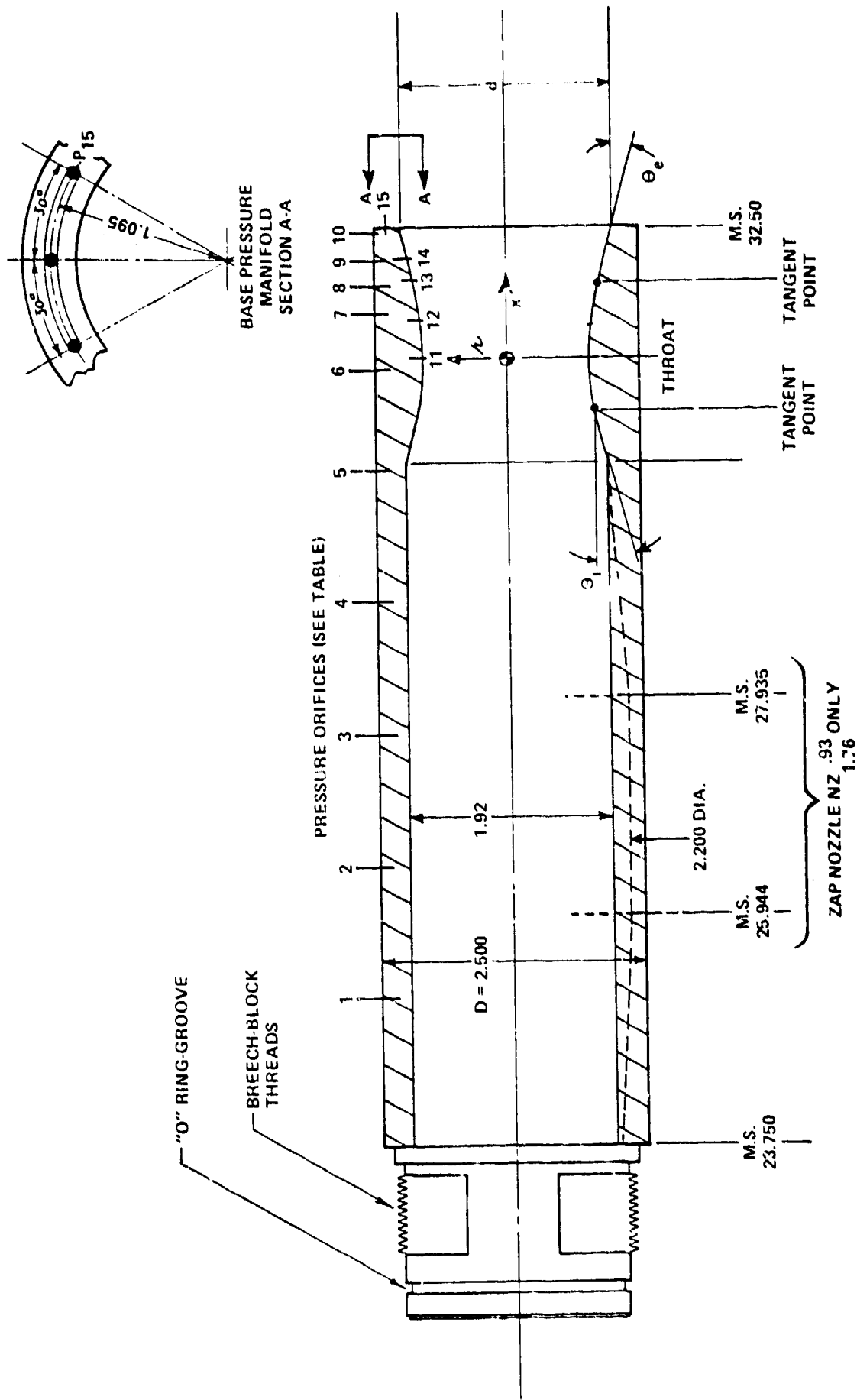
Four of the afterbodies incorporated nozzles designed to produce congruent plumes when operating at the proper jet pressure ratio (Fig. 1). Two additional afterbodies contained nozzles designed to model the plume effects of the ZAP rocket on both the 6.12- and 7.0-in diameter sled configurations. The afterbodies had nozzle exit to base diameter ratios (D_N/D_B) of 0.8 except the nozzle modeling the 7.0-in diameter sled configurations. This afterbody had a base diameter ratio of 0.93. Each nozzle had four static pressure orifices on the nozzle wall opposite the support strut.

The final afterbody was built to hold the solid plume and the normal jet simulator. This afterbody had the same distribution of external pressure orifices as the nozzle afterbodies. The solid plume was designed to match the size and shape of the plumes of the four nozzles previously mentioned. The normal jet simulator consists of 24 sonic nozzles arranged circumferentially in two rows with a common air chamber. Air is supplied to the chamber through the model. The combined exit area of the 24 nozzles represented 5% of the model base area. (The geometry of the normal jet simulator is proportional to the normal jet simulators used on sting supported model tests. In these tests the simulator was mounted on the sting and air was supplied from the rear.)

Details of the various afterbodies are presented in Fig. 4. Orifice locations in terms of model diameters from the base are presented in Table 2. Due to the lack of test time, the internal orifices on the two ZAP model nozzles were not connected.

4.3 TESTS

The model was tested at zero angle of attack except for a few runs at transonic speeds where the model was pitched to -5 deg angle of attack. During a run Mach number was held constant and jet chamber total pressure was varied up to about 600 psia. Where matching plumes were desired, the P_c/P_b value was set on or near the "design point" with additional data points close to the design point. No transition grit was applied to the model.



a. TYPICAL NOZZLE CONFIGURATION
 Fig. 4 Configuration Description

AFTERBODY EXTERNAL ORIFICES (ALL NOZZLES)

ORIFICE NO.:	1	2	3	4	5
MODEL STA.:	25.188	26.458	27.638	28.938	30.188
ORIFICE NO.:	6	7	8	9	10
MODEL STA.:	31.126	31.688	31.938	32.188	32.438
ORIFICE NO.:	15 ^o				
MODEL STA.:	32.500 (BASE MANIFOLD)				

NOZZLE INTERNAL ORIFICES

<u>M = 1.7 CONICAL NOZZLE</u> NC ^{.8} 1.7				
ORIFICE NO.:	11	12	13	14
NOZZLE STA.:	0	0.25	0.75	1.00
MODEL STA.:	31.3611	31.6111	32.1111	32.3611
<u>M = 2.0 CONICAL NOZZLE</u> NC ^{.8} 2.0				
ORIFICE NO.:	11	12	13	14
NOZZLE STA.:	0	0.375	0.750	1.125
MODEL STA.:	31.245	31.620	31.995	32.370
<u>M = 2.4 CONICAL NOZZLE</u> NC ^{.8} 2.4				
ORIFICE NO.:	11	12	13	14
NOZZLE STA.:	0	0.375	0.75	1.125
MODEL STA.:	31.1668	31.5418	31.9168	32.2918
<u>M = 2.7 CONICAL NOZZLE</u> NC ^{.8} 2.7				
ORIFICE NO.:	11	12	13	14
NOZZLE STA.:	0	0.500	1.000	1.250
MODEL STA.:	31.0509	31.5509	32.0509	32.3009
<u>SMALL ZAP NOZZLE</u> NZ ^{.8} 1.76				
ORIFICE NO.:	11	12	13	14
NOZZLE STA.:	0	0.500	1.375	2.375
MODEL STA.:	29.9978	30.4978	31.3728	32.3728
<u>LARGE ZAP NOZZLE</u> NZ ^{.93} 1.76				
ORIFICE NO.:	11	12	13	14
NOZZLE STA.:	0	0.75	1.75	2.75
MODEL STA.:	29.5014	30.3514	31.3514	32.3514

b. PRESSURE ORIFICE LOCATIONS

Fig. 4 Configuration Description (Continued)

NC .3 1.7		NC .8 2.0		NC .8 2.4		NC .8 2.7	
d = 2.0000 d/D = 0.80 $\theta_i = 7.5^\circ$ $\theta_e = 9.10^\circ$		d = 2.0000 d/D = 0.80 $\theta_i = 15^\circ$ $\theta_e = 13.60^\circ$		d = 2.000 d/D = 0.80 $\theta_i = 15^\circ$ $\theta_e = 19.35^\circ$		d = 2.000 d/D = 0.80 $\theta_i = 15^\circ$ $\theta_e = 23.30^\circ$	
x	r	x	r	x	r	x	r
.9560	.9600 ^①			1.3681	.9600 ^①		
.4889	.8985 ^②	-1.0061	.9600 ^①	.4914	.7251 ^②		
.4510	.8939	.4944	.8229 ^②	.4537	.7169		
.4137	.8898	.4535	.8159	.4177	.7093		
.3768	.8860	.4133	.8096	.3823	.7025		
.3401	.8826	.3736	.8039	.3476	.6963	-1.5954	.9600 ^①
.3035	.8795	.3341	.7987	.3129	.6907	.5210	.6721 ^②
.2666	.8767	.2943	.7941	.2785	.6857	.4361	.6537
.2299	.8743	.2547	.7901	.2435	.6812	.3596	.6396
.1922	.8722	.2138	.7865	.2089	.6773	.2867	.6284
.1282	.8695	.1425	.7817	.1724	.6738	.2158	.6199
.0641	.8679	.0713	.7788	.0867	.6681	.1414	.6134
0	.8674 ^③	0	.7778 ^③	0	.662 ^③	0	.6085 ^③
.0641	.8679	.0713	.7788	.0862	.6681	.1414	.6134
.1282	.8695	.1425	.7817	.1724	.6738	.2158	.6199
.1922	.8722	.2138	.7865	.2089	.6773	.2867	.6284
.2299	.8743	.2547	.7901	.2435	.6812	.3596	.6396
.2666	.8767	.2943	.7941	.2785	.6857	.4361	.6537
.3035	.8795	.3341	.7987	.3129	.6907	.5210	.6721
.3401	.8826	.3736	.8039	.3476	.6963	.6201	.6968
.3768	.8860	.4133	.8096	.3823	.7025	.7445	.7325
.4137	.8898	.4535	.8159	.4177	.7093	.9118	.7872
.4510	.8939	.4944	.8229	.4527	.7169	1.1533	.8771
.4889	.8985	.5615	.8355	.4914	.7251	1.4138	.9848 ^④
.5276	.9035	.6596	.8564	.5252	.7342	1.4491	1.0000 ^⑤
.5673	.9090	.7125	.8688 ^④	.5696	.7444		
.6084	.9152	1.2550	1.0000 ^⑤	.6121	.7558		
.6408	.9202 ^④			.6577	.7687		
1.1389	1.0000 ^⑤			.7071	.7835		
				.7608	.8004		
				.8194	.8199		
				.8620	.8346 ^④		
				1.3332	1.0000 ^⑤		

- ① NOZZLE ENTRANCE
- ② UPSTREAM TANGENT POINT
- ③ THROAT
- ④ DOWNSTREAM TANGENT POINT
- ⑤ NOZZLE EXIT

NOZZLE IS CONICAL BETWEEN ① AND ②, AND BETWEEN ④ AND ⑤, AT HALF ANGLES OF θ_i AND θ_e , RESPECTIVELY.

c. CONICAL NOZZLE COORDINATES

Fig. 4 Configuration Description (Continued)

NZ .8 1.76		NZ .93 1.76	
d = 2.0000 d/D = .80 $\theta_i = 5^\circ$ $\theta_e = 3.95^\circ$		d = 2.3168 d/D = .9267 $\theta_i = 5^\circ$ $\theta_e = 3.95$	
x	r	x	r
-1.6018	.9600 ^①		
-.4588	.8600 ^②		
-.4088	.8575	-1.2483	1.1000 ^①
-.3609	.8553	-.4181	.9308 ^②
-.3145	.8535	-.3643	.9887
-.2690	.8519	-.3116	.9868
-.2243	.8506	-.2598	.9854
-.1800	.8496	-.2085	.9842
0	.8478 ^③	0	.9819 ^③
.1800	.8496	.2085	.9842
.2243	.8506	.2598	.9854
.2690	.8519	.3116	.9868
.3145	.8535	.3643	.9887
.3609	.8553	.4181	.9908
.4088	.8575	.4736	.9933
.4588	.8600	.5315	.9962
.5115	.8629	.5925	.9996
.5678	.8665	.6577	1.0037
.5998	.8686 ^④	.6948	1.0062 ^④
2.5022	1.0000 ^⑤	2.8986	1.1584 ^⑤

- ① NOZZLE ENTRANCE
- ② UPSTREAM TANGENT POINT
- ③ THROAT
- ④ DOWNSTREAM TANGENT POINT
- ⑤ NOZZLE EXIT

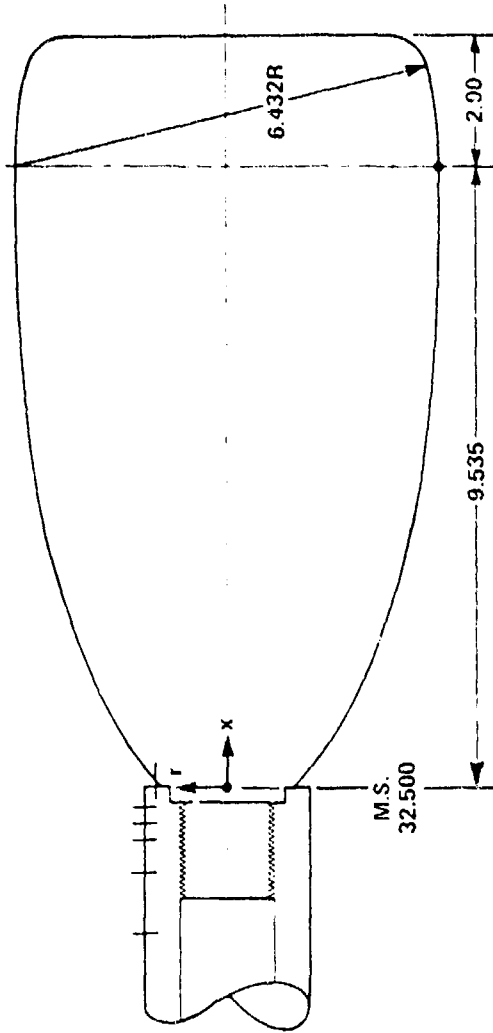
NOTE: INLET SECTION AHEAD OF NZ .93 NOZZLE IS EXPANDED TO 2.200 IN. DIA. - SEE SKETCH
1.76

d. ZAP NOZZLE COORDINATES

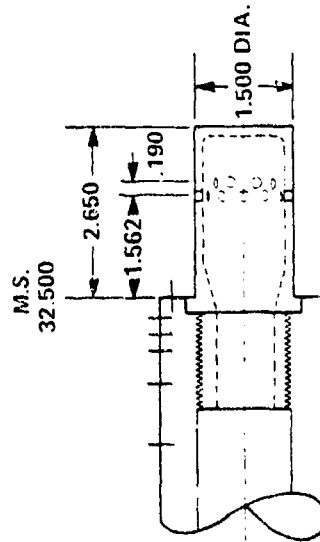
Fig. 4 Configuration Description (Continued)

SOLID PLUME SIMULATOR
COORDINATES

x	r
.000	1.000
.235	1.200
.364	1.300
.501	1.400
.806	1.600
1.160	1.800
1.565	2.000
1.790	2.100
2.302	2.300
2.588	2.400
2.902	2.500
3.249	2.600
3.640	2.700
4.081	2.800
4.585	2.900
5.189	3.000
5.591	3.100
7.038	3.190
9.535	3.216



S₂ SOLID PLUME SIMULATOR



S₁ NORMAL JET PLUME SIMULATOR

NOTE: SAME AFTERBODY USED TO ATTACH
BOTH PLUME SIMULATORS.
EXTERNAL PRESSURE ORIFICE PATTERN
SAME AS ON NOZZLE AFTERBODIES.

e. PLUME SIMULATORS

Fig. 4 Configuration Description (Continued)

Table 2 Orifice Locations (X/D Forward of Base)

BASE AND AFTERBODY ORIFICE LOCATIONS

ORIFICE NO.	X/D (CALIBERS FORWARD OF BASE)
15	0.000 (BASE)
10	0.025
9	0.125
8	0.225
7	0.325
6	0.551
5	0.925
4	1.425
3	1.945
2	2.417
1	2.925

NOZZLE ORIFICE LOCATIONS

	1.76-3.95-.8		1.76-3.95-.8		1.7-9.1-.8	
TAP	X/D	R/R _B	X/D	R/R _B	X/D	R/R _B
14	0.051	0.7955	0.059	0.9279	0.056	0.7827
13	0.451	0.7417	0.459	0.8822	0.156	0.7501
12	0.801	0.6898	0.859	0.8081	0.356	0.7005
11	1.001	0.6782	1.159	0.7855	0.456	0.6939
TAP	2.0-13.6-.8		2.4-19.35-.8		2.7-23.3-.8	
14	0.052	0.7780	0.083	0.7436	0.080	0.7328
13	0.202	0.7024	0.233	0.6375	0.180	0.6550
12	0.352	0.6433	0.383	0.5610	0.380	0.5338
11	0.502	0.6222	0.533	0.5330	0.580	0.4868

The transonic test was run at constant mass operating conditions of 1/3 atmosphere wind-off pressure. Mach number varied between 0.4 and 1.25 and Reynolds number varied between about 0.8 to 2.0 million/ft. Several data points were obtained with zero tunnel velocity. A complete description of the transonic tests is given in Ref. 29. Mr. C.F. Reid was the Project Manager for tests in the Calspan Corporation Transonic Wind Tunnel.

The supersonic tests were performed over a Mach number range from 1.6 to 2.5. Only one run was made at a Mach number of 1.6 due to the plume choking the tunnel flow. A Mach number of 1.65 was subsequently tested as the minimum Mach number. The tunnel stagnation pressure varied from about 1080 lb/ft² to about 1600 lb/ft². The Reynolds number was held constant at 2.0 million/ft. The dewpoint was maintained sufficiently low to insure negligible condensation effects. Mr. Peter F. Covell was the Project Manager for the tests in the Langley Research Center unitary plan facility.

BLANK PAGE

5.0 MODEL NOMENCLATURE

Where data from nozzle configurations are compared the more descriptive nomenclature used in previous Army Missile Command reports will be used. This nomenclature is designated by $M_J-\theta_N-D_N/D_B$ where M_J represents jet exit Mach number, θ_N represents nozzle exit angle and D_N/D_B represents the nozzle exit to model base diameter ratio. For example, the large ZAP nozzle is designated as 1.76-3.95-.93. Results of the present tests have been stored in the Army Missile Command Aerodynamic Analyzer System data base. This system was used to make plots of the basic data. A 5- or 6-character designation was used to identify configurations and are used on the plots of the basic data in Appendix A. A different model designation was used by Calspan. Figures 2 through 4 were reprinted from Ref. 29 and the Calspan designation is used. A comparison of the three designations are given in Table 3.

Table 3 Model Nomenclature

PRESENT REPORT $M_J-\theta_N-D_N/D_B$	MICOM AAS DATA BASE	CALSPAN (REF. 28)
1.7-9.1-.8	B1AZ43	NC .8 1.7
2.0-13.6-.8	B1AZ44	NC .8 2.0
2.4-19.35-.8	B1AZ45	NC .8 2.4
2.7-23.3-.8	B1AZ46	NC .8 2.7
1.76-3.95-.8	B1AZ41	NZ .8 1.76
1.76-3.95-.93	B1AZ42	NZ .93 1.76
NORMAL JET	B1AJ2	S1
SOLID PLUME	B1AS3	S2

BLANK PAGE

6.0 RESULTS AND DISCUSSION

The basic results of this investigation are presented in Appendix A. Typical distributions of base and afterbody pressures are shown for various jet total pressure ratios (P_c/P_b) for each test configuration at both transonic and supersonic speeds.

As previously mentioned, four nozzles were built which were designed to give the same plume shape when operating at the proper jet total pressure ratio. The design jet total pressure ratio and the resulting plume Mach number for these nozzles are as follows:

NOZZLE	P_c/P_b	M_F
1.7-9.1-.8	39.6	3.05
2.0-13.6-.8	55.14	3.274
2.4-19.35-.8	82.44	3.555
2.7-23.3-.8	108.2	3.75

Pressure distributions of the four nozzles at the "design" pressure ratio are compared to the solid plume (with the same shape) in Fig. 5. Generally at Mach numbers of one or less, there is little effect of plume surface Mach number on afterbody pressures. However, there is a tendency for the plumes with higher surface Mach numbers to cause higher pressures, and plumes with lower surface Mach numbers to cause lower pressures. The solid plume generally results in the highest pressures. With increasing Mach number the effect of plume Mach number increases and solid plume distribution diverges more from the air nozzle data. At the supersonic Mach numbers there is a significant difference between the various nozzles and the solid plume. In general, plume surface Mach number can be related to plume flexibility (or stiffness) with the solid plume representing zero flexibility (Ref. 8).

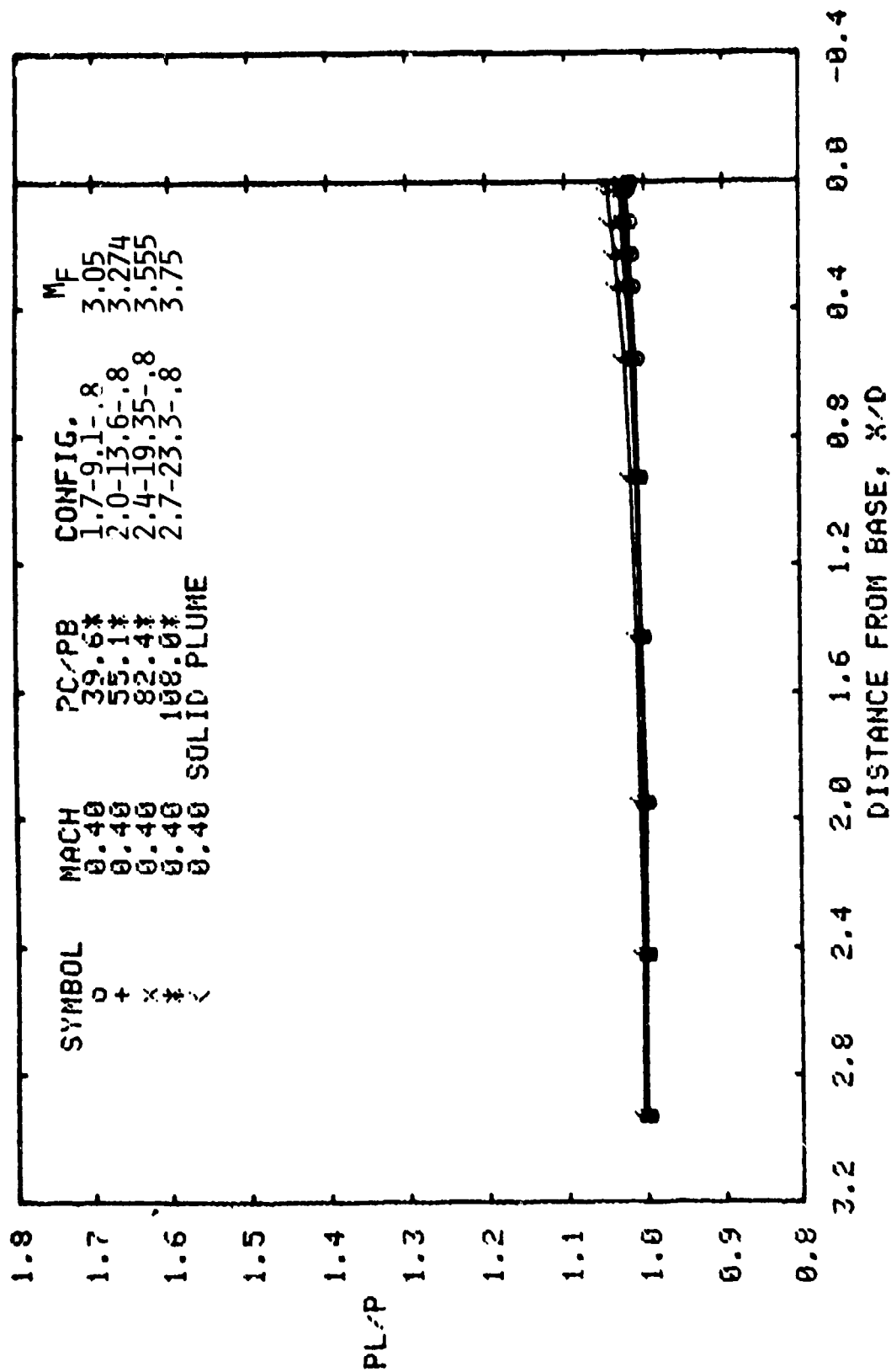


Fig. 5 Comparison of Pressure Distributions of the Four Nozzles at the Design Pressure Ratio and a Solid Plume

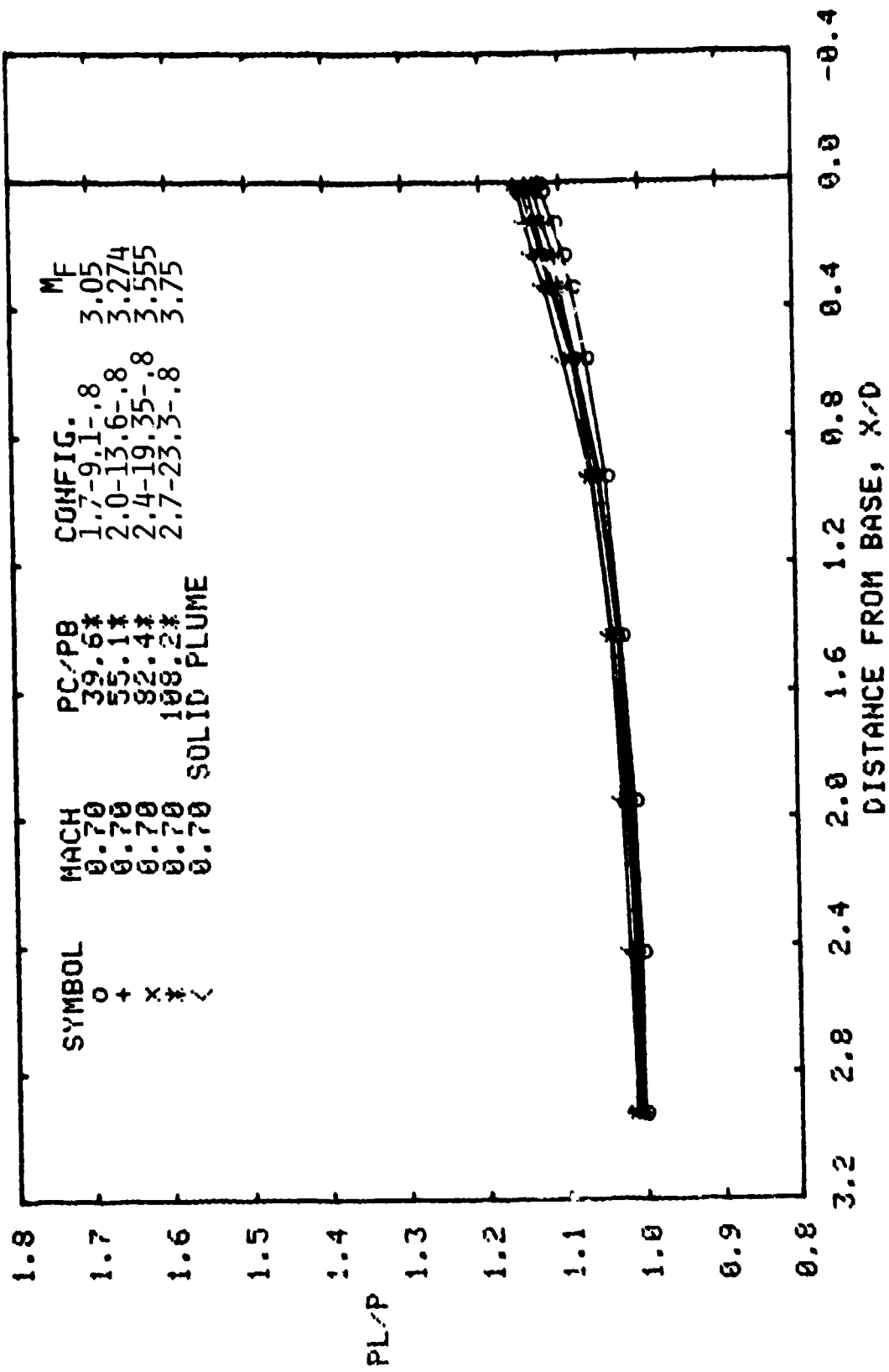


Fig. 5 Comparison of Pressure Distributions of the Four Nozzles at the Design Pressure Ratio and a Solid Plume (Continued)

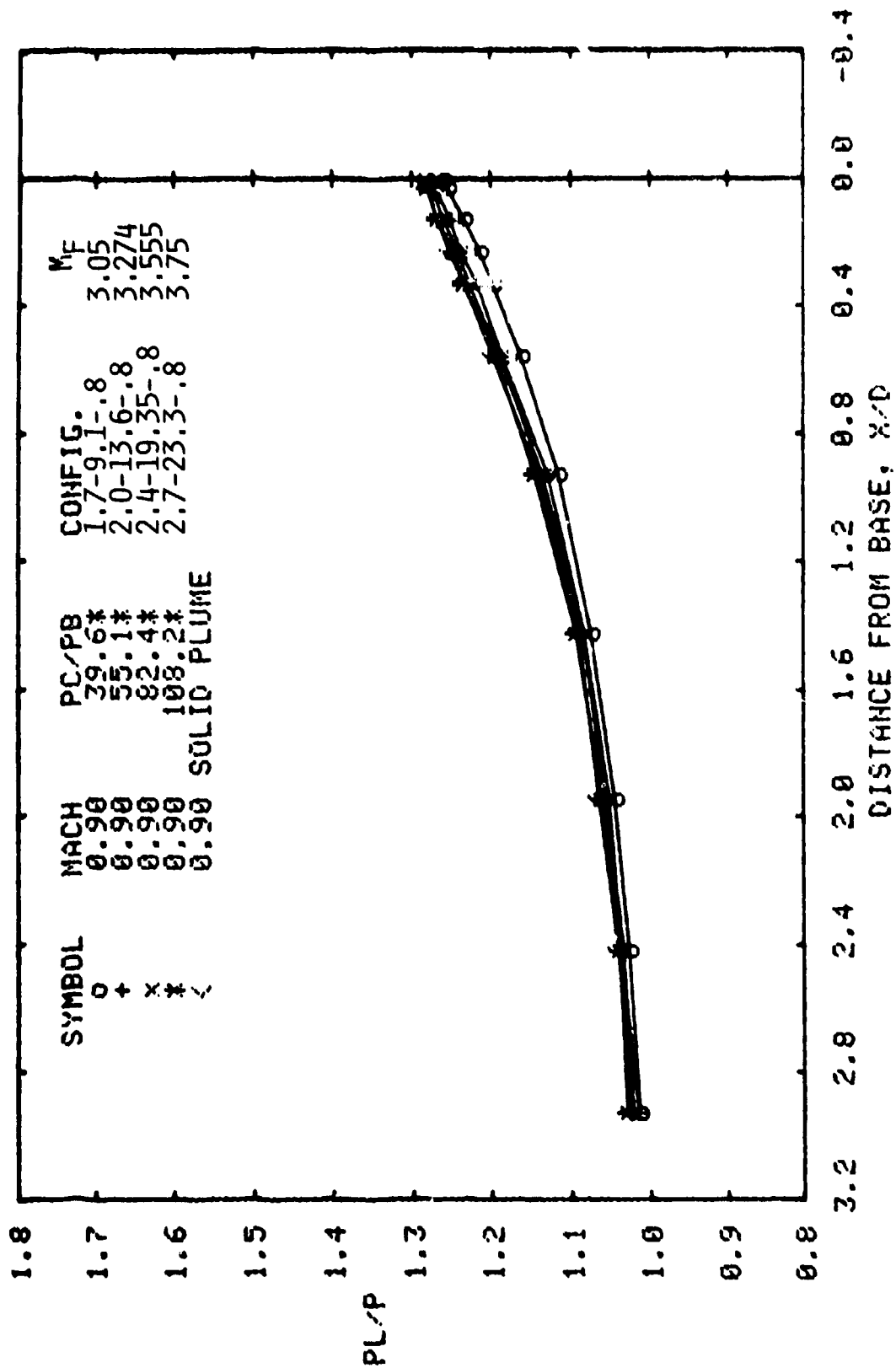


Fig. 5 Comparison of Pressure Distributions of the Four Nozzles at the Design Pressure Ratio and a Solid Plume (Continued)

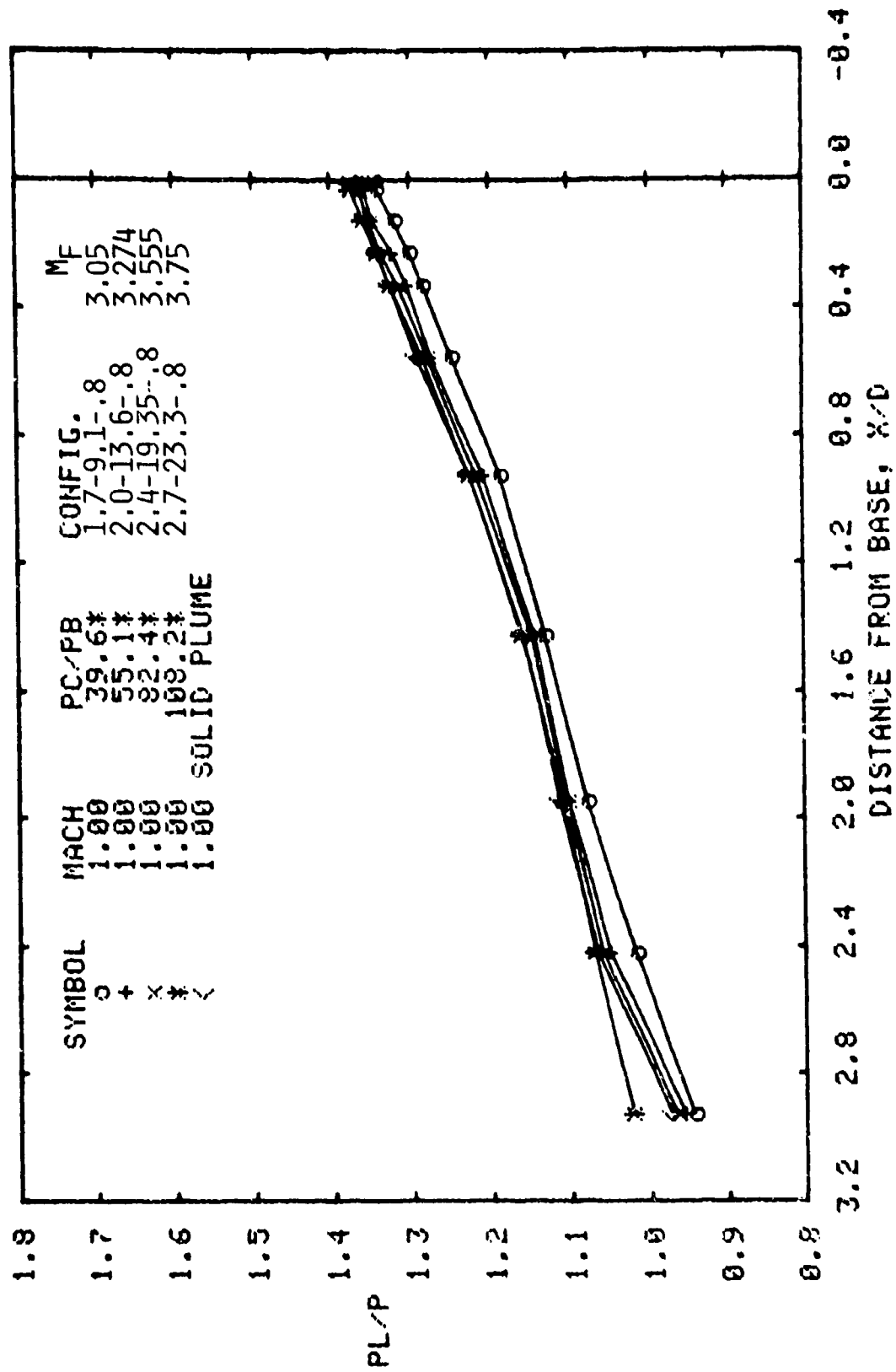


Fig. 5 Comparison of Pressure Distributions of the Four Nozzles at the Design Pressure Ratio and a Solid Plume (Continued)

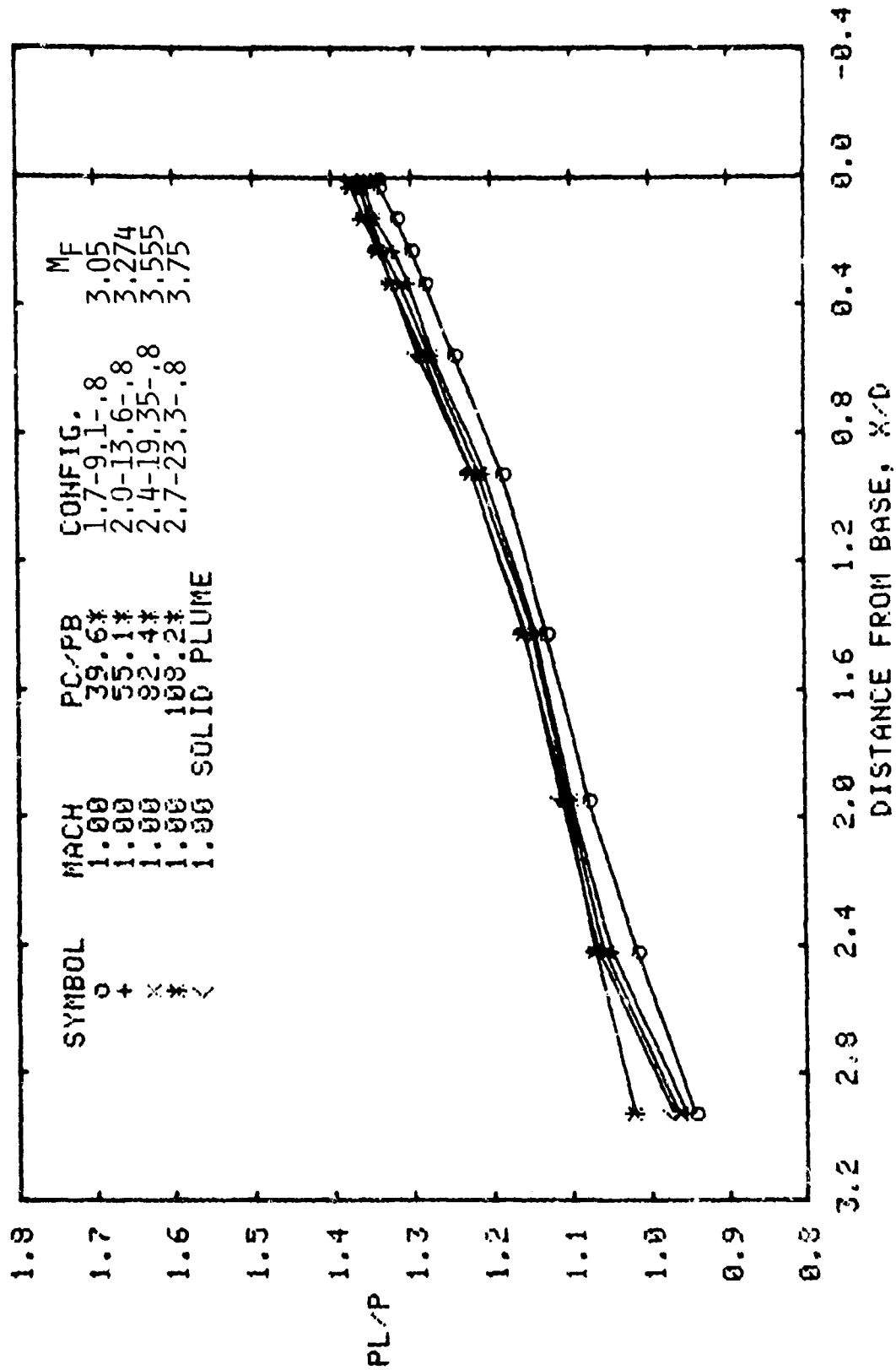


Fig. 5 Comparison of Pressure Distributions of the Four Nozzles at the Design Pressure Ratio and a Solid Plume (Continued)

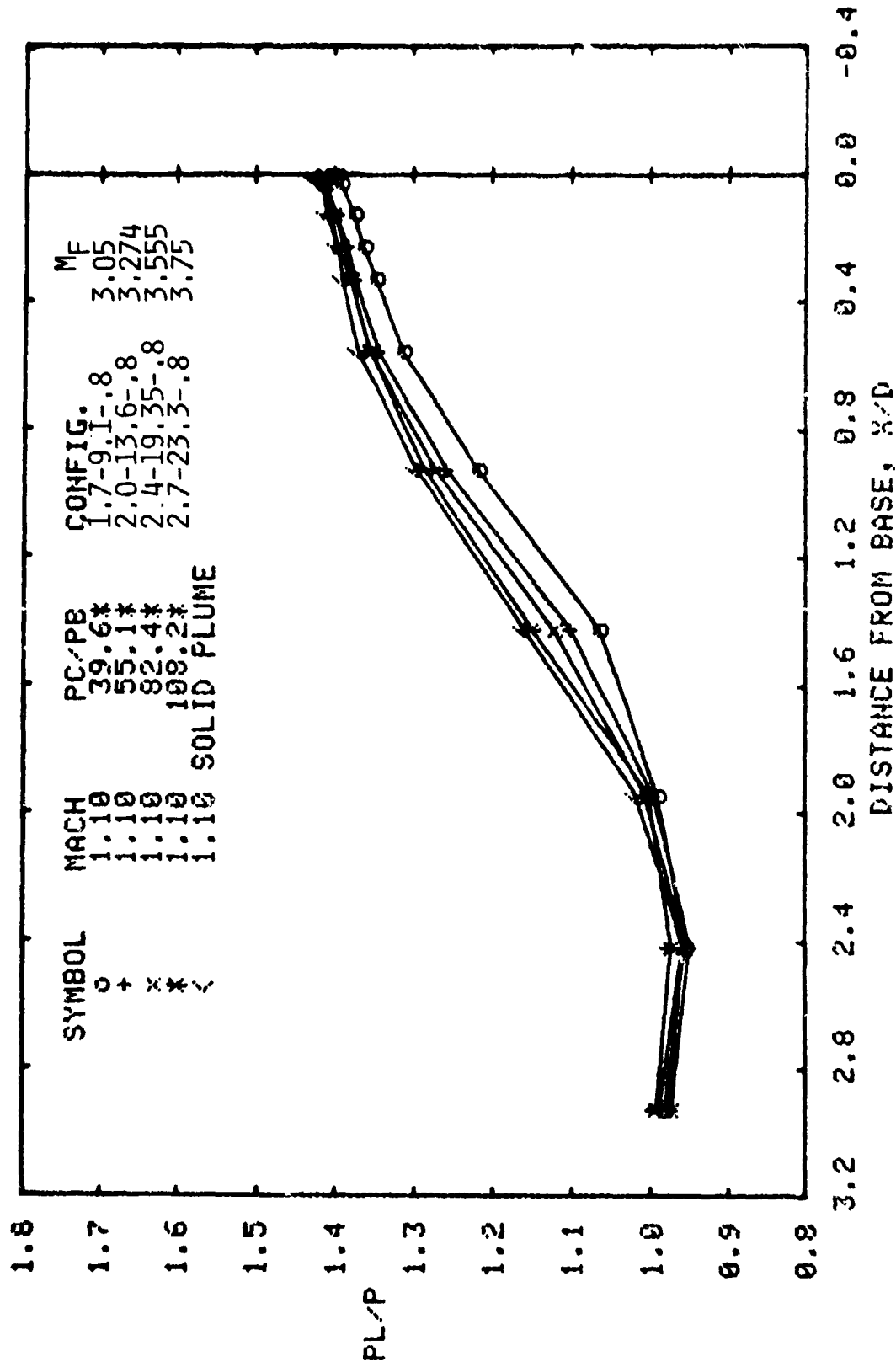


Fig. 5 Comparison of Pressure Distributions of the Four Nozzles at the Design Pressure Ratio and a Solid Plume (Continued)

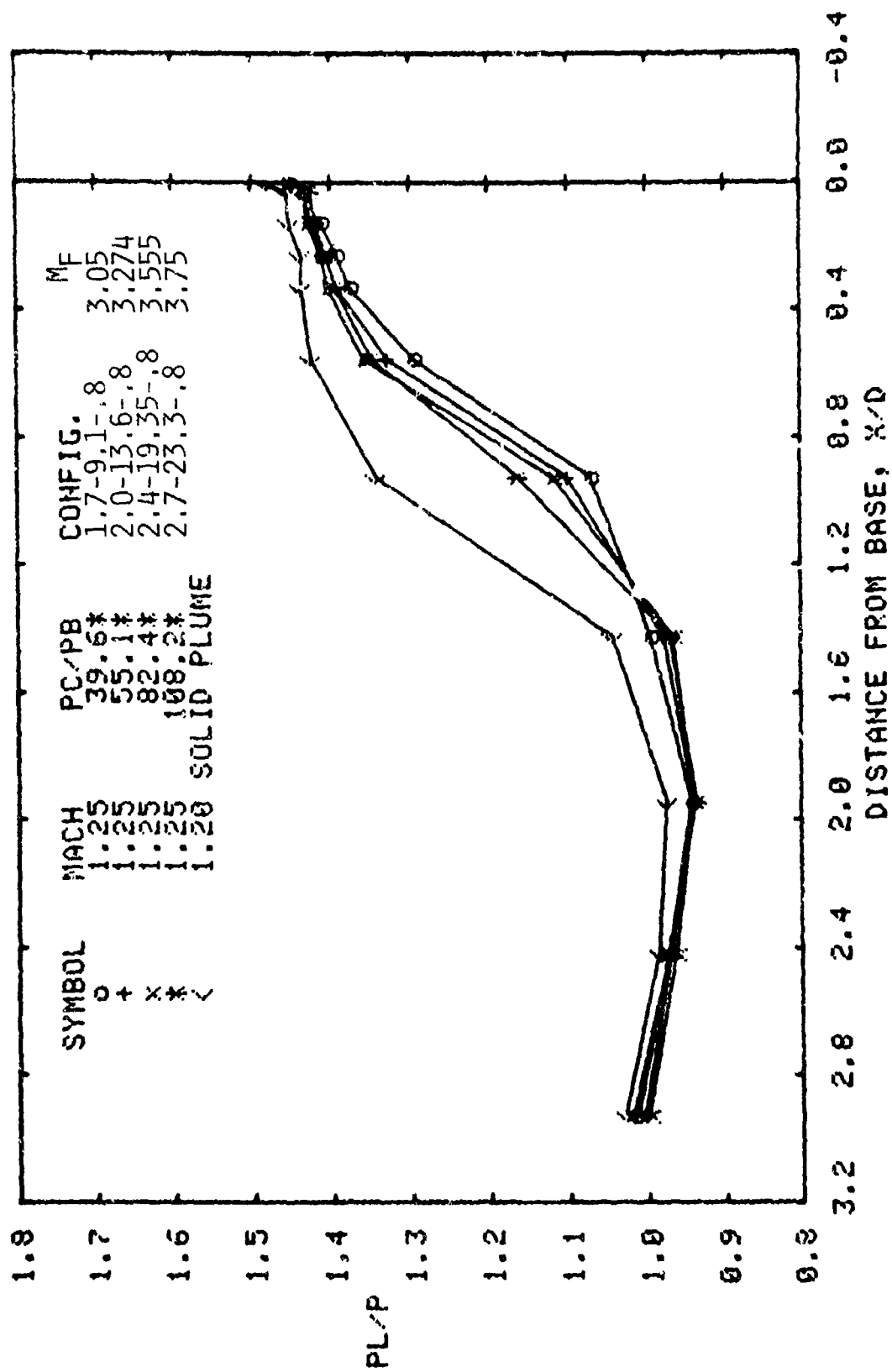


Fig. 5 Comparison of Pressure Distributions of the Four Nozzles at the Design Pressure Ratio and a Solid Plume (Continued)

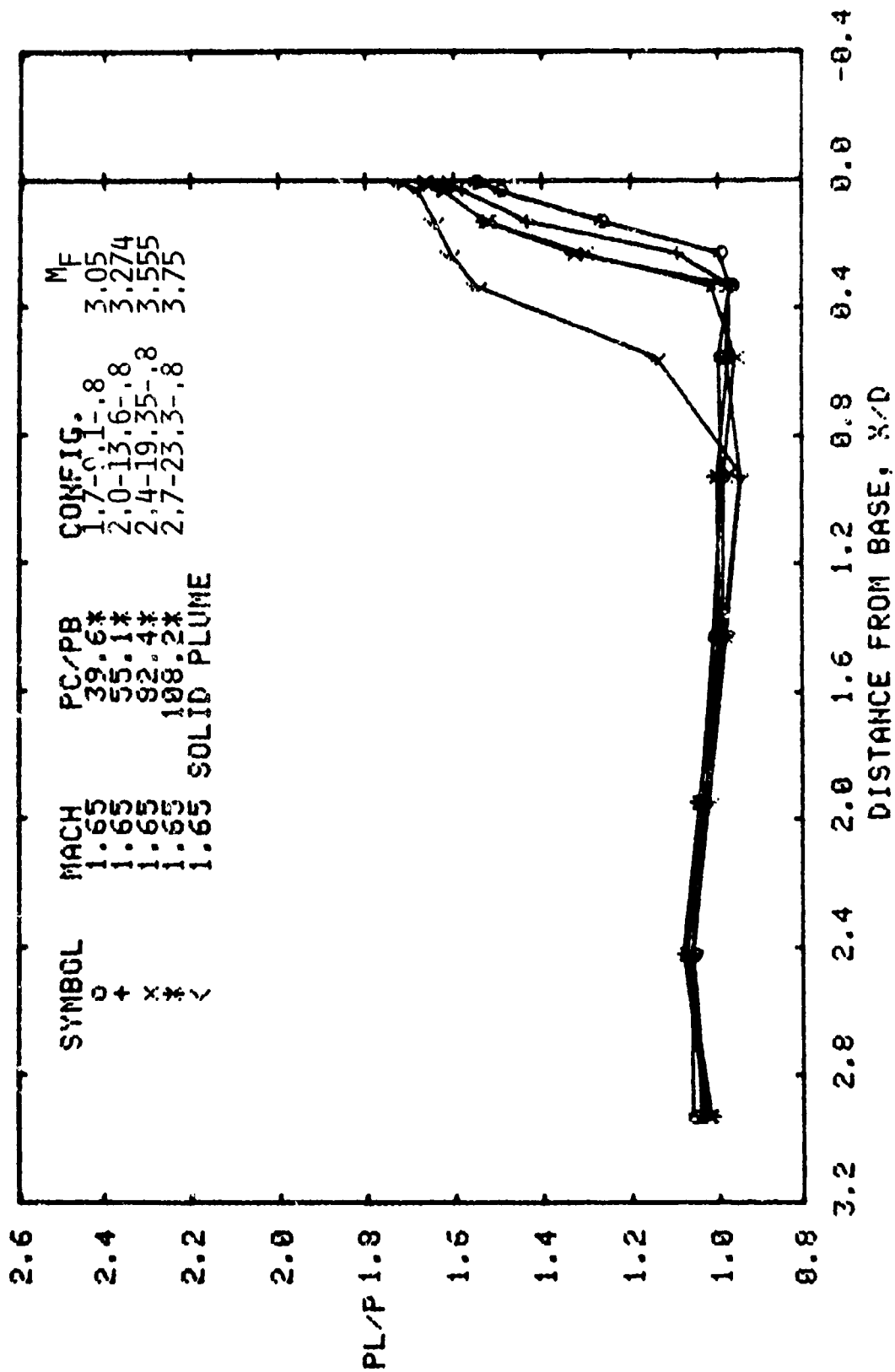


Fig. 5 Comparison of Pressure Distributions of the Four Nozzles at the Design Pressure Ratio and a Solid Plume (Continued)

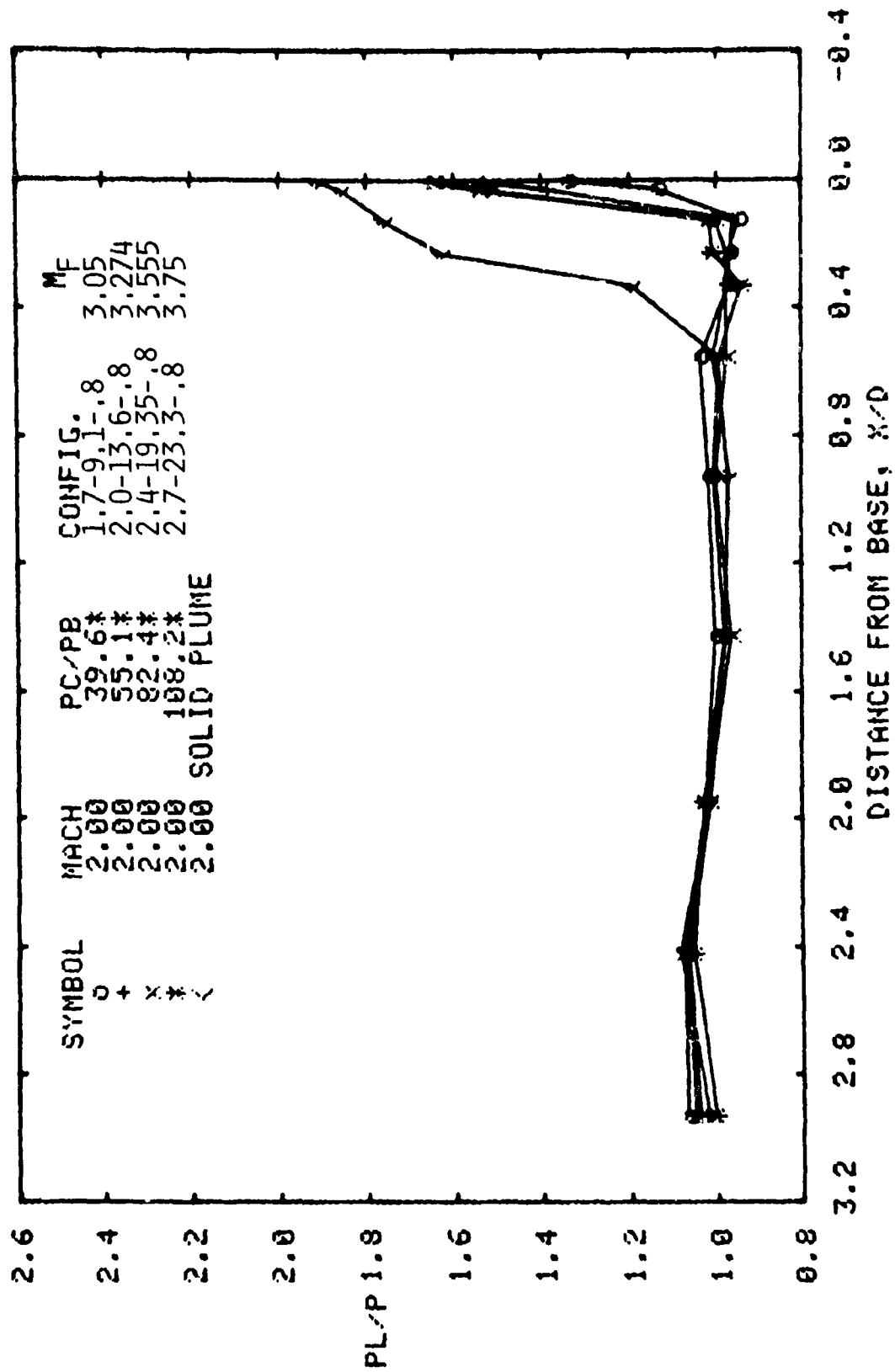


Fig. 5 Comparison of Pressure Distributions of the Four Nozzles at the Design Pressure Ratio and a Solid Plume (Continued)

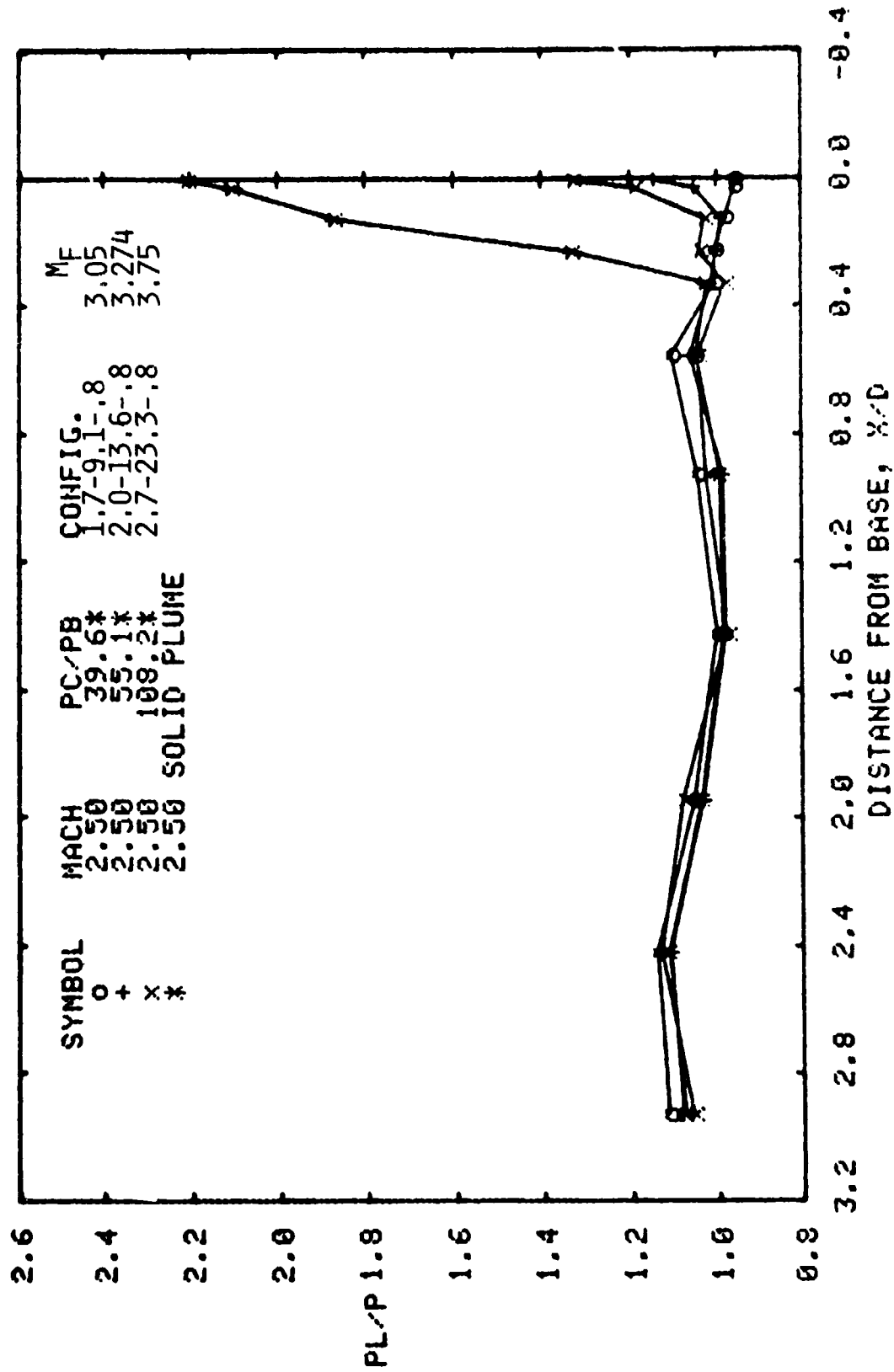
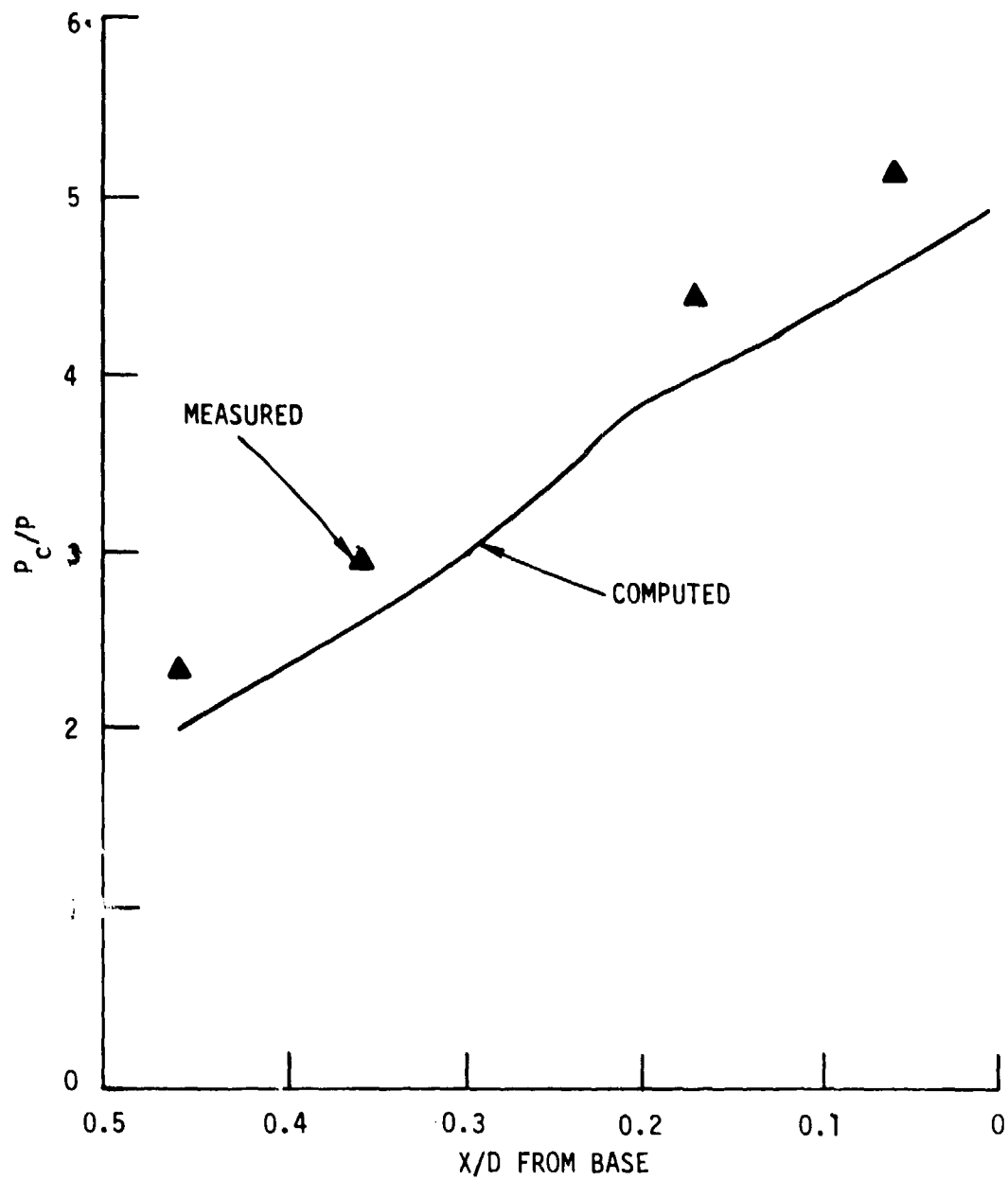


Fig. 5 Comparison of Pressure Distributions of the Four Nozzles at the Design Pressure Ratio and a Solid Plume (Continued)

There is some doubt of the precision of plume geometry at the "design" conditions. The nozzle wall pressure distributions are compared to computed distributions in Fig. 6. From extrapolation of the measured values it appears that the nozzle designed for an exit Mach number of 2.7 has an exit Mach number nearer to 2.6 and the nozzle designed for an exit Mach number of 1.7 is nearer to 1.8. The other two nozzles appear to be close to the design value. Even with the reduced precision, it is expected that the general conclusions stated will remain valid. An analysis of the transonic data by Nenni (Ref. 30) indicates that the "design" plume shapes from schlieren photographs compare well with computed plume shapes.

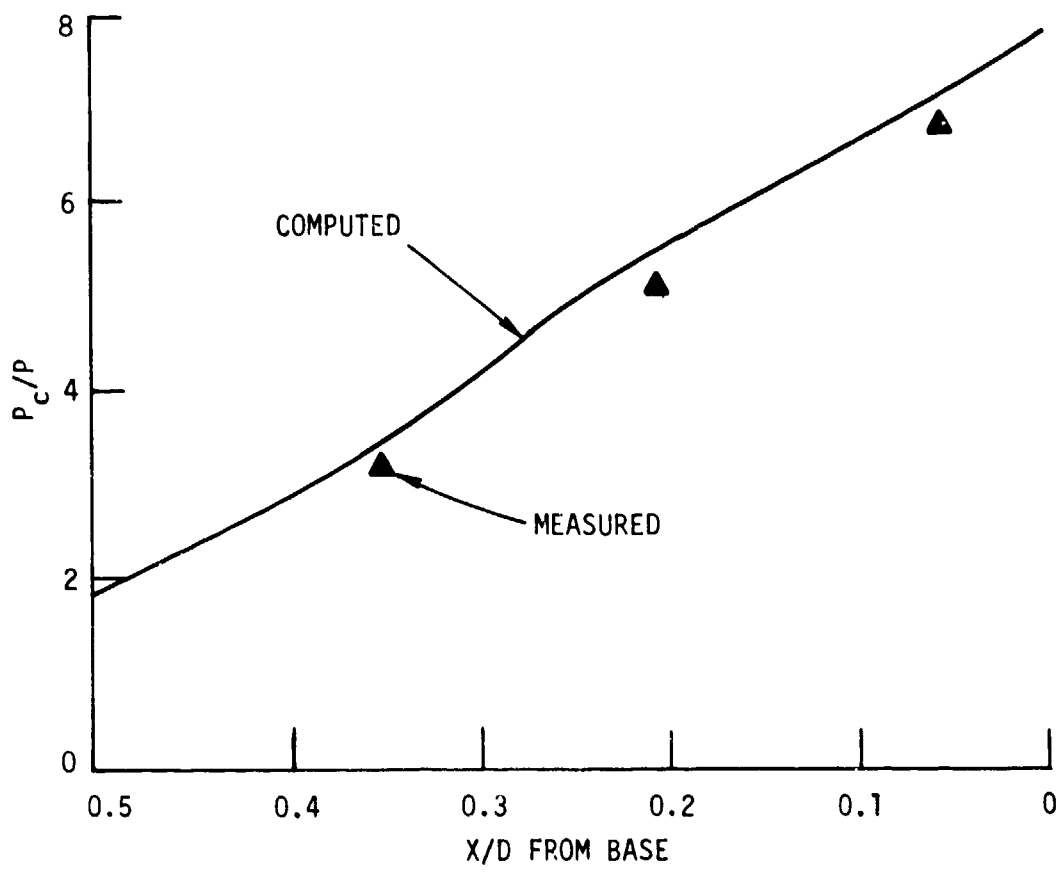
A review of the sled data was made for possible comparisons with the wind tunnel results. It appears that the sled data at conditions matching transonic tunnel measurements was affected by interference from the sled to such an extent as to make it questionable. When tests were run at the unitary tunnel, blockage resulting from the plume size voided planned tests at a Mach number of 1.5. A run was made with the smaller ZAP model nozzle (1.76-3.95-.8) at a Mach number of 1.6 and blockage occurred at values of $P_c/P_b > 40$. The remaining ZAP configuration (1.76-3.95-.93) was tested at a minimum Mach number for the test of 1.65.

No exact comparisons were available between the sled data and wind tunnel data. However some off-design comparison can be made where the two Mach numbers are slightly different. For thrust levels where the prototype (ZAP) is not exactly modeled, the comparison should still be valid (Ref. 7). Where initial plume angles are matched there is only a small discrepancy in initial plume radius of curvature. The variation of P_c/P_b with initial plume angle for both the prototype ($\gamma=1.235$) and the model ($\gamma=1.4$) is shown in Fig. 7. Comparison between the 6.12-in sled data ($M=1.56$, $P_c/P_b=105$) and the model ($M=1.6$, $P_c/P_b=40$) is shown in Fig. 8. From the preceding figure it is apparent the plumes nearly match. The data in Fig. 8 compare both the jet-on and jet-off pressure distributions. For this case the sled plume effects are greater than the model plume effects.



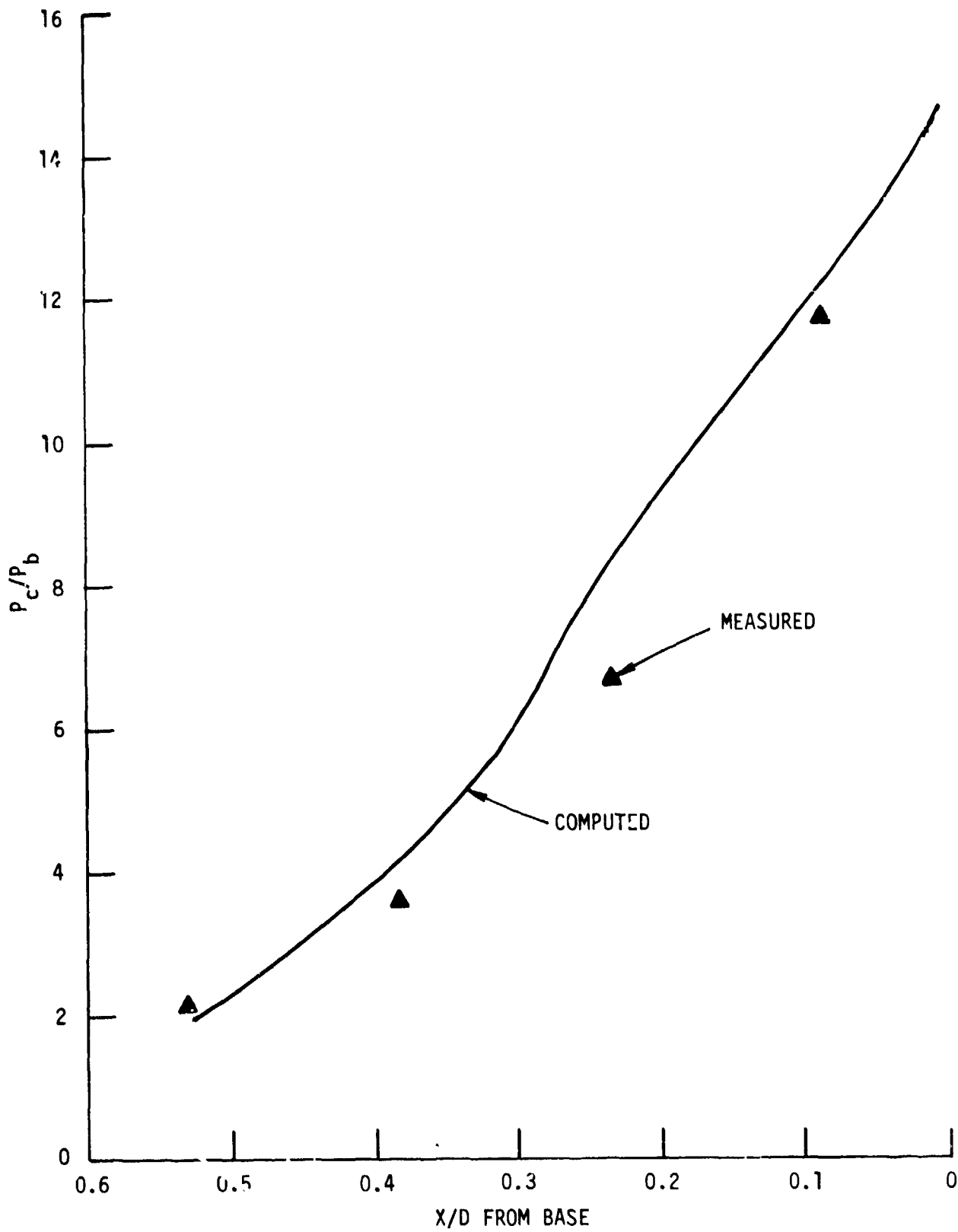
a. NOZZLE 1.7-9.1-.8

Fig. 6 Comparison of Measured Nozzle Pressures with Computed Distribution



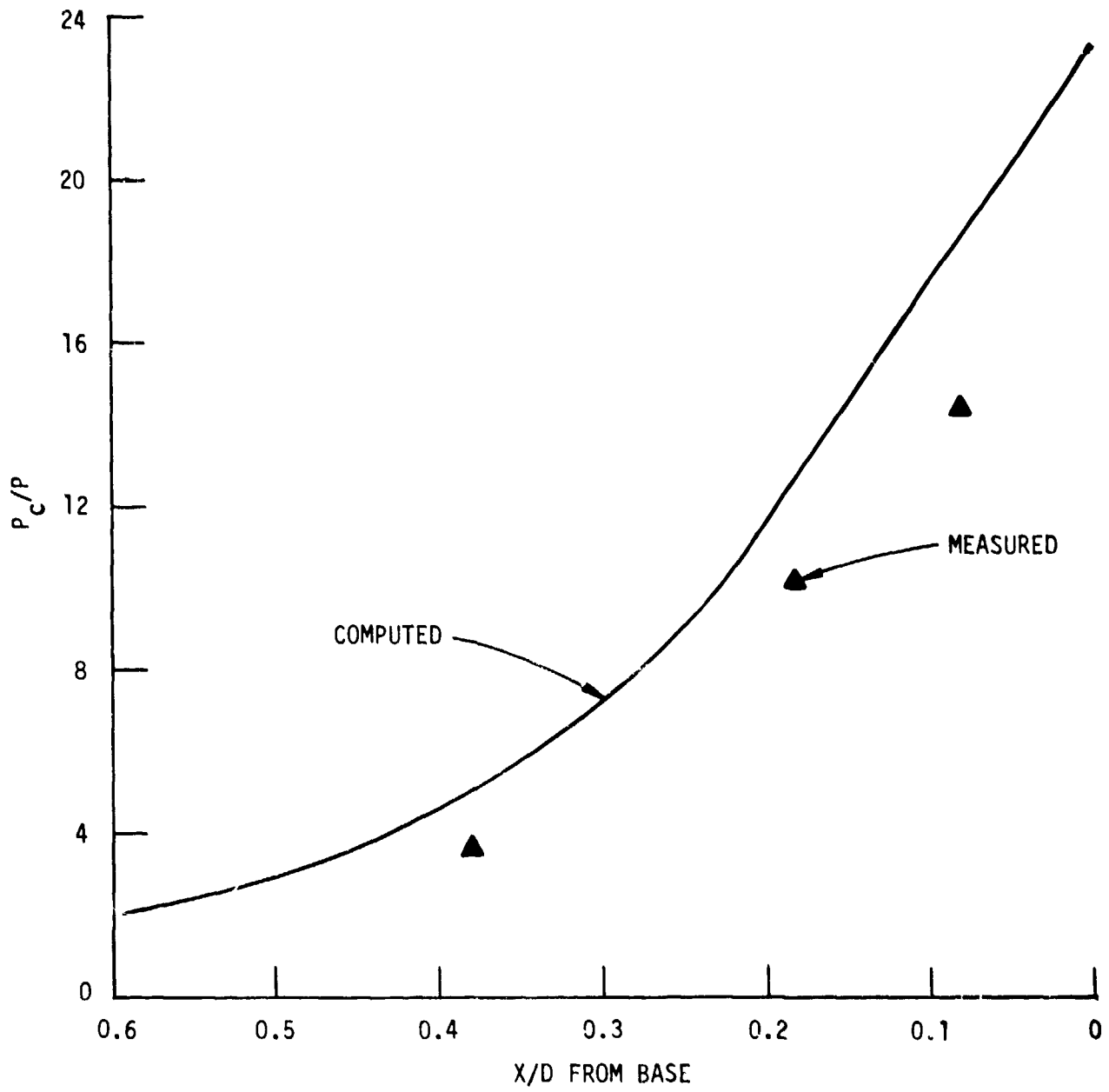
b. NOZZLE 2.0-13.6-.8

Fig. 6 Comparison of Measured Nozzle Pressures with Computed Distribution (Continued)



c. NOZZLE 2.4-19.35-.8

Fig. 6 Comparison of Measured Nozzle Pressures with Computed Distribution (Continued)



d. NOZZLE 2.7-23.3-.8

Fig. 6 Comparison of Measured Nozzle Pressures with Computed Distribution (Continued)

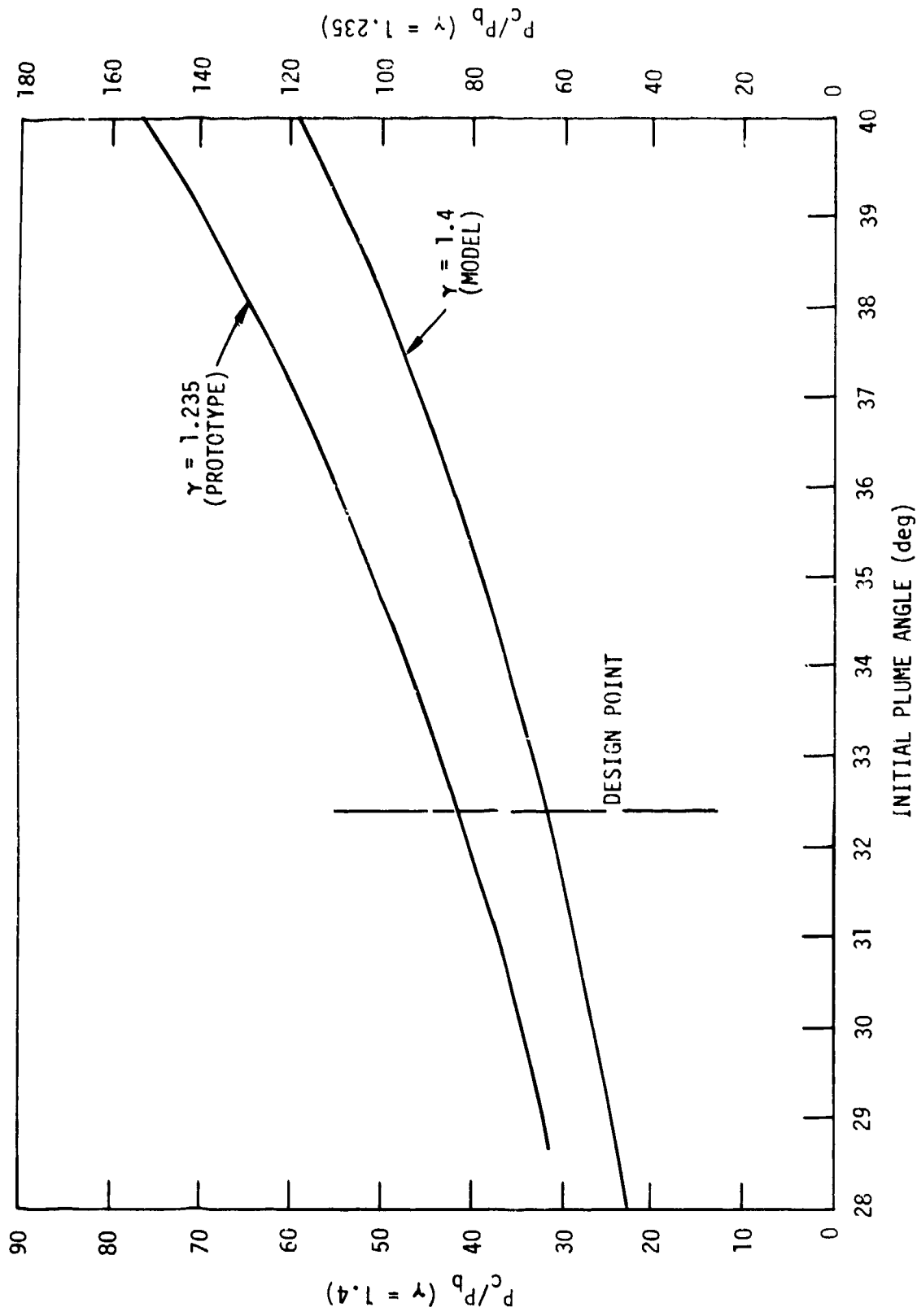


Fig. 7 Variation of Initial Plume Angle with Jet Total Pressure Ratio for ZAP Nozzle and ZAP Model Nozzle

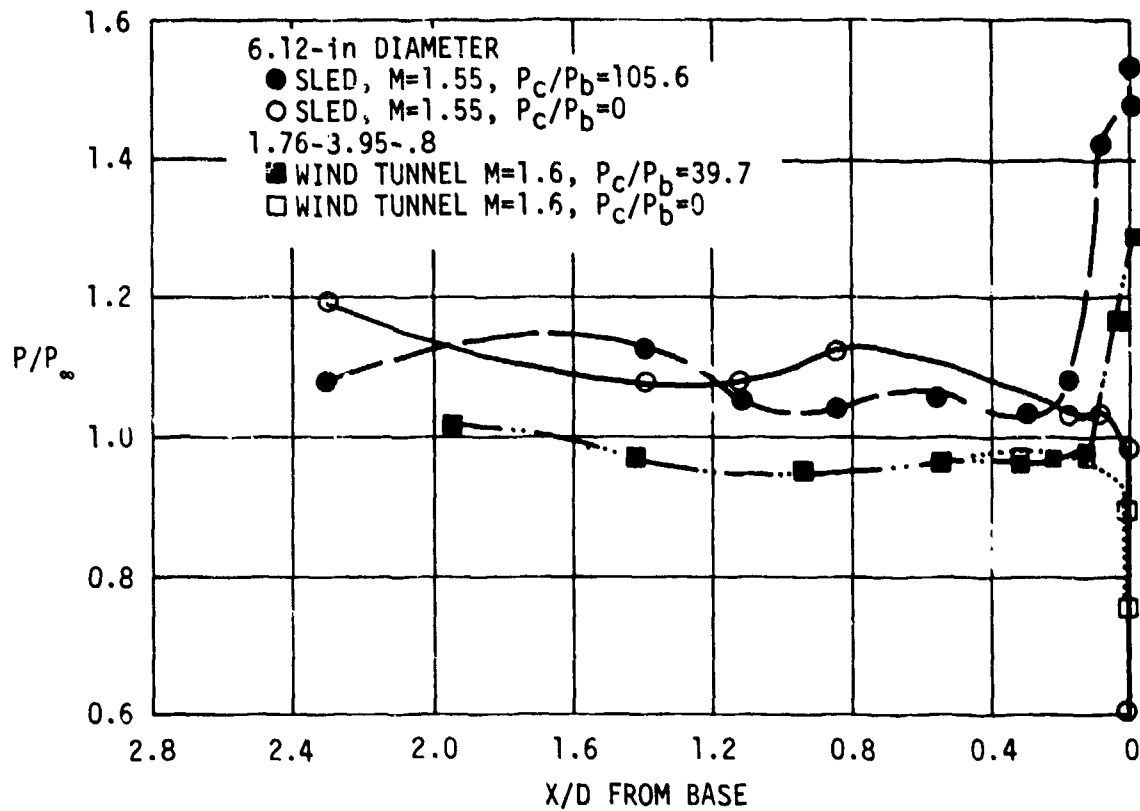


Fig. 8 Comparison of Jet-On and Jet-Off Base and Afterbody Pressures Between the 6.12-in Sled Configuration and Wind Tunnel Configuration (1.76-3.95-.8)

There appears to be more matching conditions for the earlier 6-in ZAP configuration and the modeled nozzle (1.76-3.95-.8). Unfortunately, the orifice distribution on the sled was designed to measure pressures at transonic speeds and consequently few orifices are located near the base of the model where the plume effects are restricted to a small area at supersonic speeds. The variation of base and afterbody pressures on the wind tunnel configuration (1.76-3.95-.8) with sled jet total pressure ratio at a Mach number of 1.65 is shown in Fig. 9. The wind tunnel P_c/P_b was related to the sled P_c/P_b by using Fig. 7. Also shown in Fig. 9 is the variation of base pressure on the 7-in sled at a Mach number of 1.63. The base pressure was the only usable data during this sled run. The only other orifice in the area influenced by the plume appeared to be plugged. However, there appears to be a fairly good match between sled and wind tunnel base pressures.

Brazzel (Ref. 31) used thrust coefficient (C_T) as a parameter for correlating sustainer level jet effects on base pressure. Although jet-on base pressure is influenced by many variables, the use of C_T allowed the analysis of experimental data in a manner where adequate design information could be obtained. Thrust coefficient is given by

$$C_T = \frac{\gamma_j p_j A_j M_j^2 + A_j (p_j - p_\infty)}{1/2 \gamma_\infty p_\infty A_B M_\infty^2} = \frac{\text{Thrust}}{q_\infty A_B} \quad (2)$$

where the subscripts j and ∞ represent the jet and freestream, respectively.

For simulated sustainer thrust levels where the base is aspirated by the jet, the use of C_T appears to account for all the variables except jet Mach number (assuming the use of air or similar gas for the jet). At the thrust levels high enough for the plume to influence the afterbody, there is the added effect of nozzle exit angle and nozzle exit to base diameter ratio.

Since four of the nozzles of the present tests were built to give the same "design" plume shape, it appeared reasonable that C_T should be a good parameter to correlate base pressure. Shown in Fig. 10 is a comparison of the variation of P_b/p_∞ with C_T for these nozzles for Mach numbers of 0.9 to 2.5.

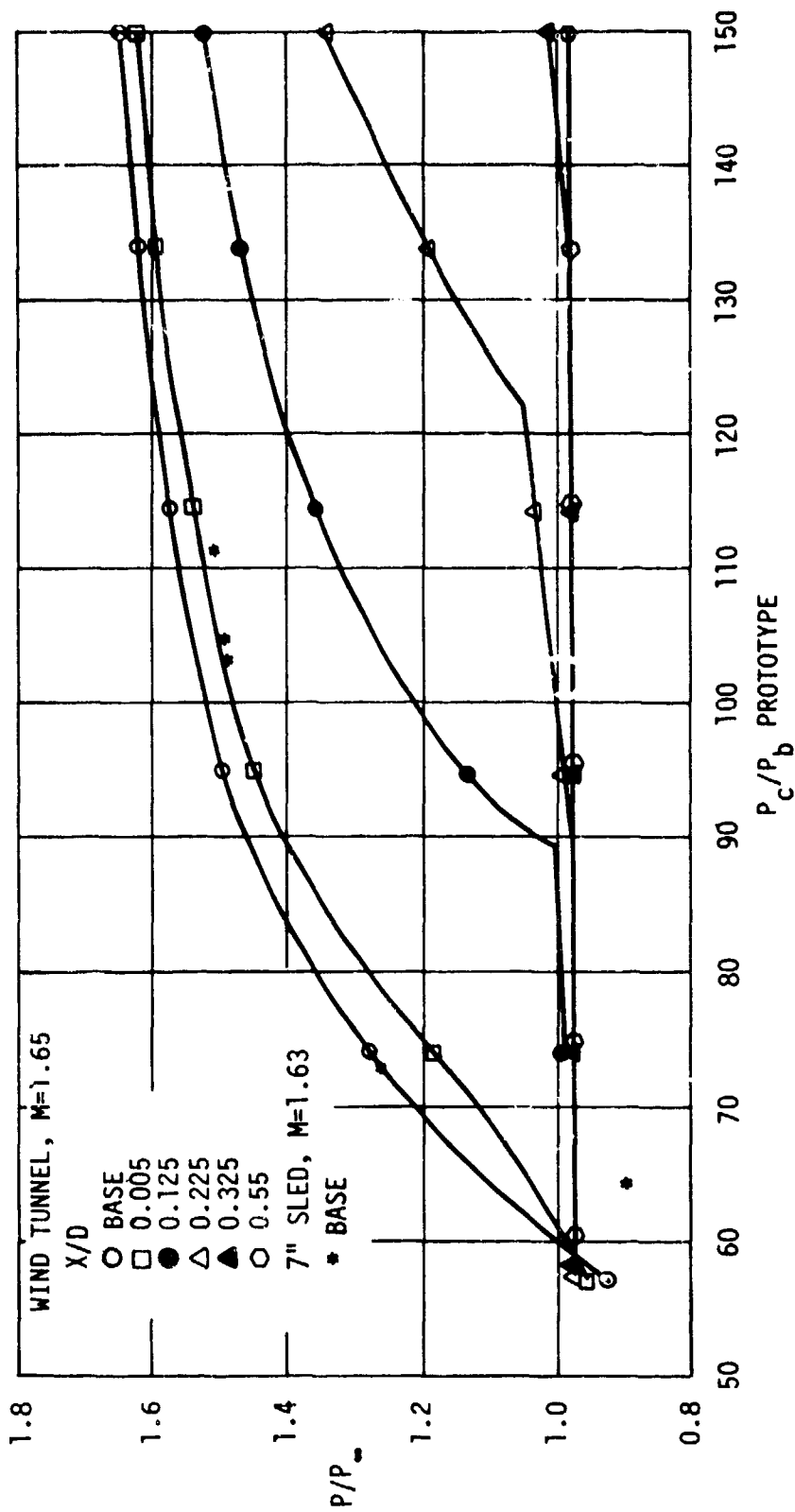


Fig. 9 Comparison of Wind Tunnel Model (1.76-3.95-.93) Pressures Related to Sled P_c/P_b at $M=1.65$ to 7-in Diameter Sled Base Pressures at $M=1.63$

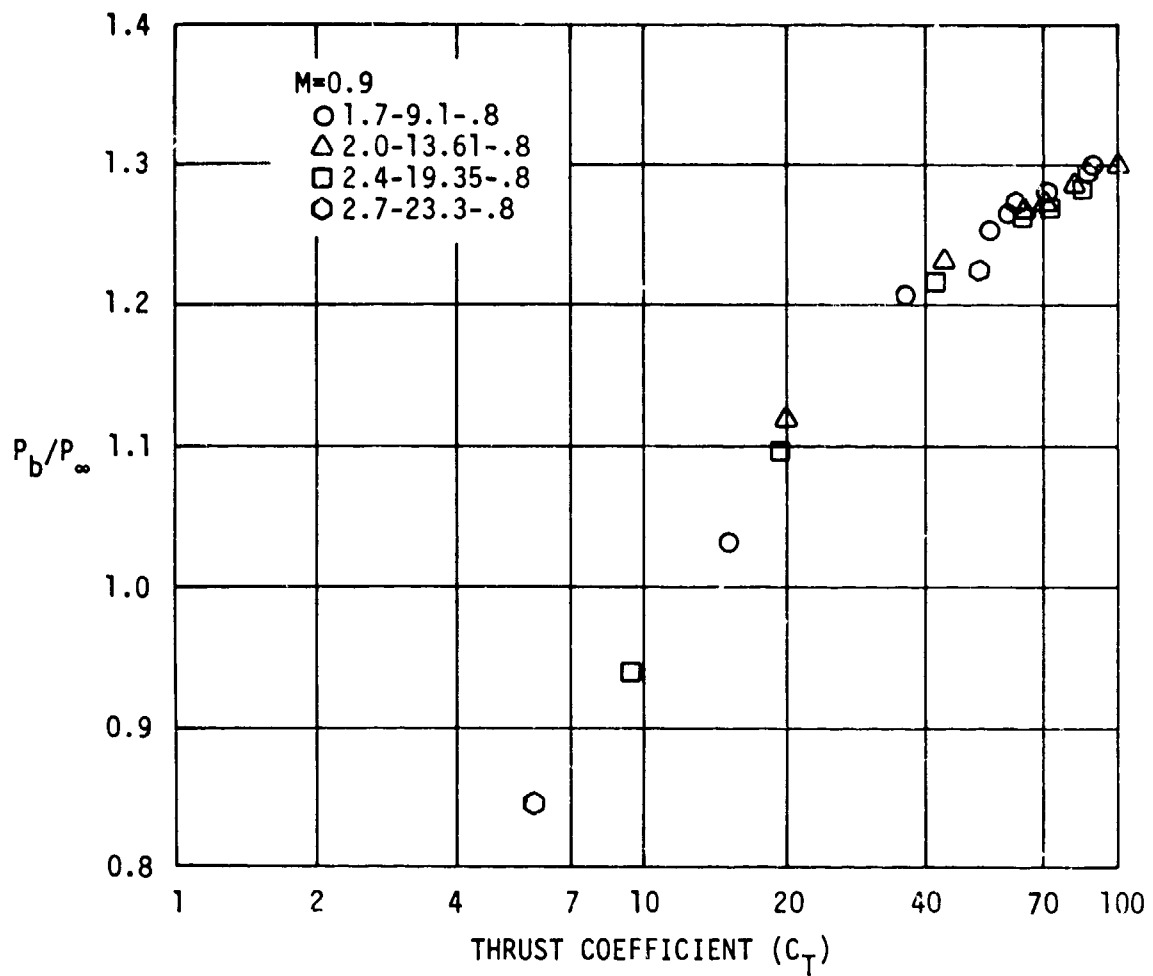


Fig. 10 Variation of Base Pressure with Thrust Coefficient for the Four Nozzles with Same "Design" D'ume Shape

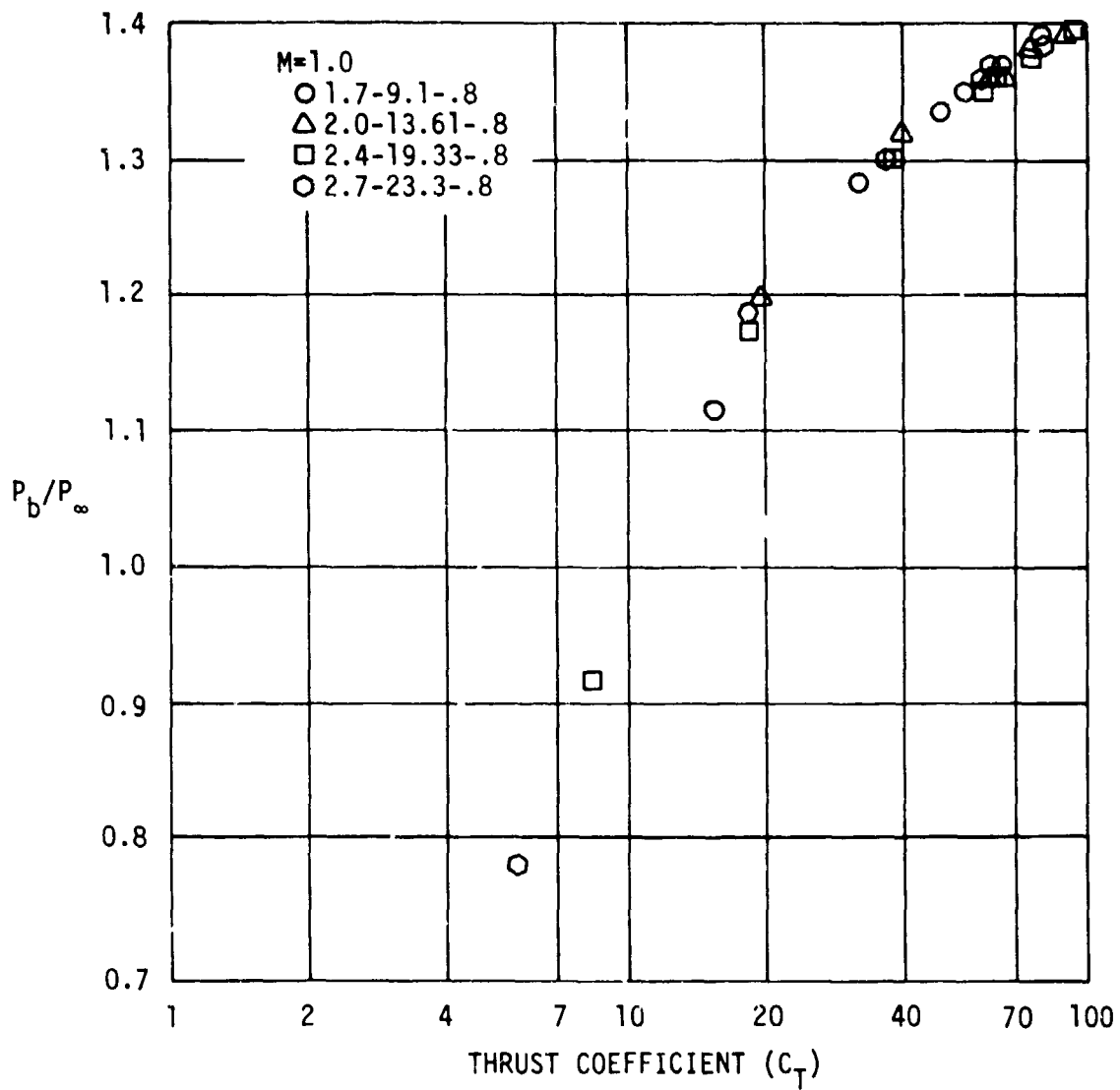


Fig. 10 Variation of Base Pressure with Thrust Coefficient for the Four Nozzles with Same "Design" Plume Shape (Continued)

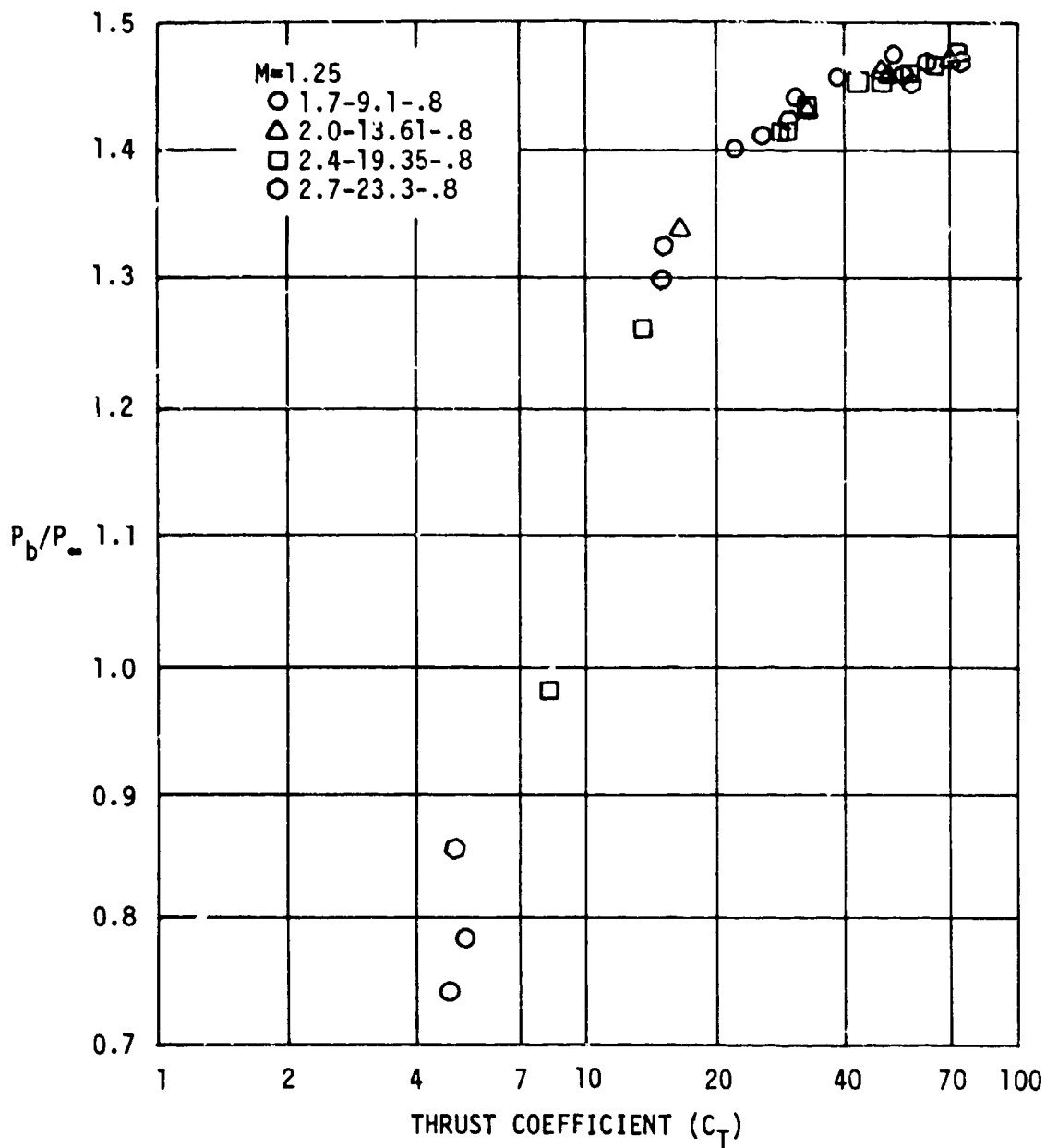


Fig. 10 Variation of Base Pressure with Thrust Coefficient for the Four Nozzles with Same "Design" Plume Shape (Continued)

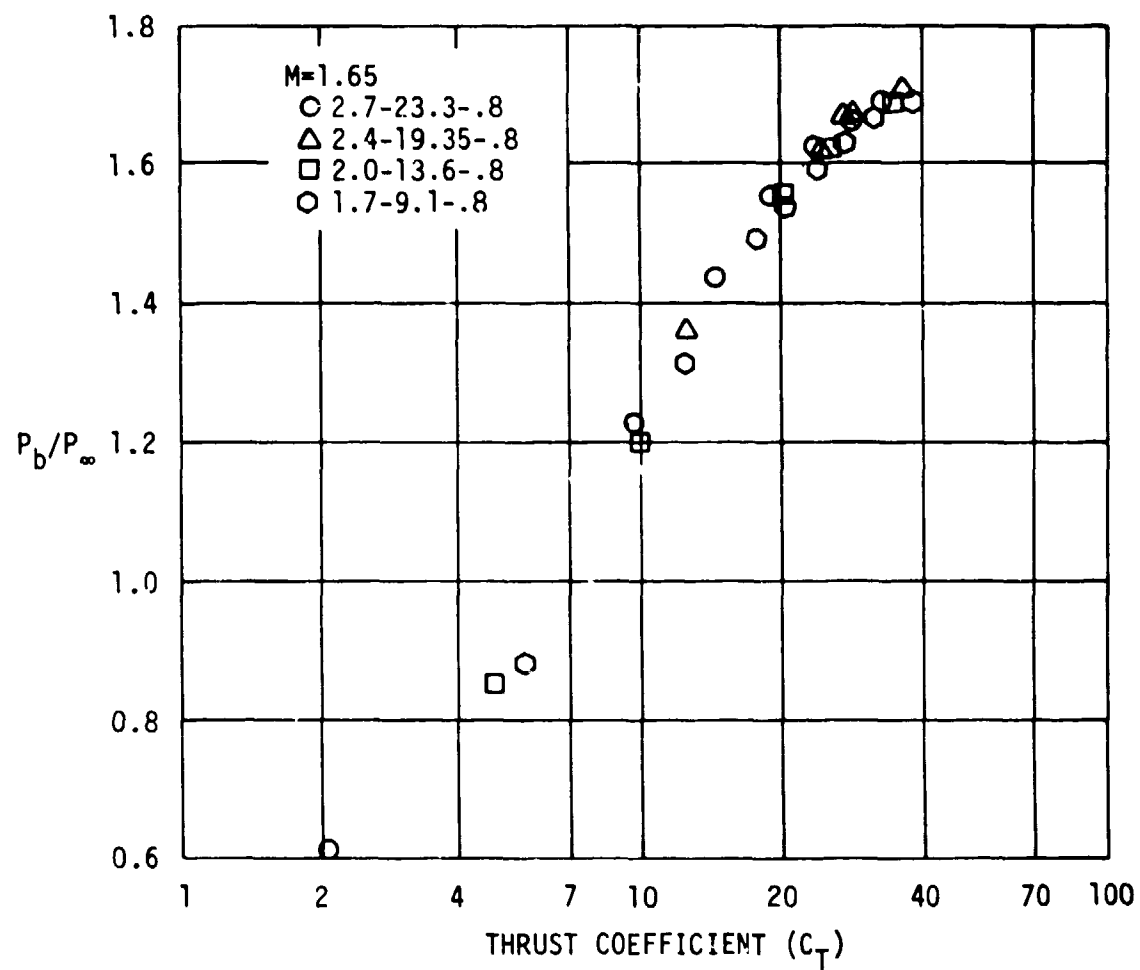


Fig. 10 Variation of Base Pressure with Thrust Coefficient for the Four Nozzles with Same "Design" Plume Shape (Continued)

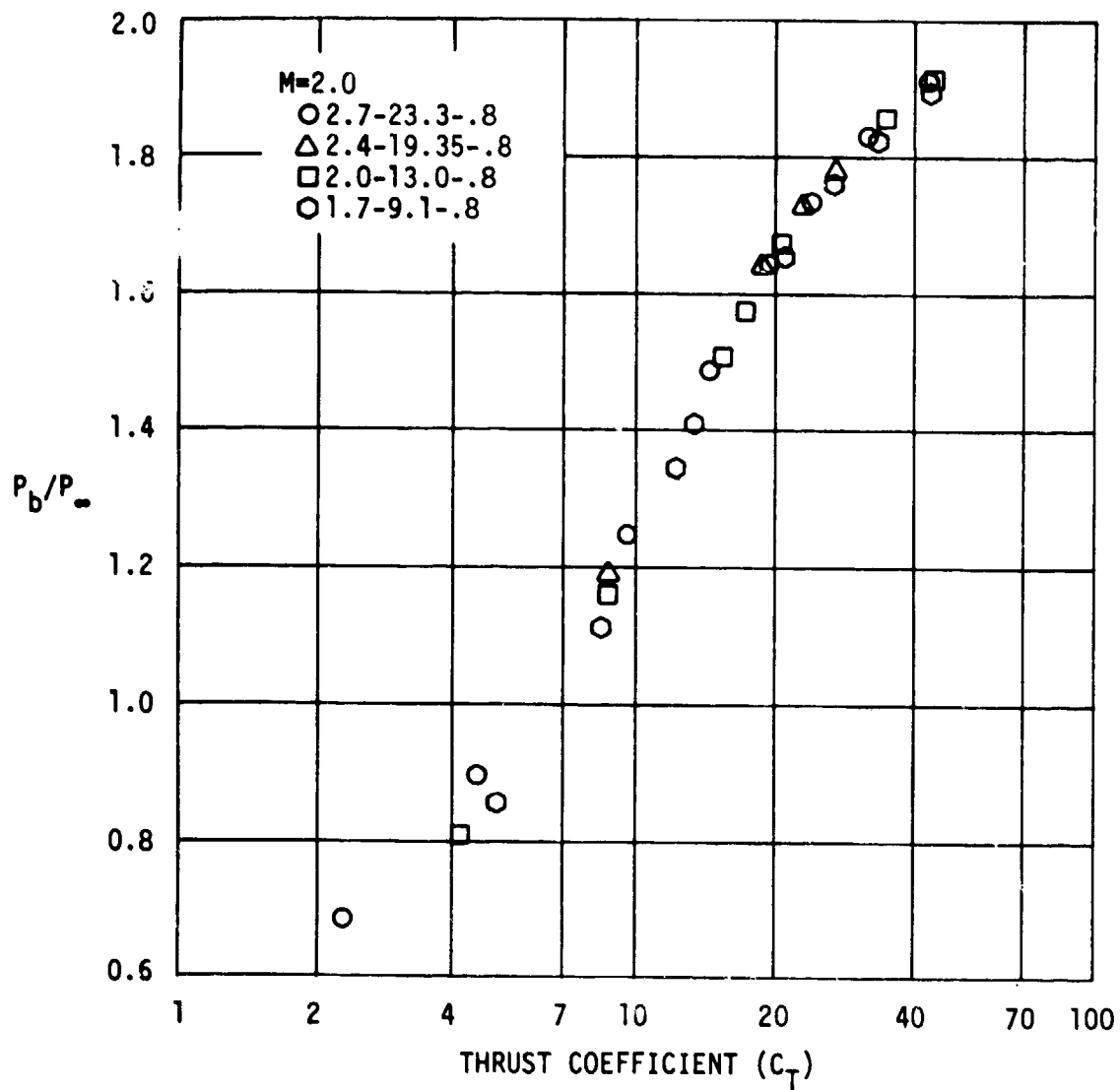


Fig. 10 Variation of Base Pressure with Thrust Coefficient for the Four Nozzles with Same "Design" Plume Shape (Continue.)

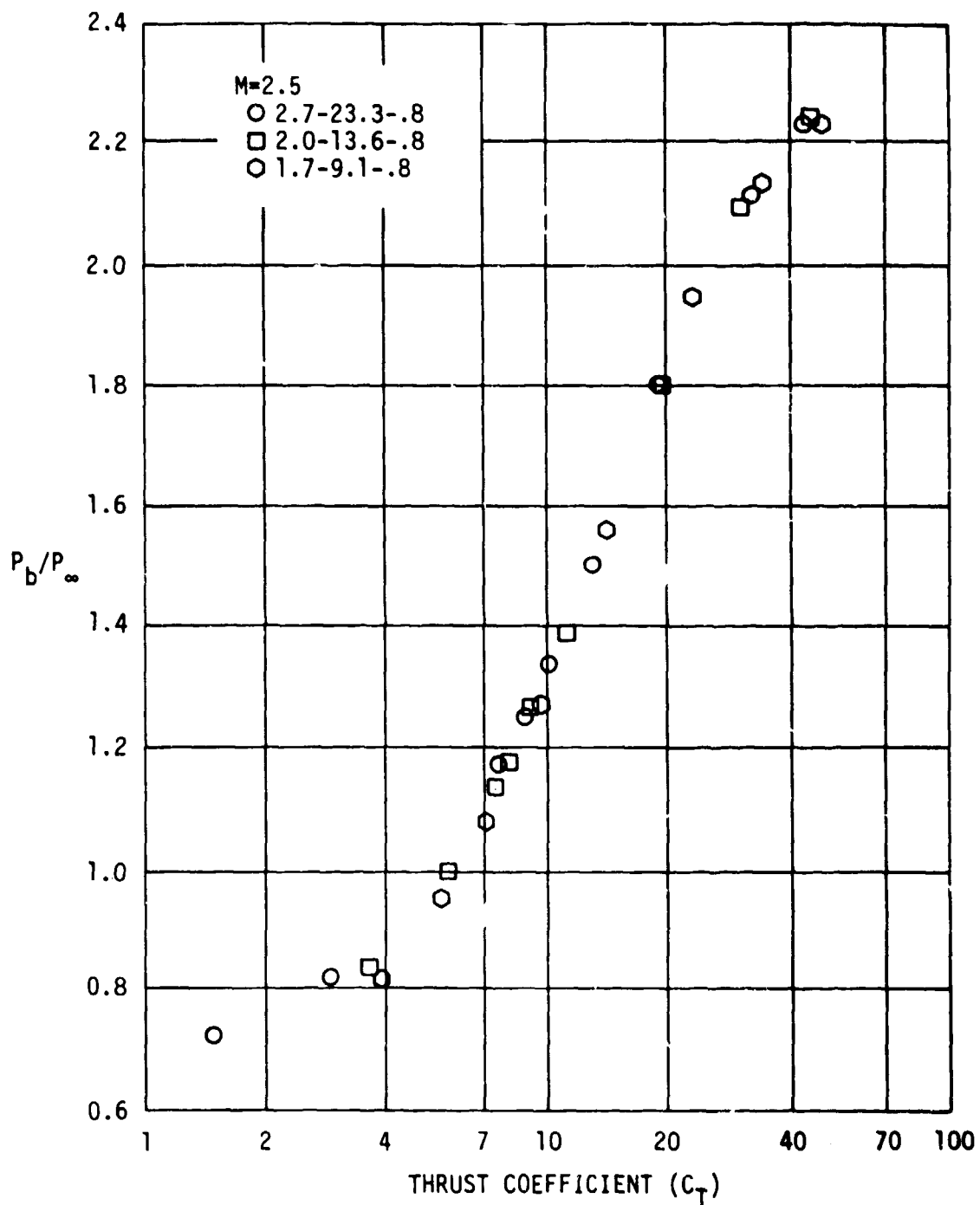


Fig. 10 Variation of Base Pressure with Thrust Coefficient for the Four Nozzles with Same "Design" Plume Shape (Continued)

It appears that a fairly good correlation is obtained for all of the freestream Mach numbers shown. The approximate value of P_b/P_∞ for the "design" plumes may be obtained from Fig. 5.

The correlation obtained in Fig. 10 suggests a slight change in approach of modeling plume effects on aerodynamics. For high acceleration tactical missiles and free rockets, the exit Mach number is usually between about 2.3 to 2.7. Using the Korst modeling technique the model nozzle exit Mach number will vary from less than two to nearly sonic. When the exit Mach number is close to sonic, the nozzle will be difficult to fabricate with precision required to give an accurate exit Mach number. However, a higher exit Mach number and higher exit angle nozzle designed to match the plume shape of the model nozzle could be utilized. For example, a model nozzle having an exit Mach number of 1.7 and an exit angle of 4 deg could be replaced by a nozzle having an exit Mach number of 2.5 and an exit angle of 15 deg. The plume Mach number for the $M_j = 2.5$ nozzle would be higher than that of the model nozzle resulting in plume with a higher stiffness factor, but this fact would tend to account for the effects of afterburning (Ref. 32).

The variation of base pressure with C_T for the two ZAP configurations is shown in Fig. 11. Base pressure is not correlated by C_T as well as for the nozzles in Fig. 10.

The variation of base pressure with radial thrust coefficient (C_{RT}) for the normal jet plume effects simulator is presented in Fig. 12. Radial thrust coefficient is given by

$$C_{RT} = \frac{\text{radial thrust}}{q_\infty A_{\text{ref}}}$$

where radial thrust is the total thrust from the 24 nozzles on the simulator. The normal jet simulator, which is used on sting-mounted force models, tends to simulate the radial component of momentum of an axial plume. By comparing the variation of base pressure with C_T from Figs. 10 and 11, and variation of base pressure with C_{RT} in Fig. 12, an indication can be obtained of the amount of radial thrust required to simulate the same plume effect as the axial jet.

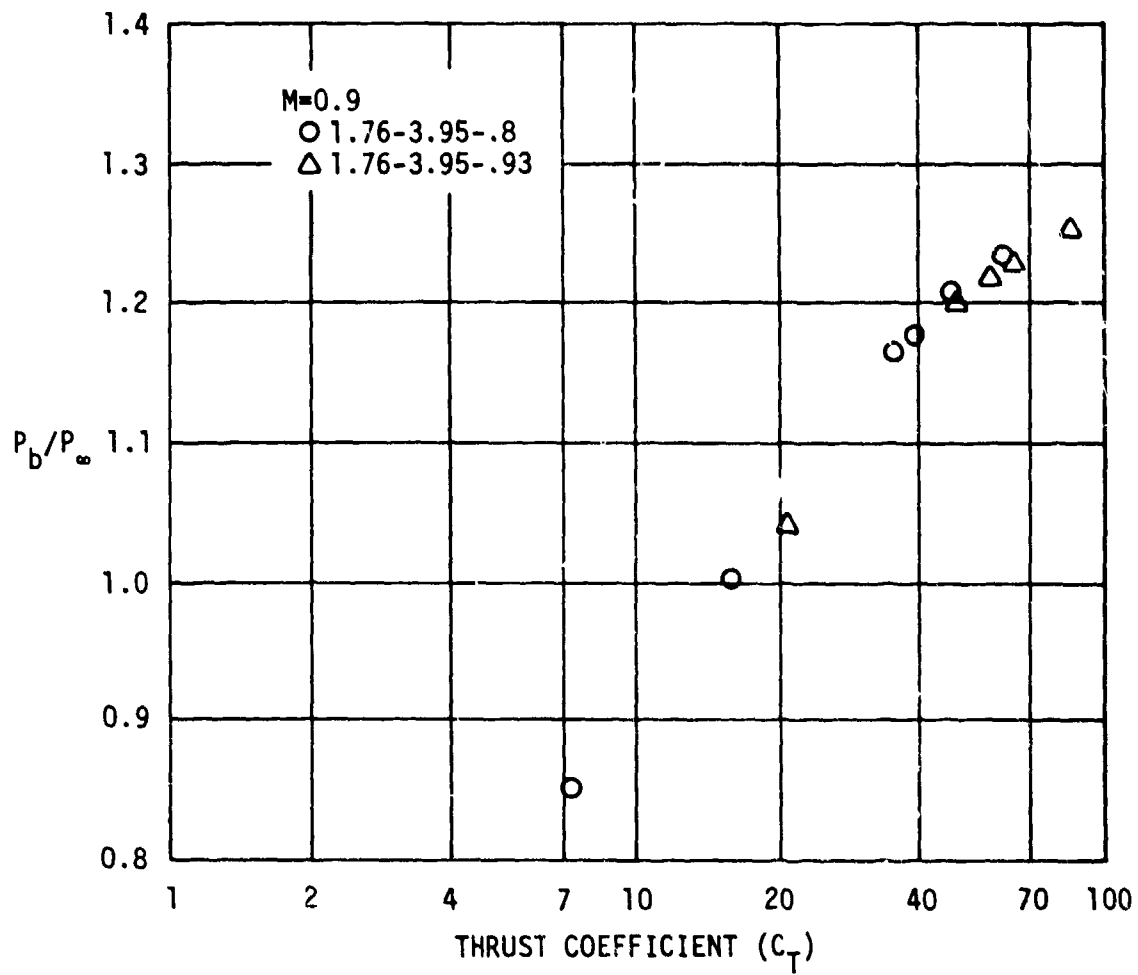


Fig. 11 Effect of D_N/D_B on Variation of Base Pressure with Thrust Coefficient

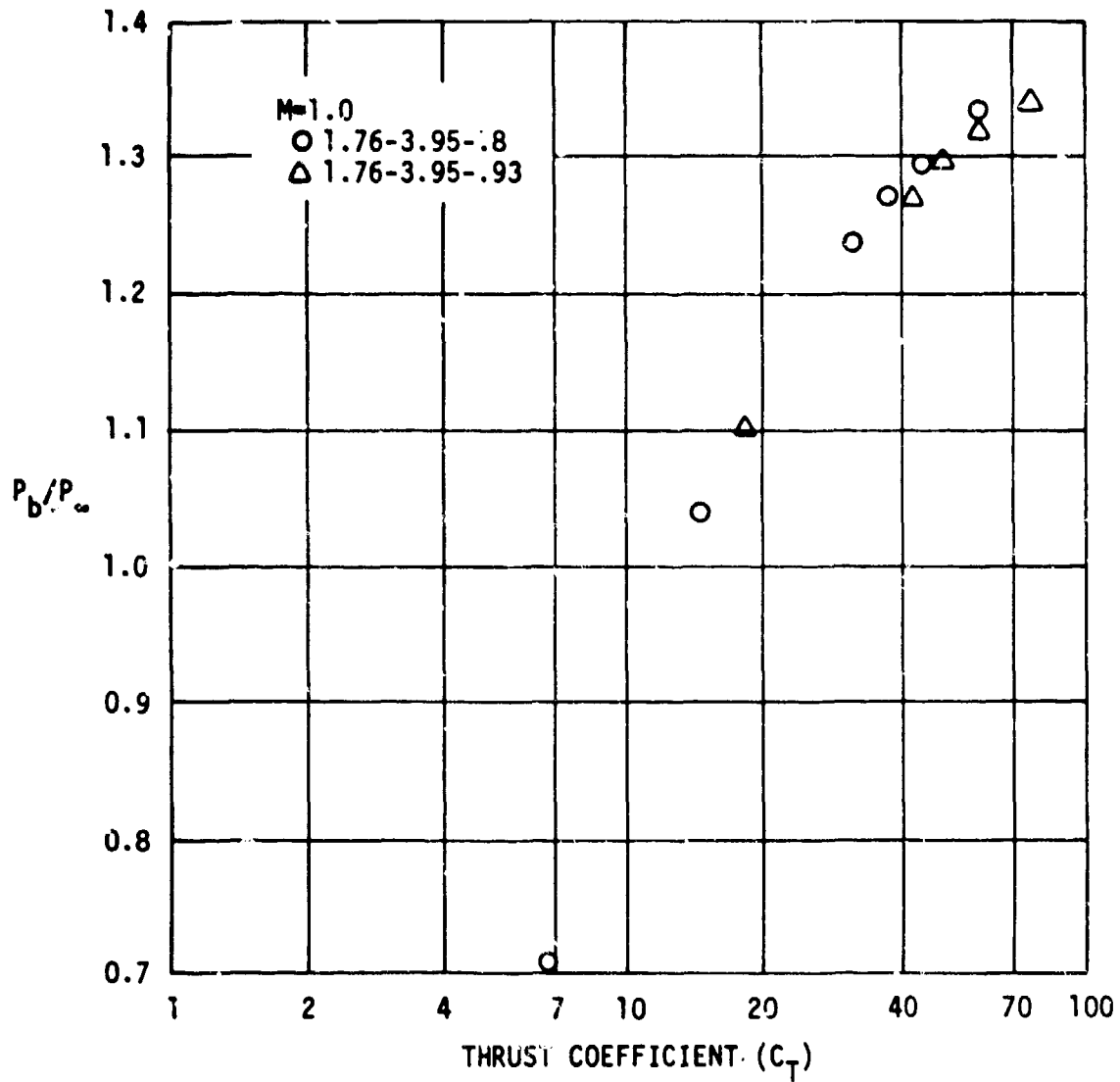


Fig. 11 Effect of D_N/D_B on Variation of Base Pressure with Thrust Coefficient (Continued)

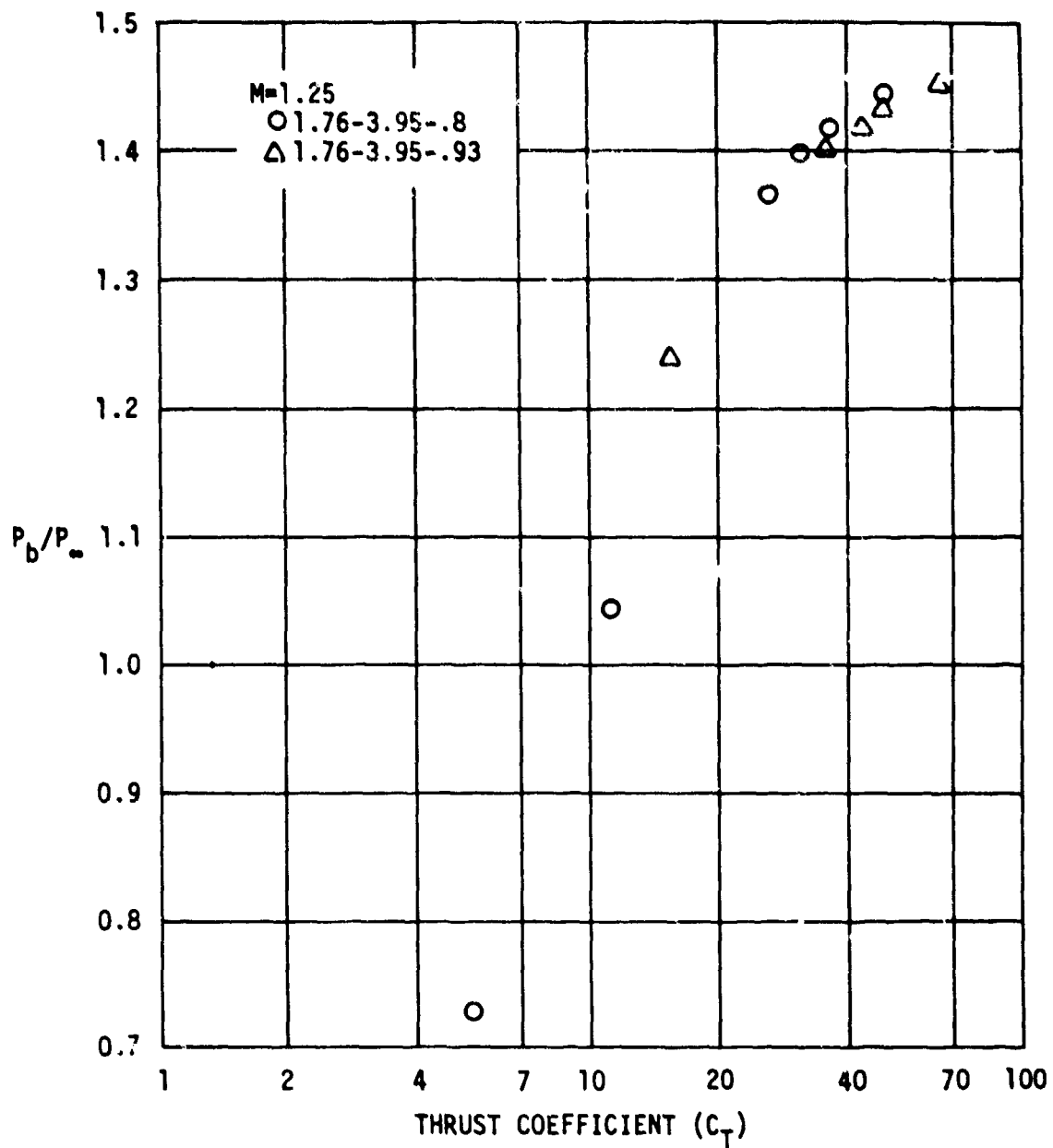


Fig. 11 Effect of D_N/D_B on Variation of Base Pressure with Thrust Coefficient (Continued)

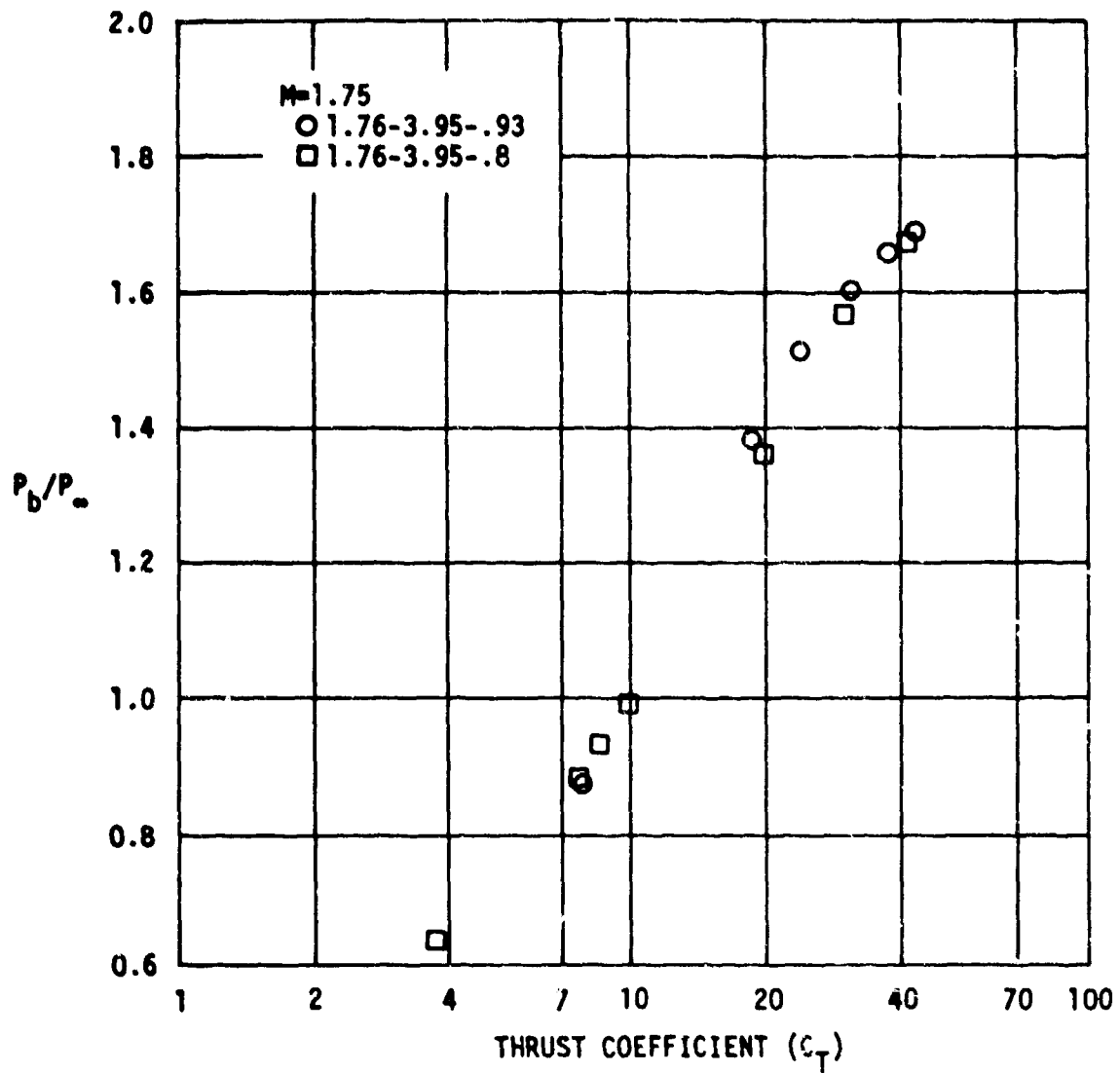


Fig. 11 Effect of D_n/D_B on Variation of Base Pressure with Thrust Coefficient (Continued)

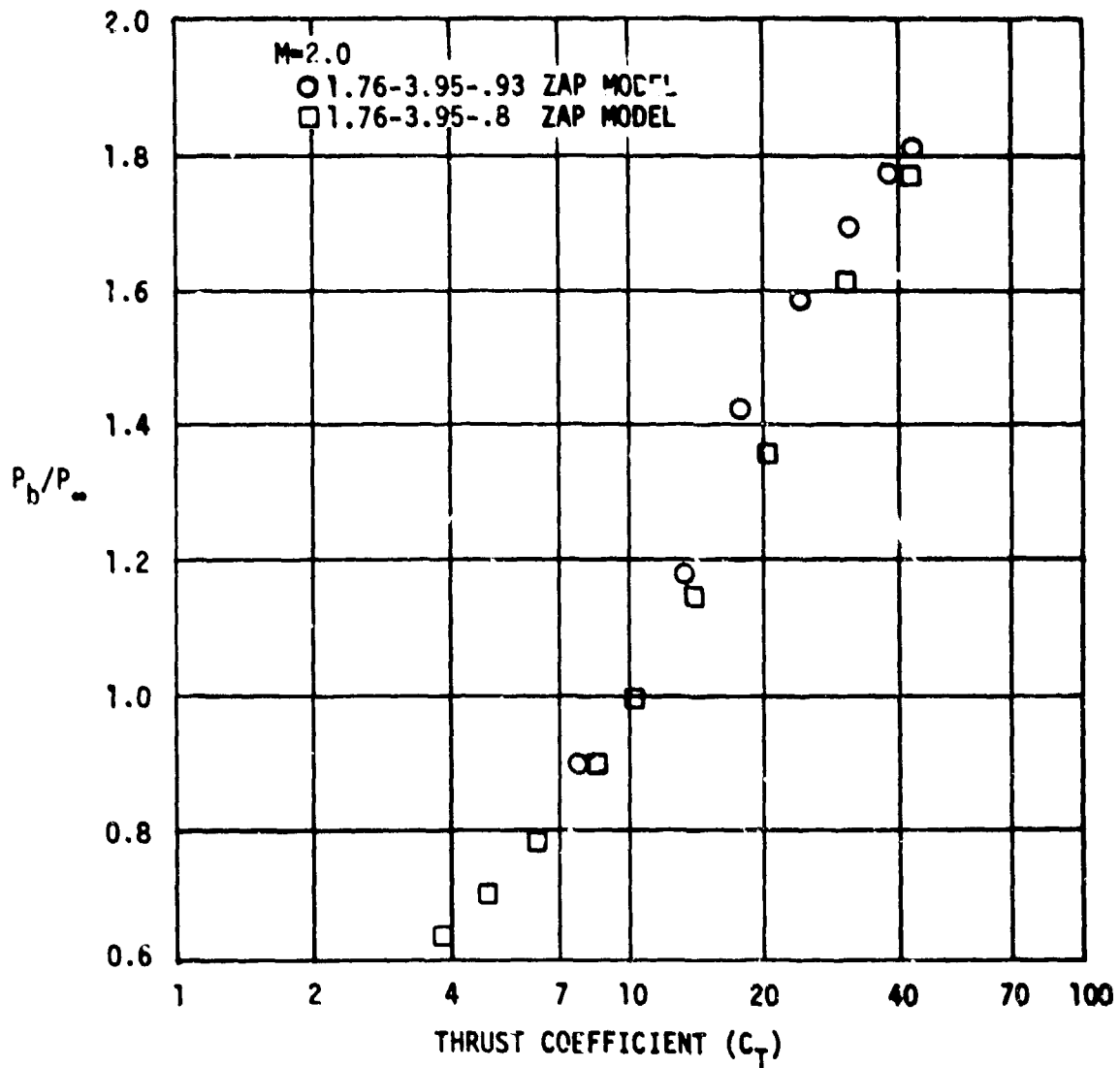


Fig. 11 Effect of D_n/D_b on Variation of Base Pressure with Thrust Coefficient (Continued)

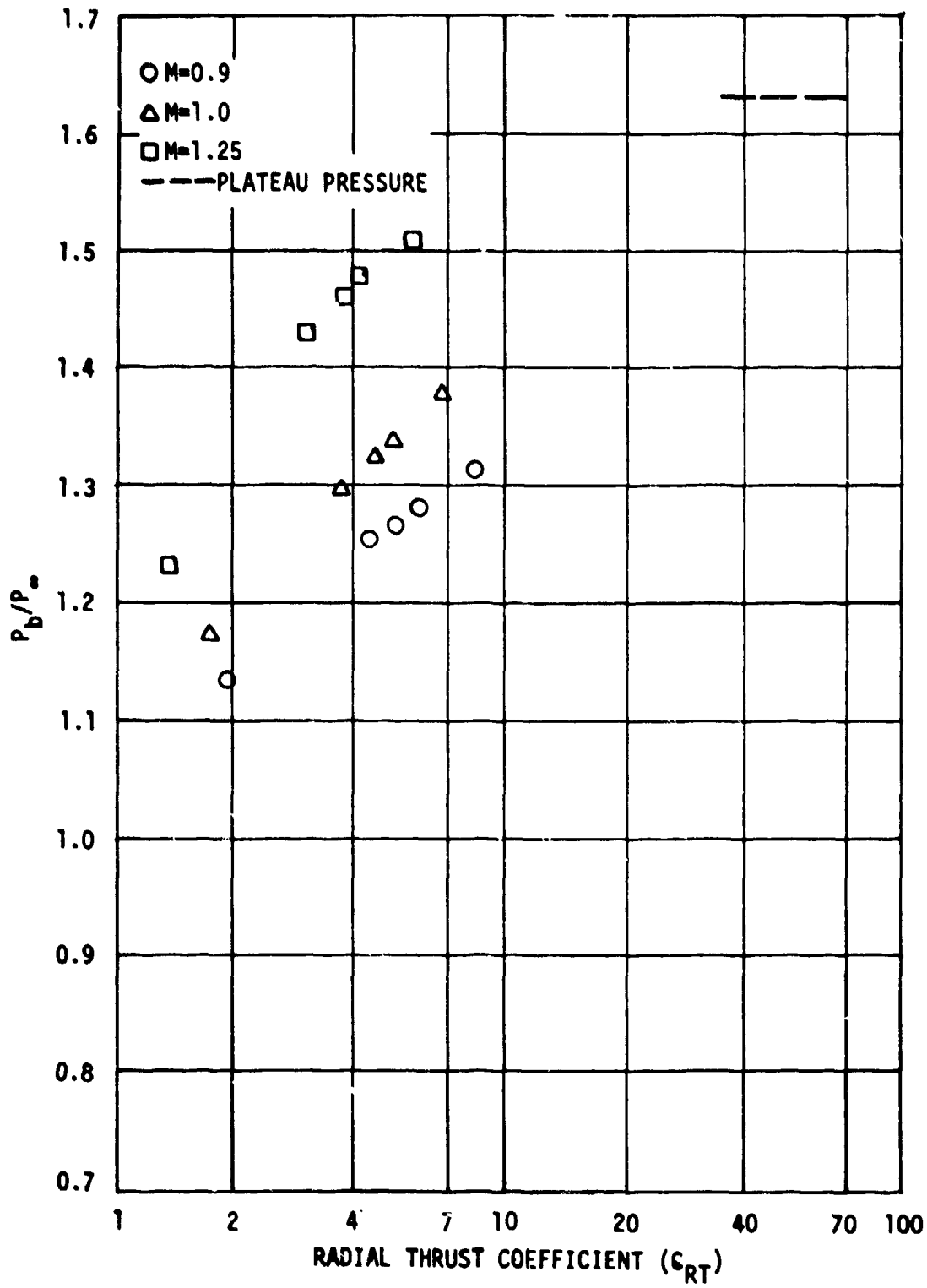


Fig. 12 Variation of Base Pressure with Radial Thrust Coefficient for the Normal Jet Plume Effects

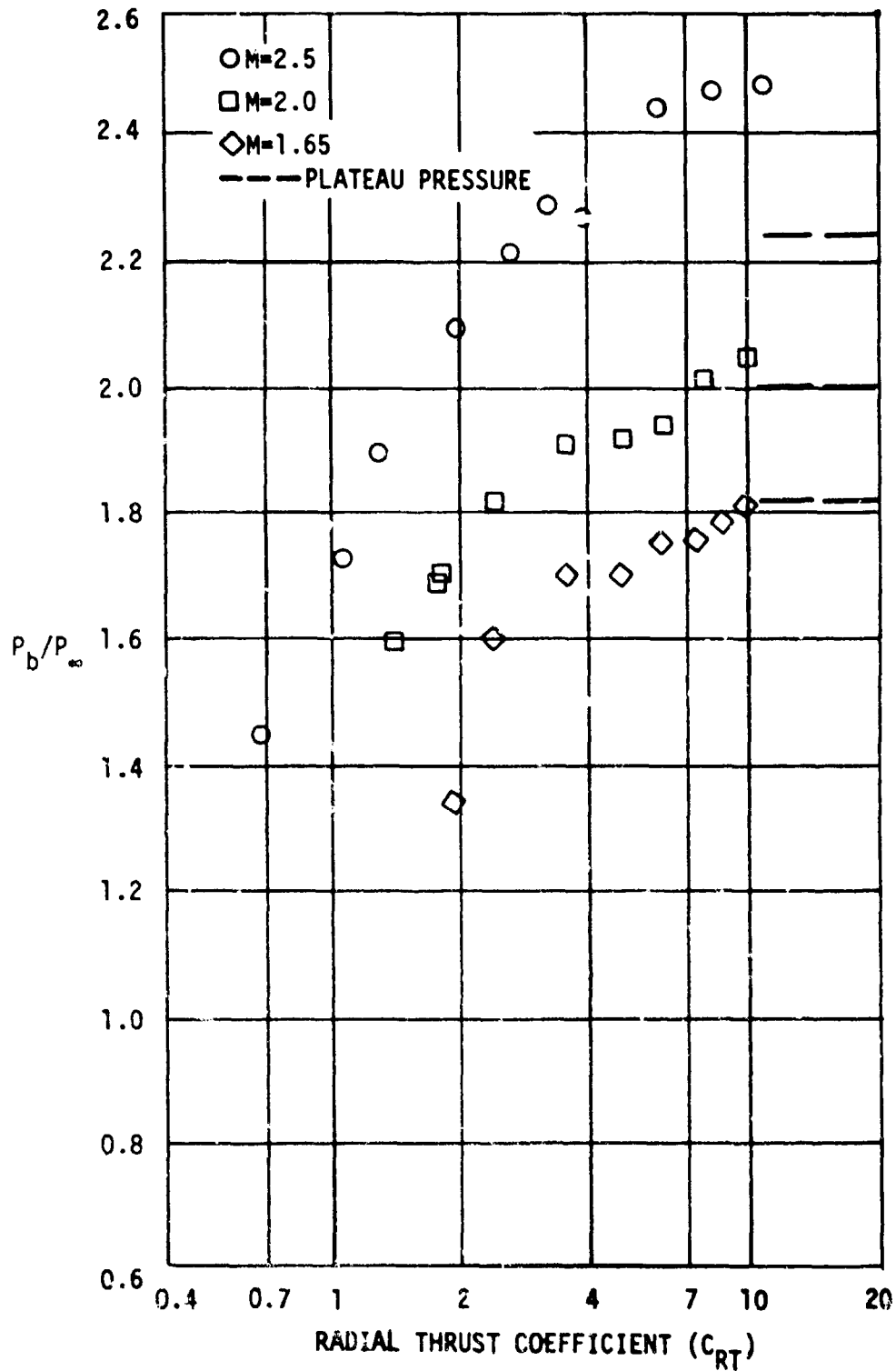


Fig. 12 Variation of Base Pressure with Radial Thrust Coefficient for the Normal Jet Plume Effects (Continued)

The fraction of radial to axial thrust required to simulate about the same plume effects is shown in Fig. 13 for the two families of nozzles in the present investigation.

At high values of C_{RT} and for the supersonic Mach numbers in Fig. 12(b), the base pressures induced by the normal jet simulator exceed the plateau pressure established by Zukoski (Ref. 33). If thrusts at this level are to be simulated, better results would probably be obtained with the simulator moved further aft.

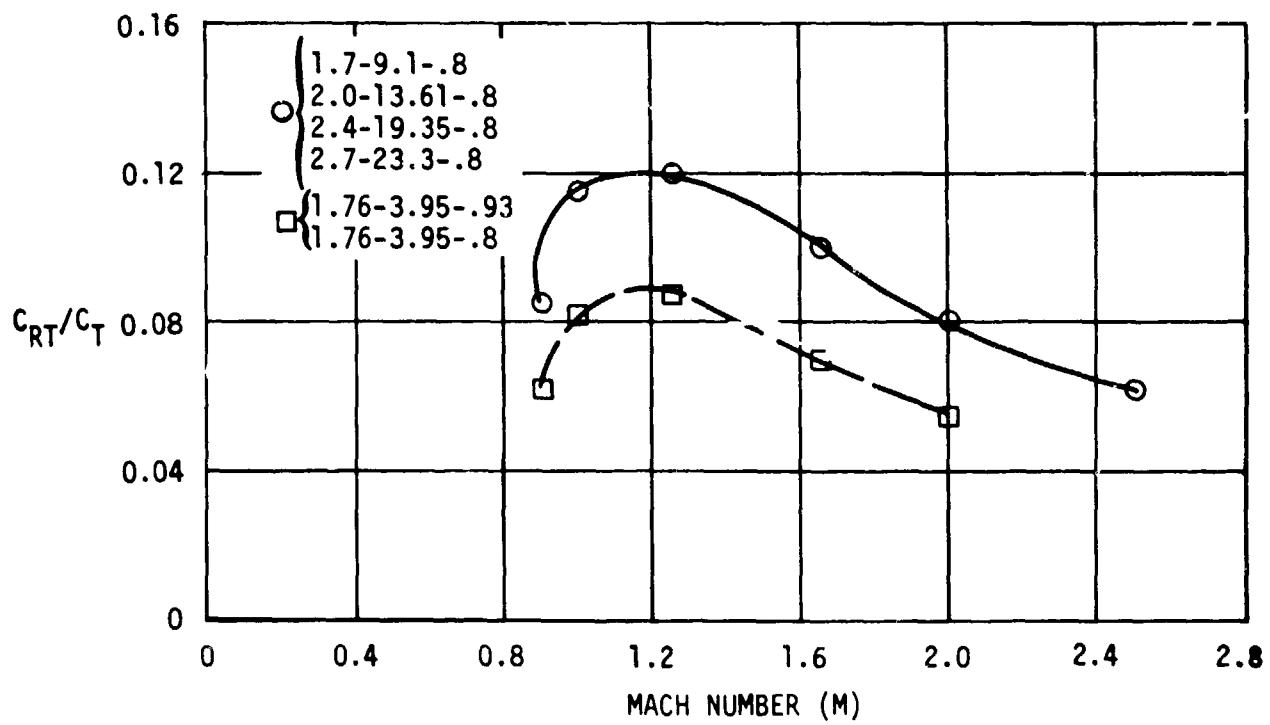


Fig. 13 Ratio of Radial Thrust to Axial Thrust Required for the Same Plume Effect

BLANK PAGE

7.0 CONCLUDING REMARKS

An investigation of concepts for modeling jet plume effects on missile aerodynamics has been made. The experimental results tend to verify the modeling concepts proposed by Korst. Comparisons were made of afterbody pressure distributions under the influence of different air plumes having the same shape but with different surface Mach numbers. The comparisons indicate that increasing plume Mach number generally increases the plume effect on afterbody pressures with this effect becoming more pronounced with increasing Mach number. A solid plume with the same shape as the air plumes has the greatest effect on afterbody pressures with the effect increasing considerably at freestream Mach numbers of 1.25 and higher.

The shape of afterbody pressure distributions under the influence of plume effects simulated by the normal jet simulator compared favorably with the distributions under the influence of axial jets. The ratio of normal to axial thrusts, C_{RT}/C_T , required to simulate the same level of effects varies with both freestream Mach number and axial jet nozzle geometry.

An attempt was made to compare sled tests of the ZAP rocket with an air nozzle modeled by Korst's concept. No exact match of test conditions was available, but the few cases where comparisons were possible tended to confirm the validity of the modeling concept.

BLANK PAGE

8.0 REFERENCES

1. Pettis, W. Jr., "Effects on Normal Force of Streamwise Gaps Between the Body and Fins of a Missile Configuration," Master of Science Thesis, Department of Aerospace Engineering, Mechanical Engineering and Engineering Mechanics, University of Alabama, University, Alabama, 1971.
2. "Design of Aerodynamically Stabilized Free Rockets," Engineering Design Handbook, U.S. Army Material Command, AMCP 706-280, 1968.
3. Davis, L., Jr., J.W. Follin, Jr. and L. Blitzer, The Exterior Ballistics of Rockets, D. Van Nostrand Company, Inc., Princeton, N. J., 1958.
4. Dahlke, C.W. and W. Pettis, "Normal Force Effectiveness of Several Fin Planforms with Streamwise Gaps at Mach Numbers of 0.8 to 5.0," Technical Report RD-TR-70-8, U.S. Army Missile Command, Redstone Arsenal, Alabama, April 1970.
5. Korst, H.H., "Approximate Determination of Jet Contours Near the Exit of Axially Symmetrical Nozzles as a Basis for Plume Modeling," U.S. Army Missile Command, Redstone Arsenal, Alabama, Report No. TR-RD-72-14, August 1972.
6. Korst, H.H., "An Analysis of Jet Plume Modeling by Dissimilar Propellant Gases," Proceedings, 43rd Semi-Annual Meeting, Supersonic Tunnel Association, Pasadena, California, 2-3 April 1975.
7. Korst, H.H. and R.A. Deep, "Modeling of Plume Induced Problems in Missile Aerodynamics," Proceedings, 17th Annual Aerospace Sciences Meeting (AIAA), New Orleans, Los Angeles, 15-17 January 1979.
8. Korst, H.H., R.A., White, et al, "The Simulation and Modeling of Jet Plumes in Wind Tunnel Facilities," Proceedings, 11th Annual Aerodynamic Testing Conference (AIAA), Colorado Springs, Colorado, 18-20 March 1980, Pages 80-430.
9. Deep, R.A., J.H. Henderson, and C.E. Brazzel, "Thrust Effects on Missile Aerodynamics," U.S. Army Missile Command, Redstone Arsenal, Alabama, Report No. RD-TR-71-9, May 1971.
10. Henderson, J.H., "Transonic Wind Tunnel Investigation of Thrust Effects on the Longitudinal Stability Characteristics of Several Body-Fin Configurations (Sting-Mounted Model with Normal-Jet Plume Simulator)," U.S. Army Missile Command, Redstone Arsenal, Alabama, Technical Report RD-75-14, 31 December 1974.
11. Henderson, J.H., "An Investigation of Jet Plume Effects on the Stability Characteristics of a Body of Revolution in Conjunction with Fins of Various Geometry and Longitudinal Positions at Transonic Speeds (Sting-Mounted Model with Normal Jet Plume Simulator)," U.S. Army Missile Command, Redstone Arsenal, Alabama, Technical Report RD-75-37, 12 June 1975.
12. Henderson, J.H., "Investigation of Jet Plume Effects on the Longitudinal Stability Characteristics of a Body of Revolution with Various Fin Configurations at Mach Numbers from 0.2 to 2.3 (Normal Jet Simulator)," U.S. Army Missile Command, Redstone Arsenal, Alabama, Technical Report RD-76-22, February 1976.

REFERENCES (Continued)

13. Dahlke, W., "An Investigation of Flow and Stability Characteristics for a Body of Revolution with Fins and Flare in Presence of Plume Induced Separation at Mach Numbers 0.7 to 1.4," U.S. Army Missile Command, Redstone Arsenal, Alabama, Report No. TR-TD-77-11, May 1977.
14. Henderson, J.H., C.W. Dahlke, and G. Batiuk, "An Experimental Investigation Using a Normal Jet Plume Simulator to Determine Jet Plume Effects on a Long Slender Rocket Configuration at Mach Numbers from 0.2 to 1.5 U.S. Army Missile Command, Redstone Arsenal, Alabama, Report No. TR-TD-77-2, 4 February 1977.
15. Burt, J.R., Jr., "An Experimental Investigation of the Effect of Several Rocket Plume Simulators on the Pressure Distribution of a Body of Revolution at Freestream Mach Numbers of 0.9 to 1.2.," U.S. Army Missile Command, Redstone Arsenal, Alabama, Report No. RD-TR-70-23, September 1970.
16. Rubin, D.V., "A Transonic Investigation of Jet Plume Effects on Base and Afterbody Pressures of Boattail and Flared Bodies of Revolution," U.S. Army Missile Command, Redstone Arsenal, Alabama, Report No. RD-TR-70-10, October 1970.
17. Craft, J.C., and C.E. Brazzel, "An Experimental Investigation of Base Pressure on a Body of Revolution at High Thrust Levels and Freestream Mach Numbers of 1.5 to 2.87," U.S. Army Missile Command, Redstone Arsenal, Alabama, Report No. RD-TM-70-6, July 1970.
18. Henderson, J.H., "Results of Transonic Wind Tunnel Investigations to Determine the Effects of Nozzle Geometry and Jet Plume on the Aerodynamics of a Body of Revolution," U.S. Army Missile Command, Redstone Arsenal, Alabama, Report No. TR-RD-72-17, November 1972.
19. Martin, T.A. and R.A. Deep, "Aerodynamic Testing on a High-Speed Test Track," Presented at AIAA 16th Aerospace Sciences Meeting, U.S. Army Missile Command, Redstone Arsenal, Alabama, 16-18 January 1978.
20. Martin, T.A., "Investigation of Plume Induced Separation on a Full-Sized Missile at Supersonic Velocities," U.S. Army Missile Command, Redstone Arsenal, Alabama, Technical Report RD-80-12, 20 June 1980.
21. Johannesen, N.H. and R.E. Meyer, "Axially-Symmetrical Supersonic Flow Near the Centre of an Expansion," The Aeronautical Quarterly, Vol. 2, 1950, pp. 127-142.
22. Addy, A.L., "Analysis of the Axisymmetric Base Pressure and Base Temperature Problem with Supersonic Interacting Freestream Nozzle Flows Based on the Flow Model of korst, et al., Part III: A Computer Program and Representative Results for Cylindrical, Boattailed, or Flared Afterbodies," U.S. Army Missile Command, Redstone Arsenal, Alabama, Report No. RD-TR-69-14, February 1970.

REFERENCES (Continued)

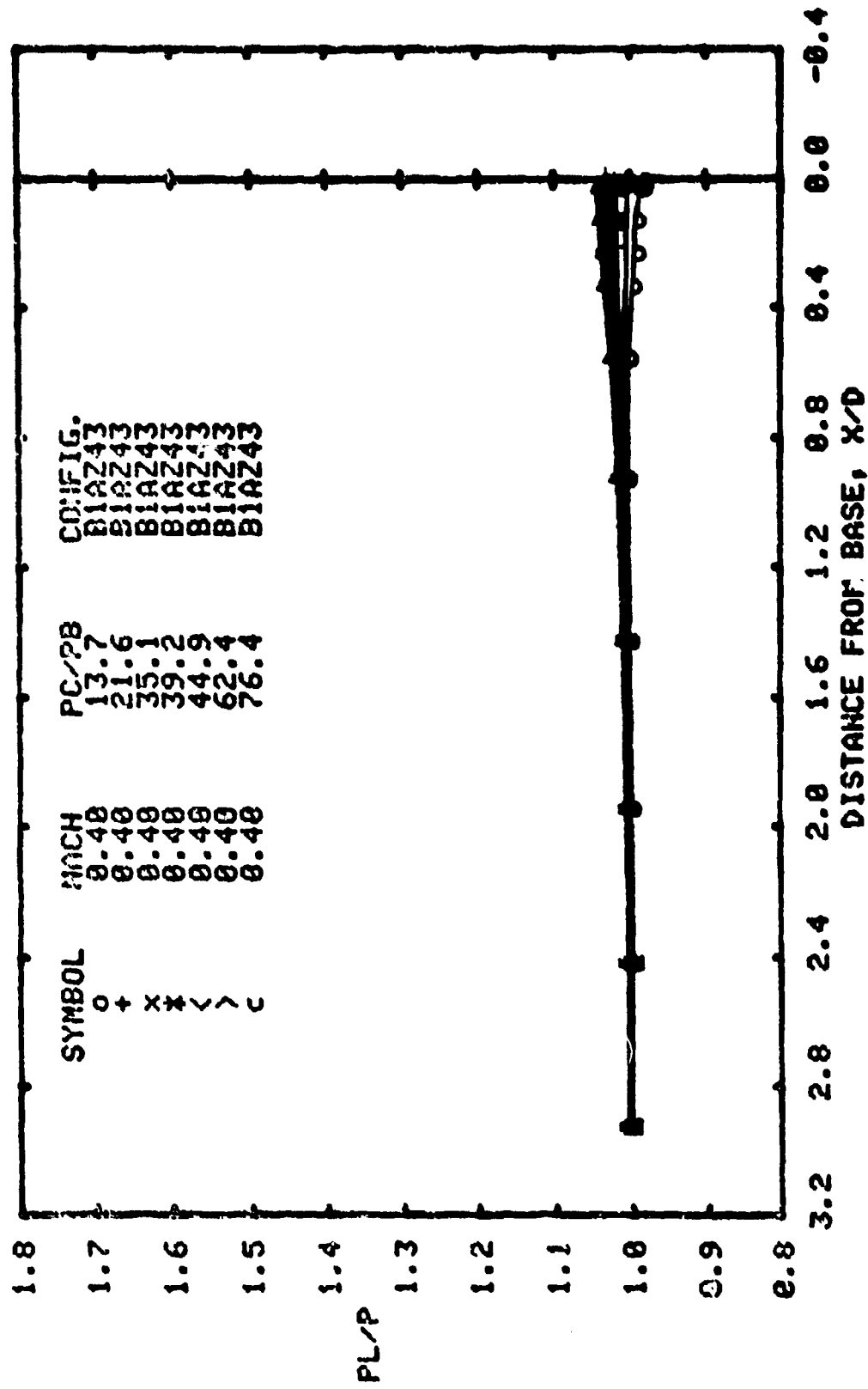
23. Nyberg, W.E. and J. Agrell, "Investigation of Modeling Concepts for Plume-Afterbody Flow Interactions," European Research Office, U.S. Army, London, England, Final Report, FFA Technical Note AU-138A, November 1981.
24. Korst, H.H. and R.A. White, "Internal and External Ballistics of Missiles with Special Consideration of Jet-Plume Interference Effects During Launch and Free Flight Phases," University of Illinois at Urbana-Champaign, Report No. UILU ENG80-4007, Urbana, IL, December 1980.
25. Oswatitsch, K. and W. Rothstein, "Flow Pattern in a Converging-Diverging Nozzle," NACA TN 1215, 1949.
26. Sauer, R., "General Characteristics of the Flow Through Nozzles at Near Critical Speeds," NACA TM 1147, 1947.
27. "8-Foot Transonic Wind Tunnel," Calspan Corporation Transonic Wind Tunnel Report No. WT0-300, Revised September 1973.
28. Langley Research Center, "Manual For Users of the Unitary Plan Wind Tunnel Facilities of the National Advisory Committee for Aeronautics," 1965.
29. Reid, C.F., "Effects of Jet Plumes on Pressure Distributions over a Cylindrical Afterbody at Transonic Speeds," Calspan Report AA-4017-W-15, February 1979.
30. Nenni, J.P., "Analysis of Experiments on the Effects of Jet Plumes on Pressure Distribution over a Cylindrical Afterbody at Supersonic Speeds," Calspan Advanced Technology Center, Aerodynamic Research Department, Buffalo, New York, AROD Project No. 13797-E, January 1980.
31. Brazzel, C., "The Effects of Base Bleed and Sustainer Rocket Nozzle Diameter and Location on The Base Drag of a Body of Revolution with Concentric Boost and Sustainer Rocket Nozzles," U.S. Army Missile Command, Redstone Arsenal, Alabama, Report No. RF-TR-63-23, 15 July 1963.
32. Walker, B.J., and A.L. Addy, "Preliminary Investigation of the Effect on Afterburning on Base Pressure," U.S. Army Missile Command, Redstone Arsenal, Alabama, Report No. RD-TM-71-6, December 1971.
33. Zukoski, E.E., "Turbulent Boundary Layer Separation in Front of a Forward Facing Step," AIAA Journal, Vol. 5, No. 10, October 1967, pp. 1746-1753.

BLANK PAGE

APPENDIX A

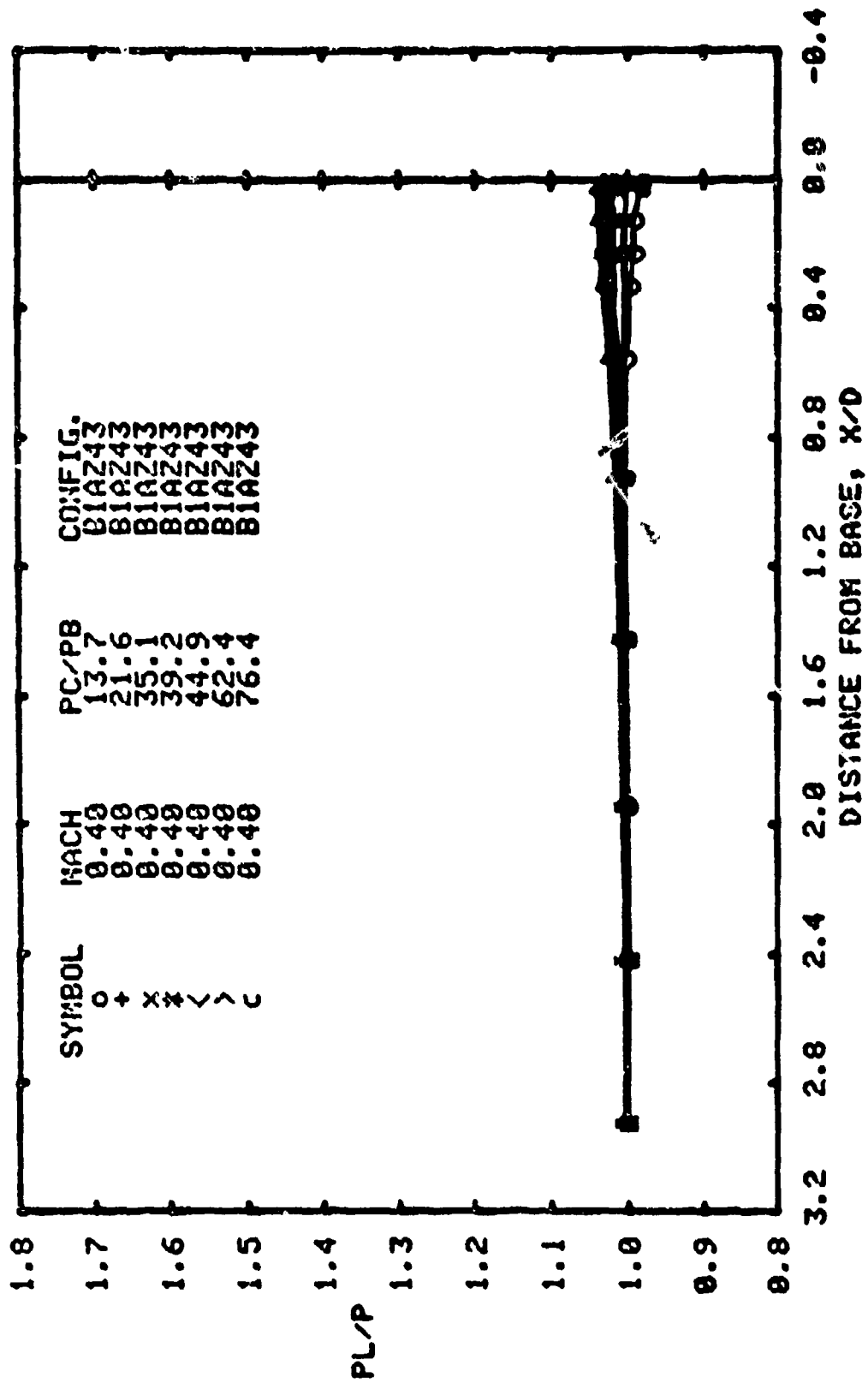
DATA BASE

BLANK PAGE



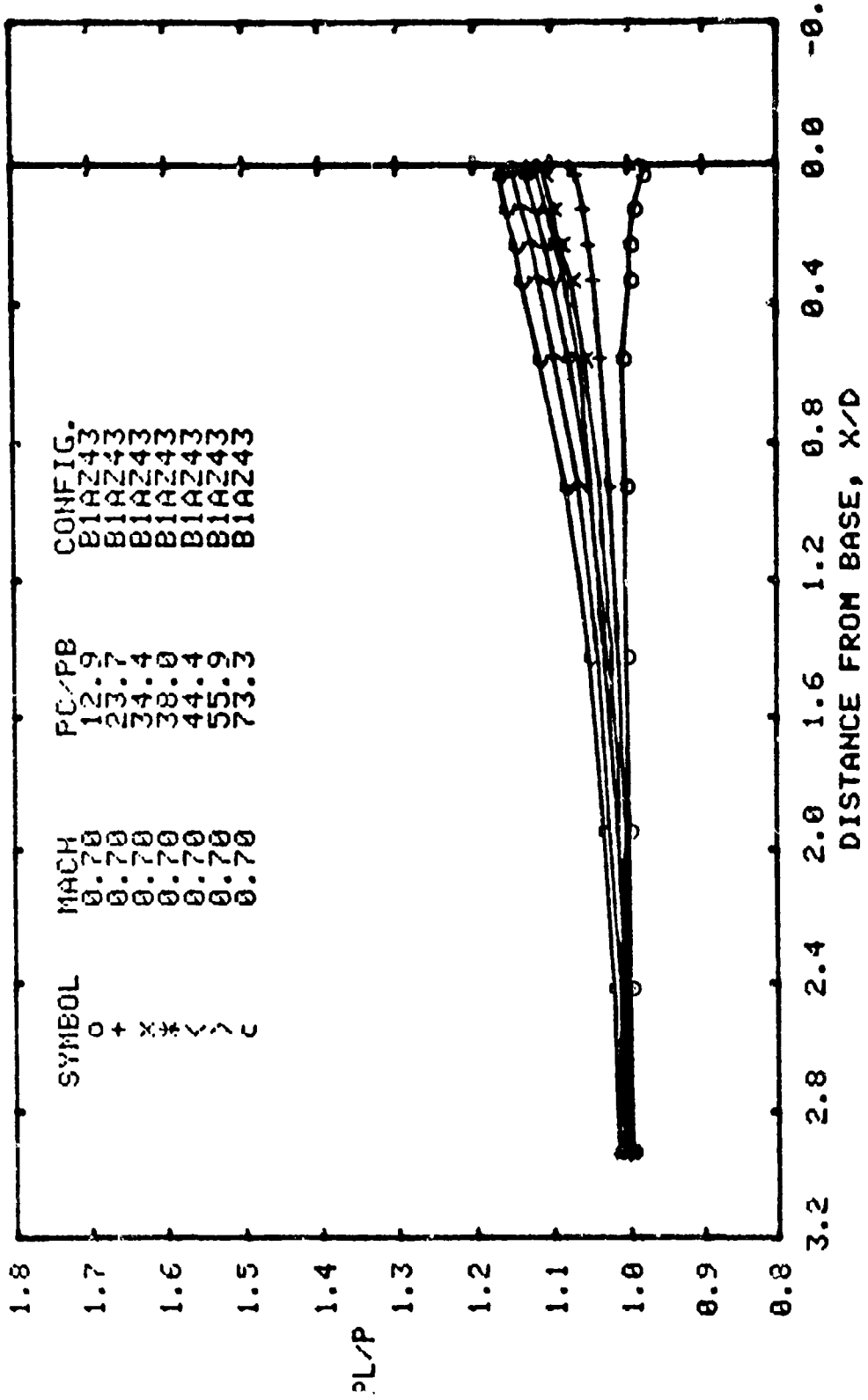
(a). $M=0.4$

Figure A1: Effect of jet total pressure ratio on body pressure distribution at various free stream Mach numbers. Configuration BIAZ43: $M_J=1.7$, $\theta_N=9.1^\circ$, $D_N/D_B=0.8$.

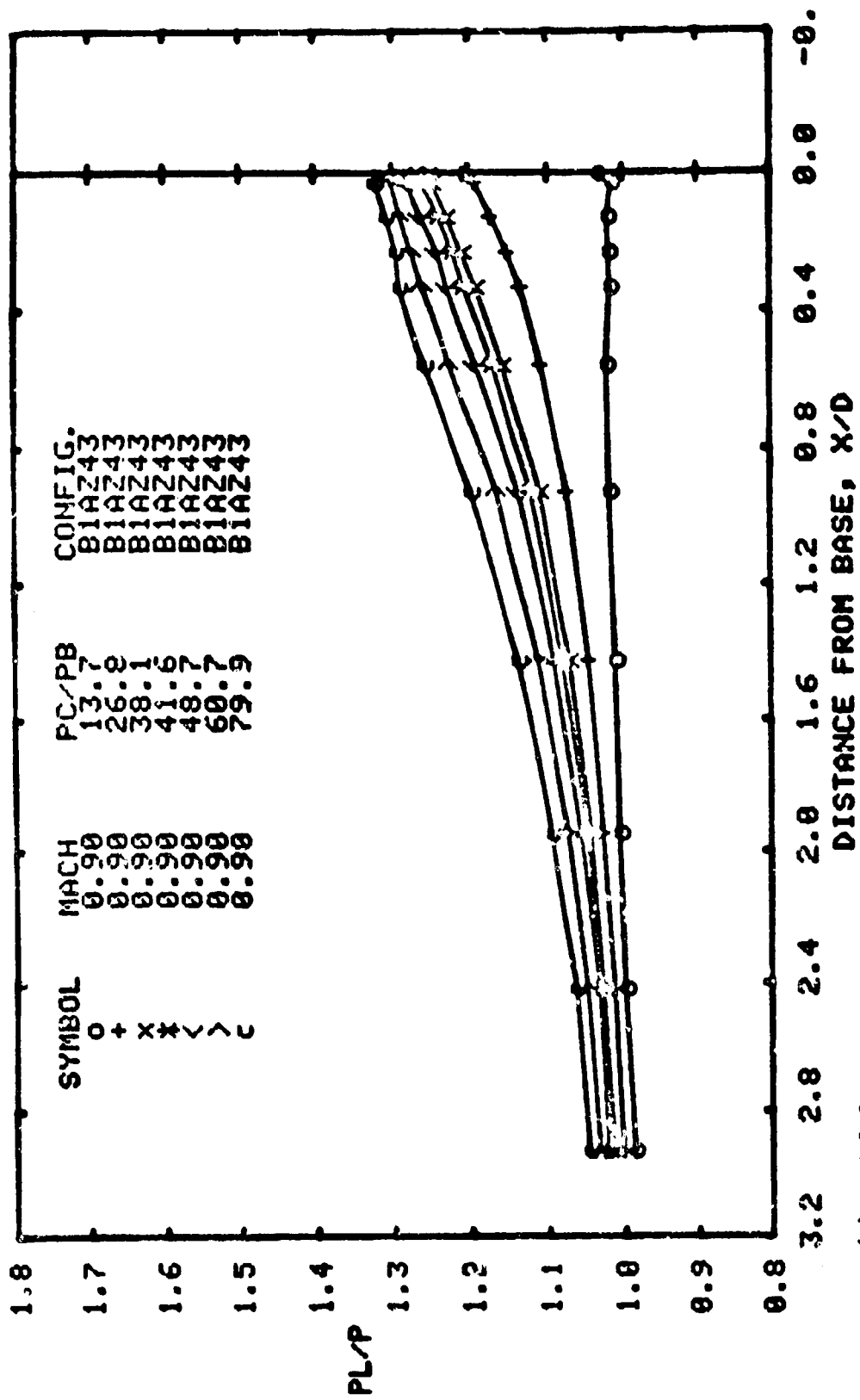


(a). $M=0.40$

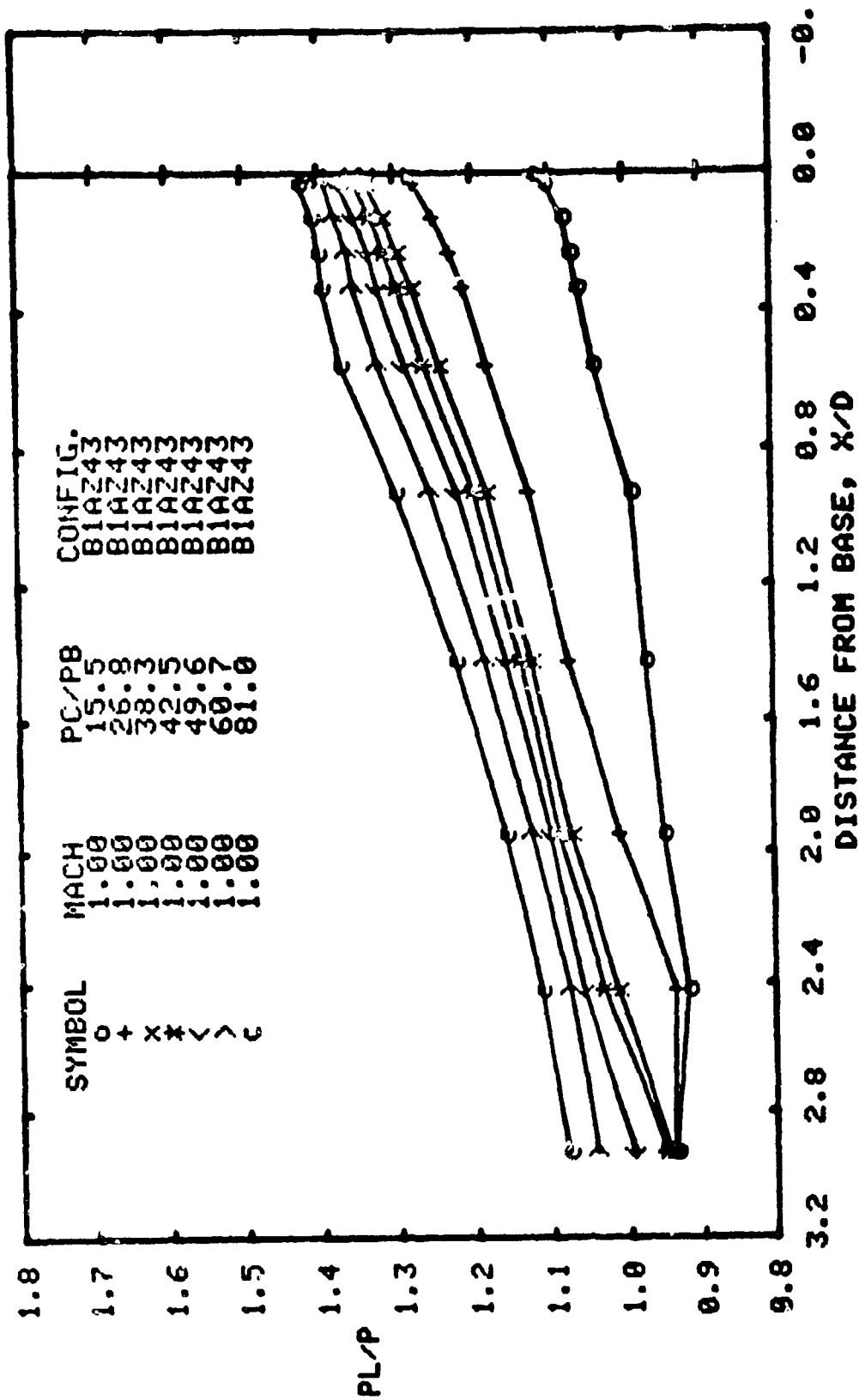
Figure A1: Effect of jet total pressure ratio on body pressure distribution at various free-stream Mach numbers. Configuration BIAZ43: $M_j=1.7$, $\theta_i=9.1^\circ$, $D_N/D_B=0.80$.



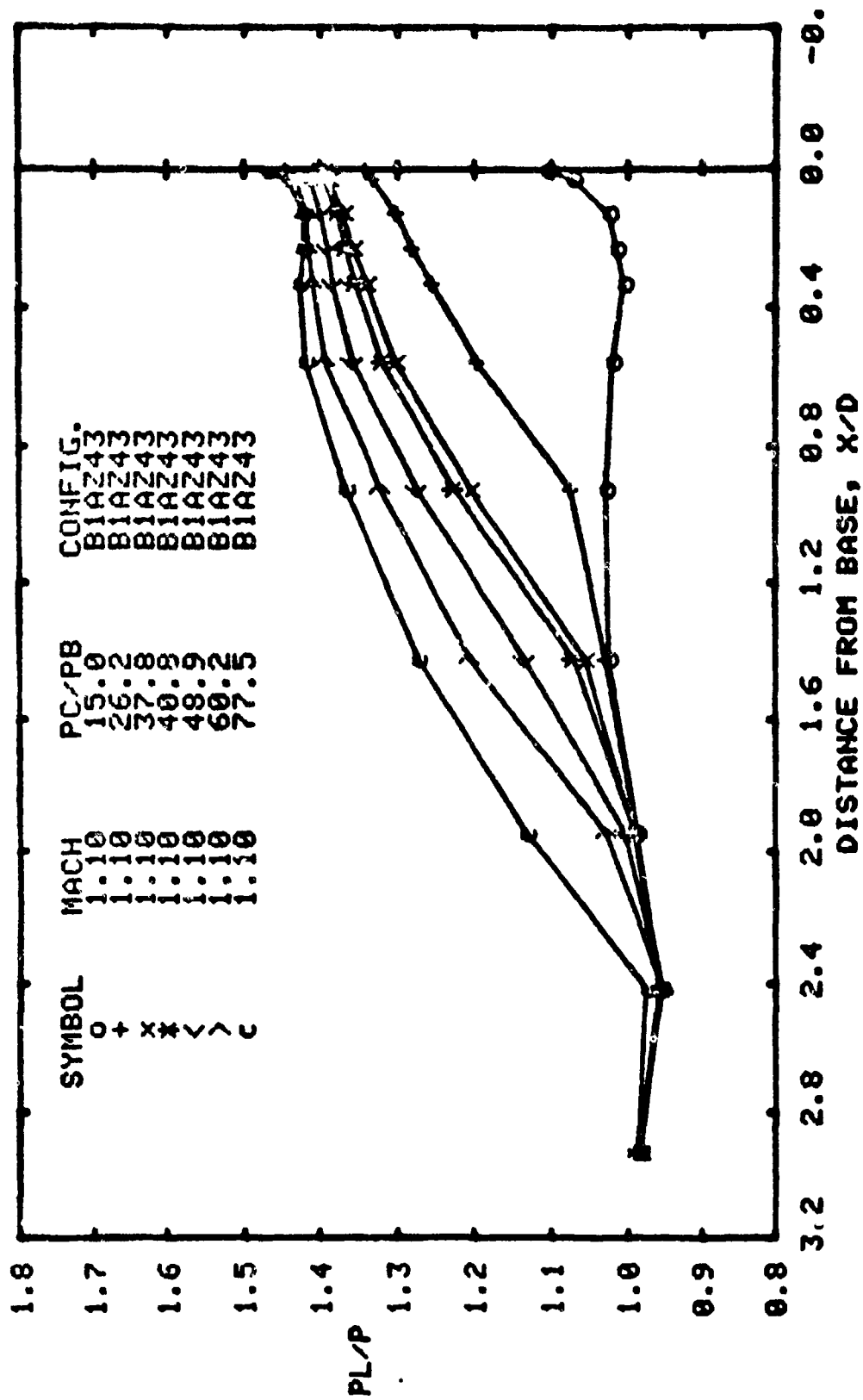
(b). M=0.7
figure A1: cont'd



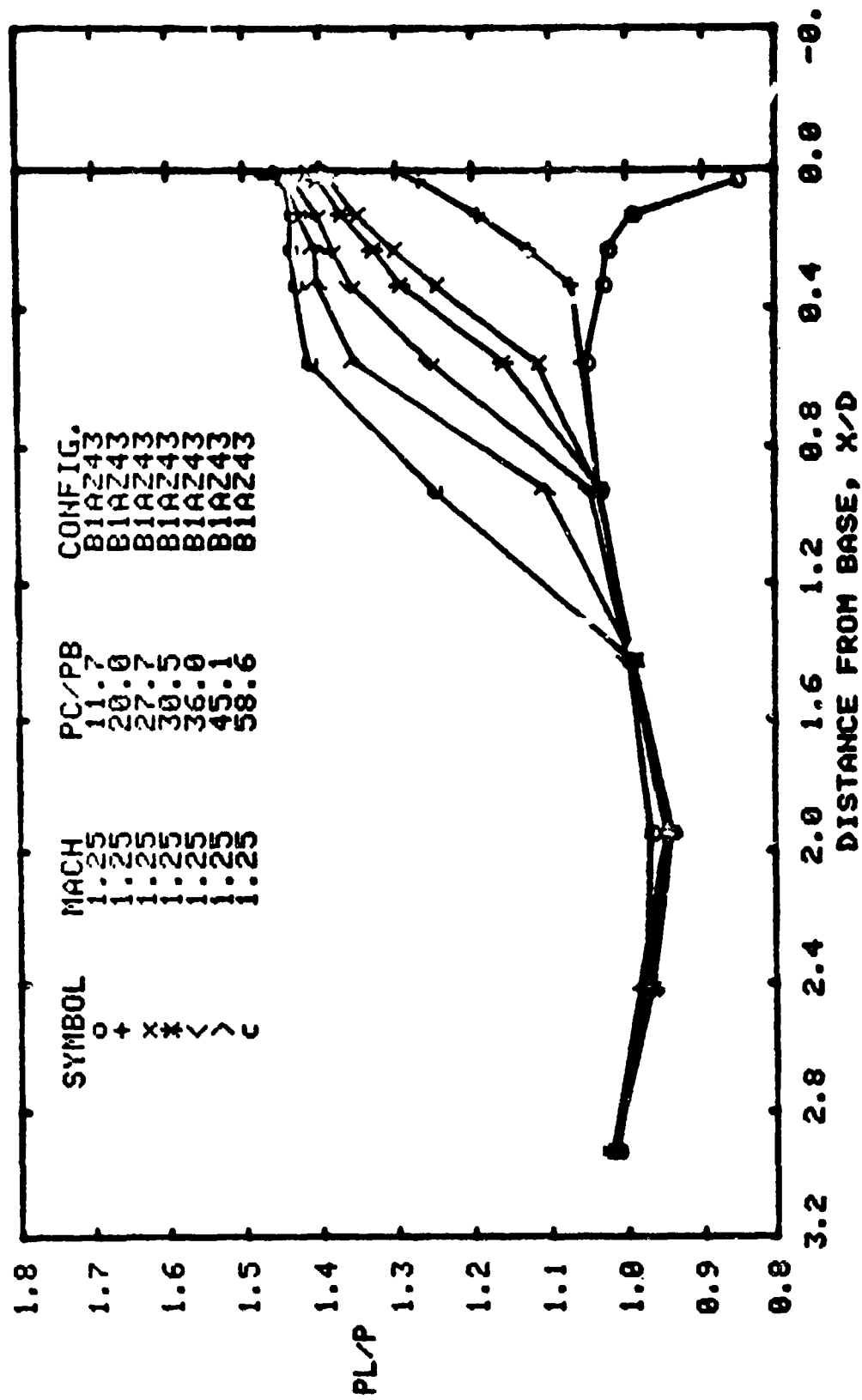
(c). M=0.9
Figure A1: cont'd



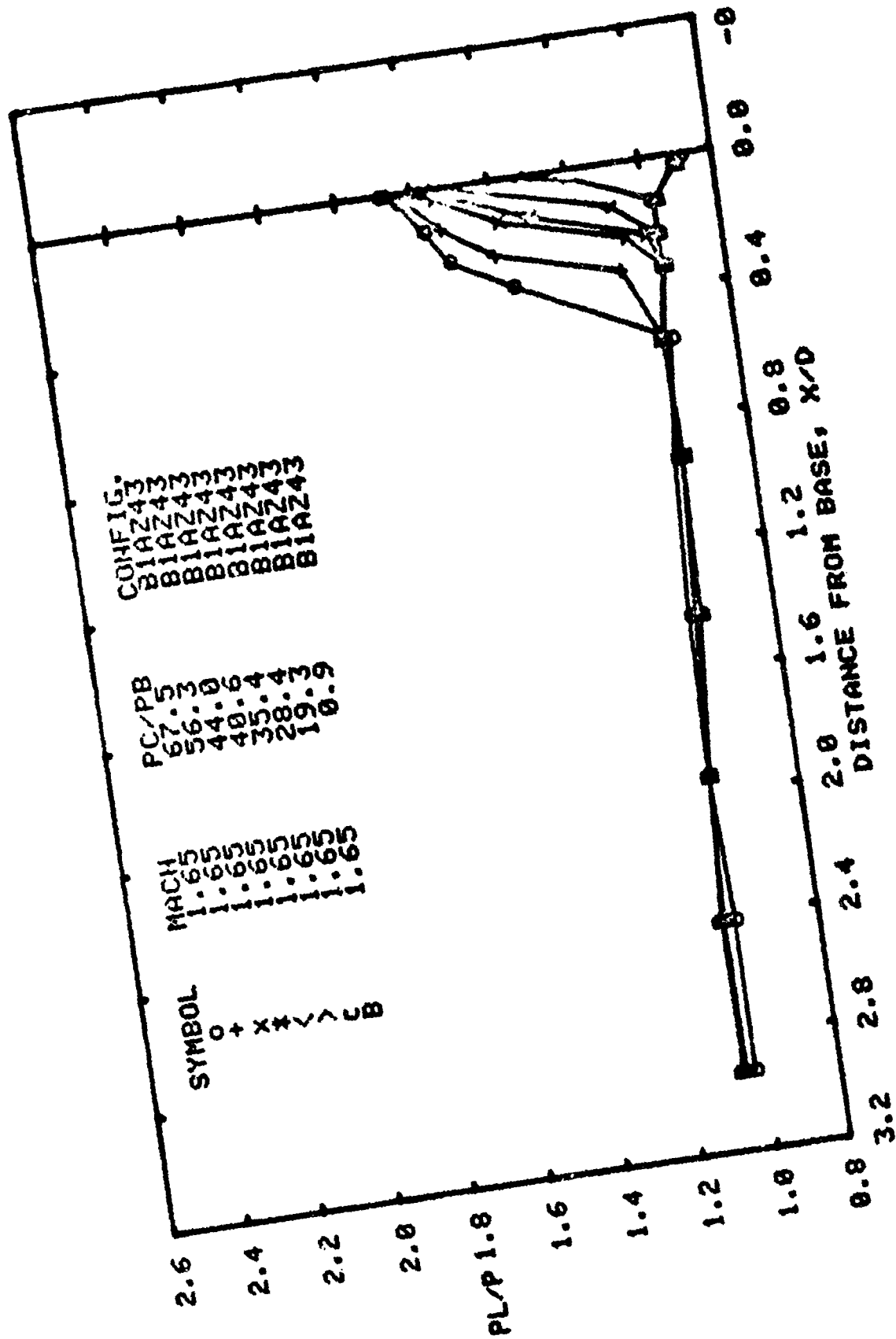
(d). M=1.0
Figure A1: cont'd



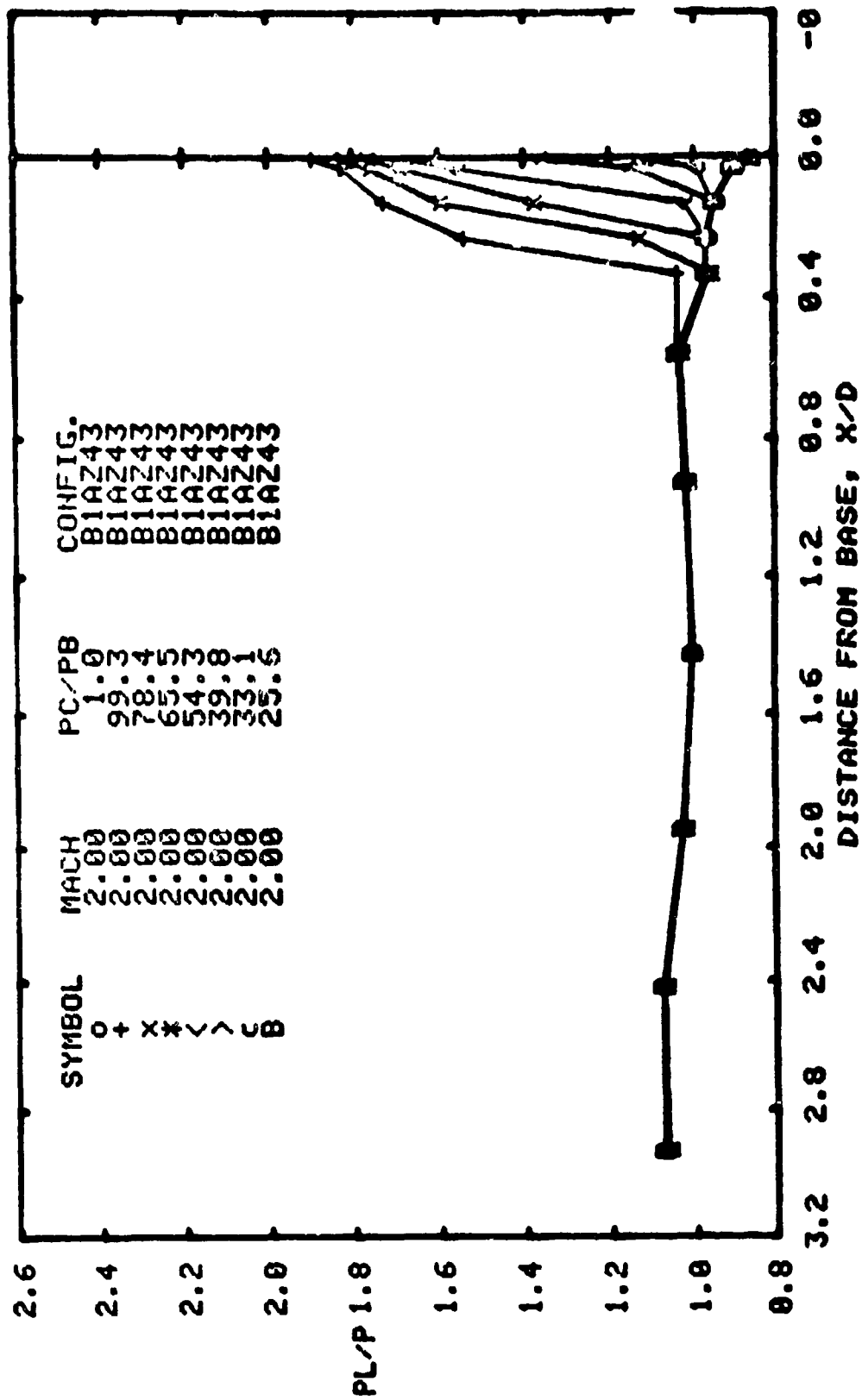
(e). M=1.1
Figure A1: cont'd



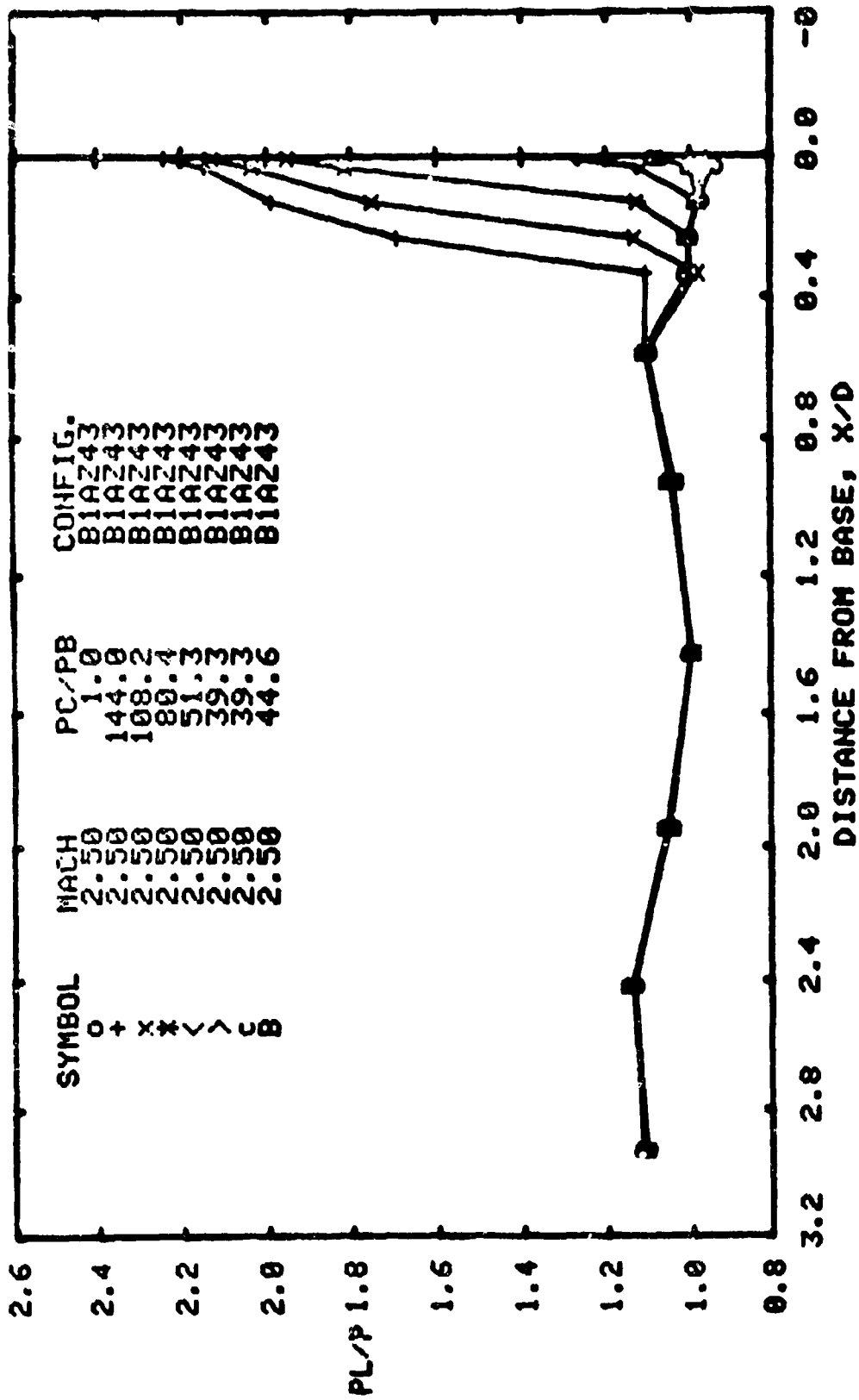
(f). M=1.25
Figure A1: cont'd



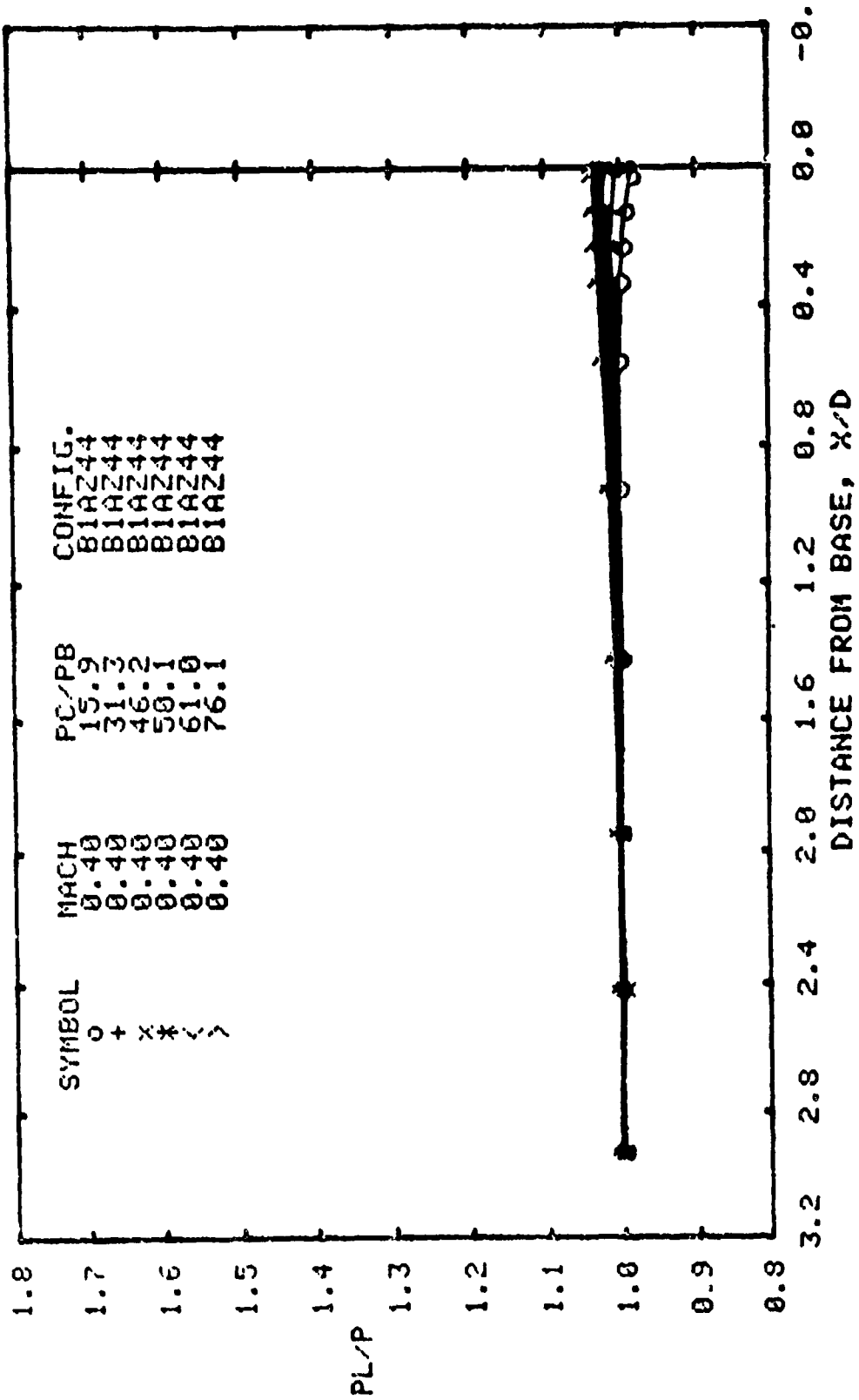
(g). M=1.65
Figure A1: cont'd



(h). $M=2.0$
Figure A1: cont'd

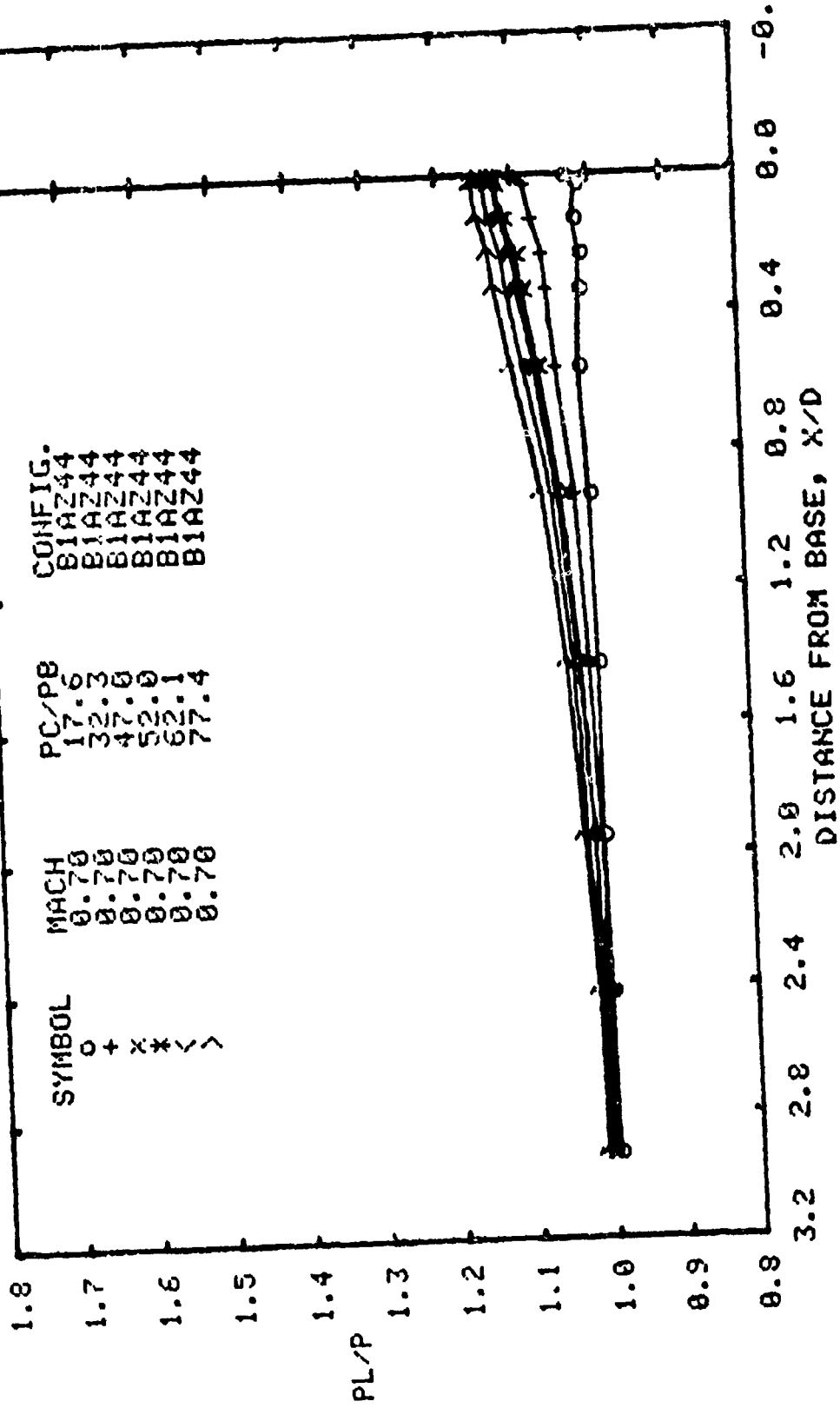


(1). M=2.5
Figure A1: concl'd.

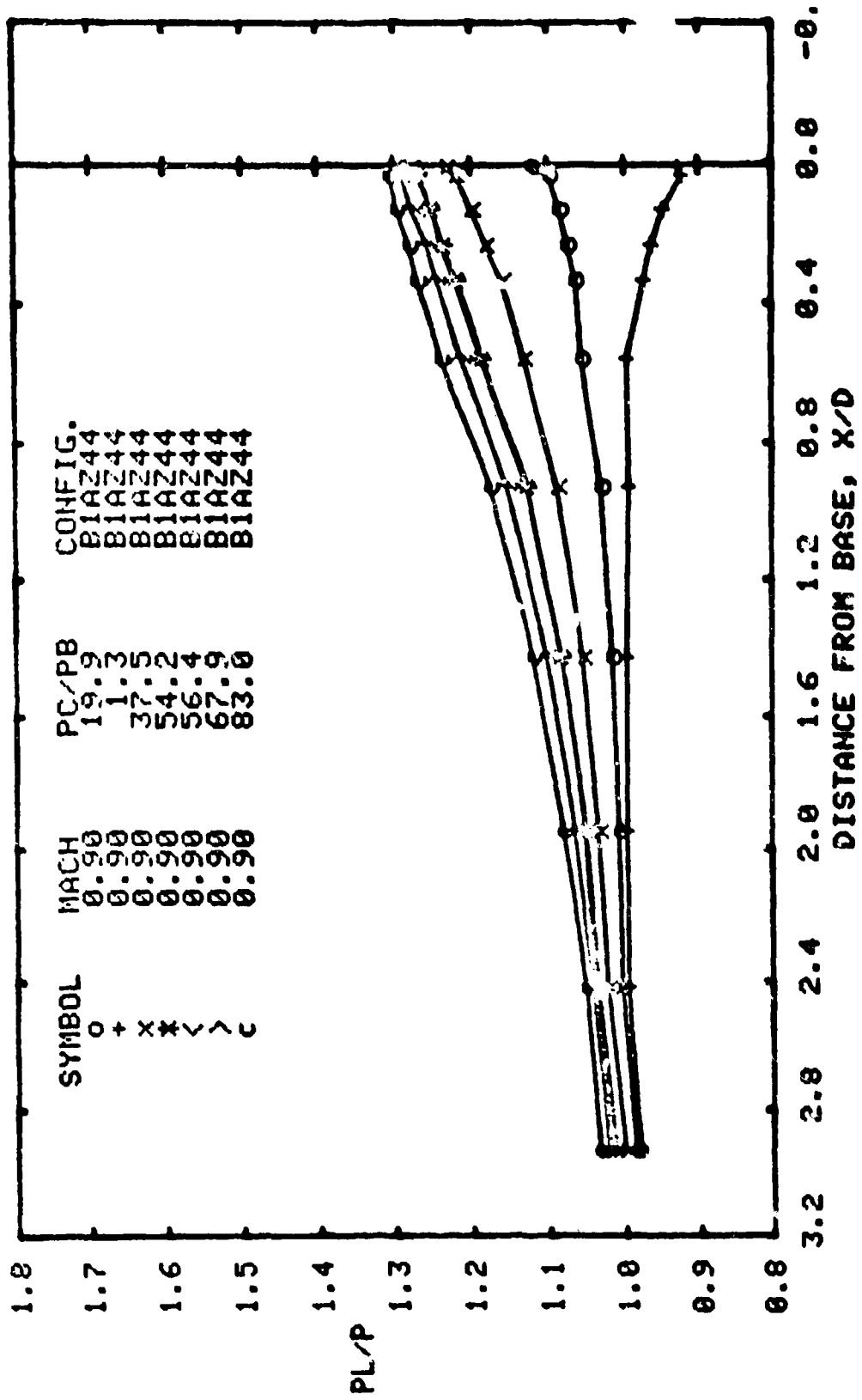


(a). M=0.4

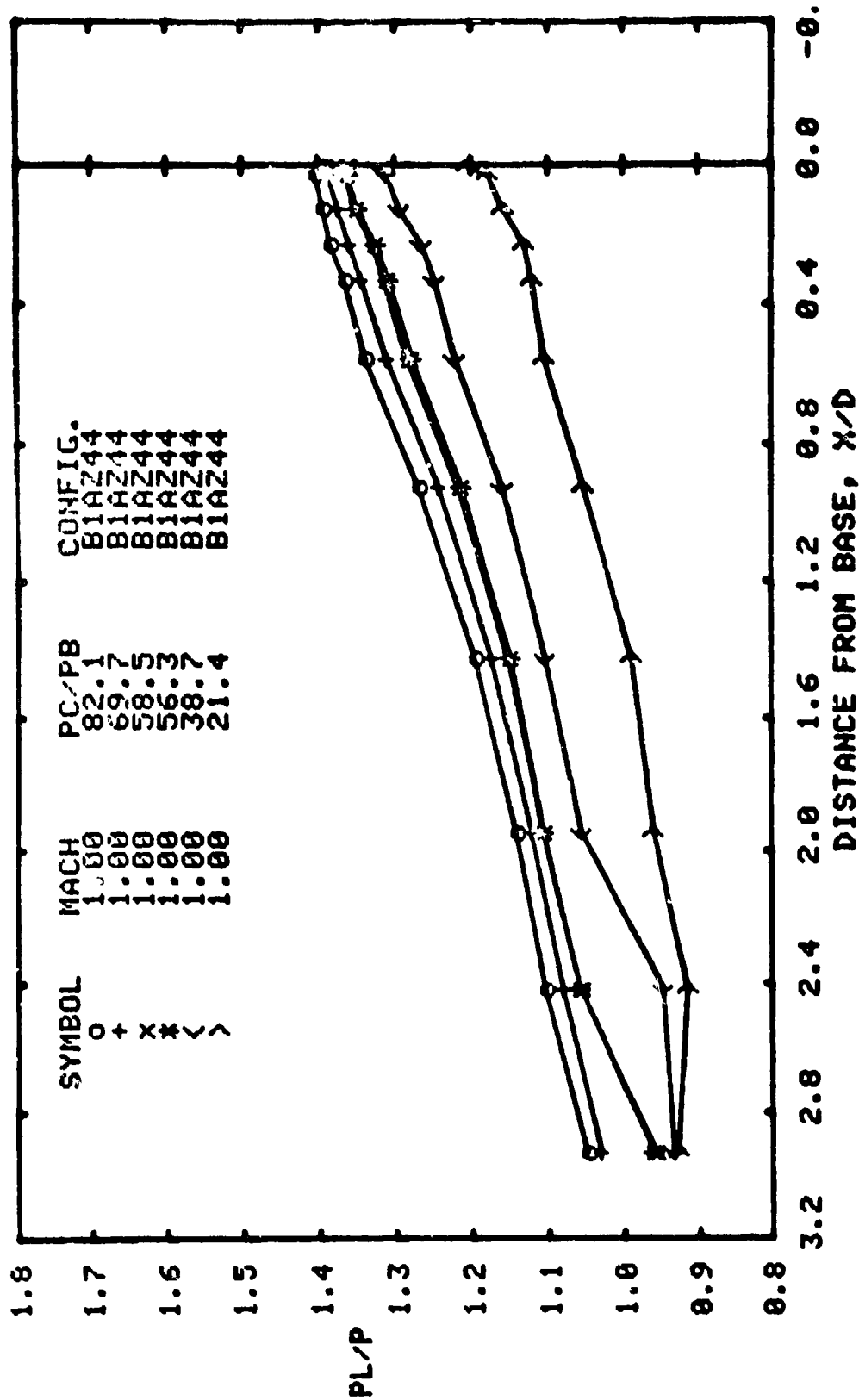
Figure A2: Effect of jet total pressure ratio on body pressure distribution at various free-stream Mach numbers. Configuration BIAZ44: $M_j=2.0$, $\theta=13.6$, $D_N/D_B=0.8$



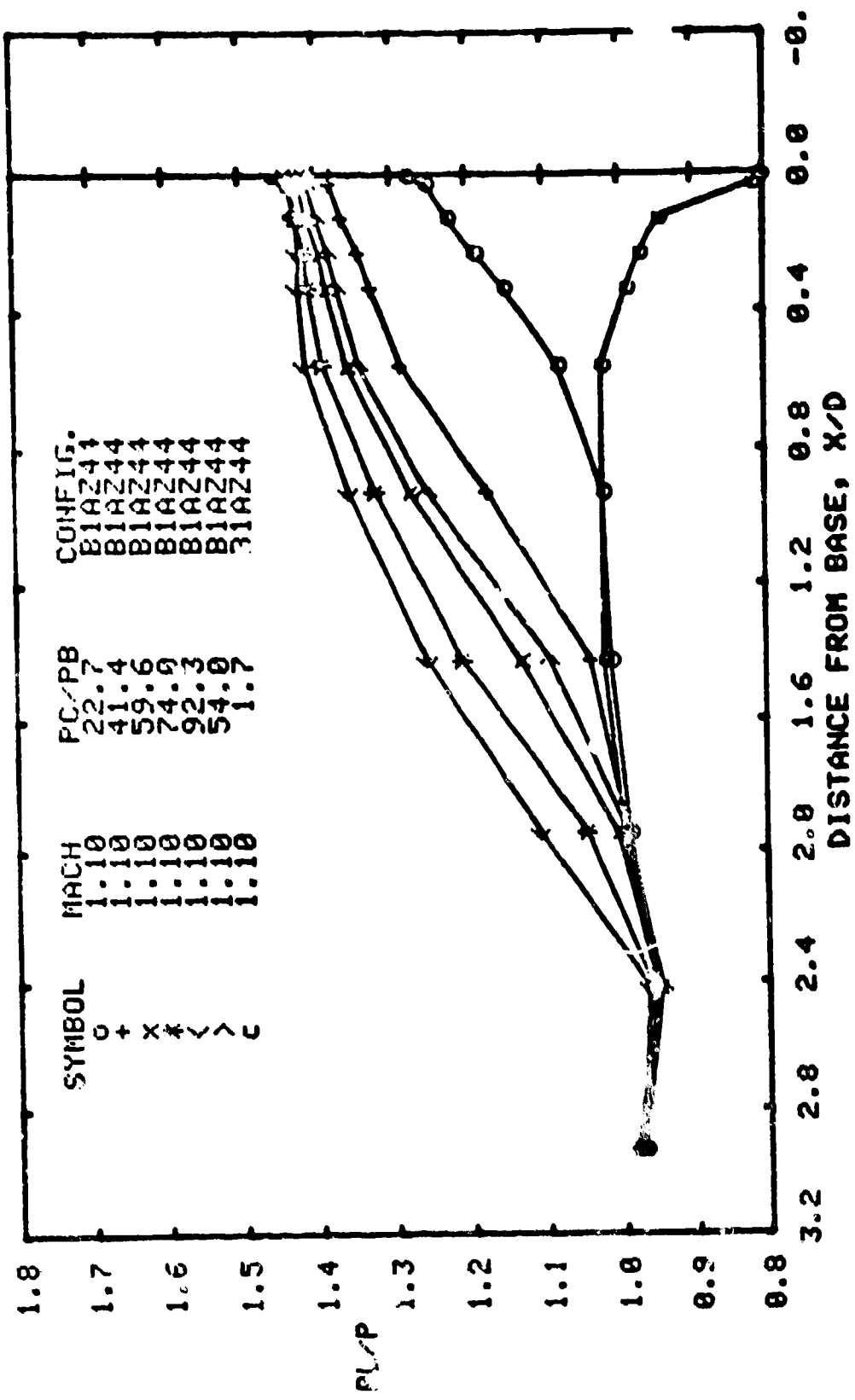
(b). M=0.7
Figure A2: cont'd



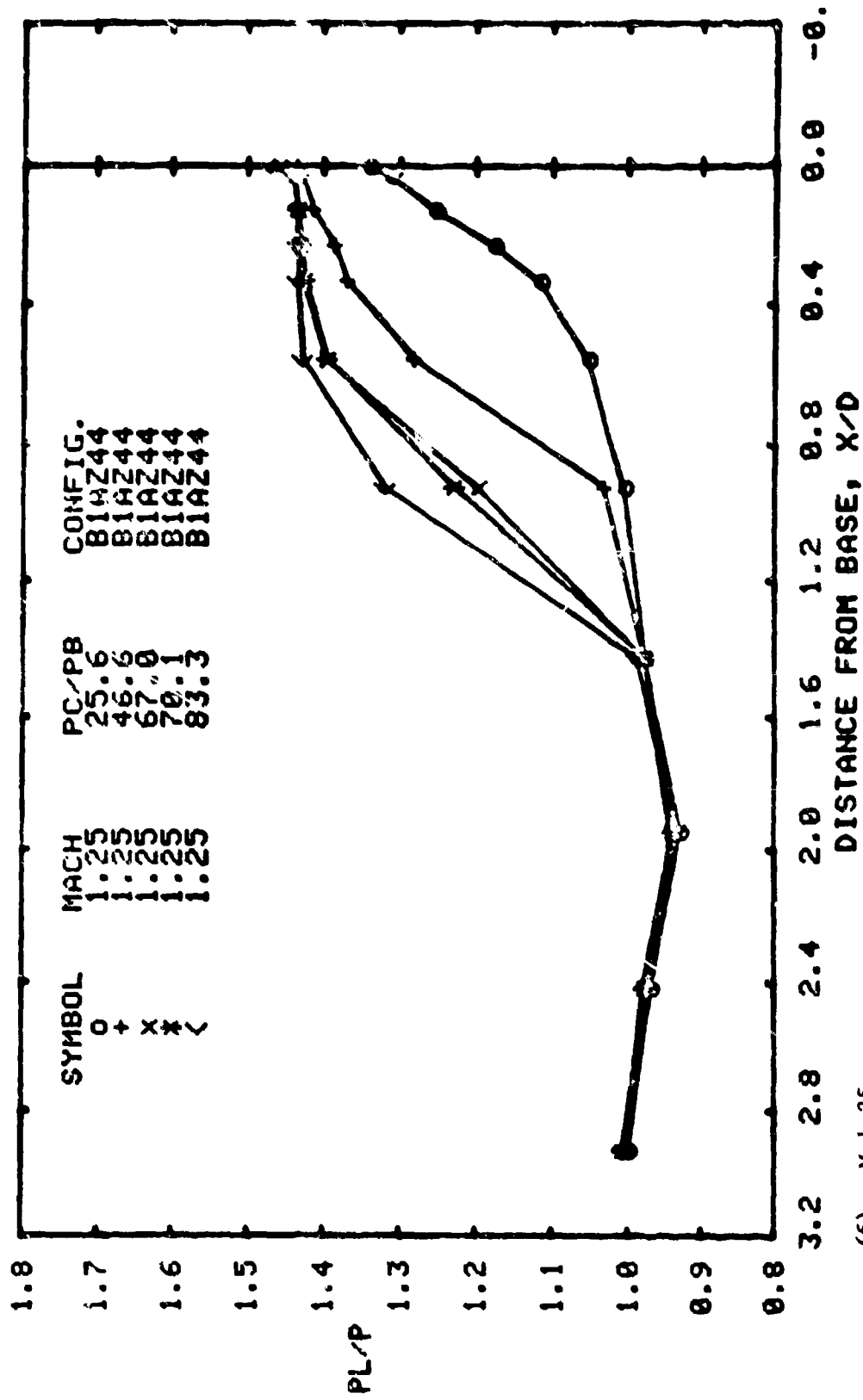
(c). M=0.9
Figure A2: cont'd



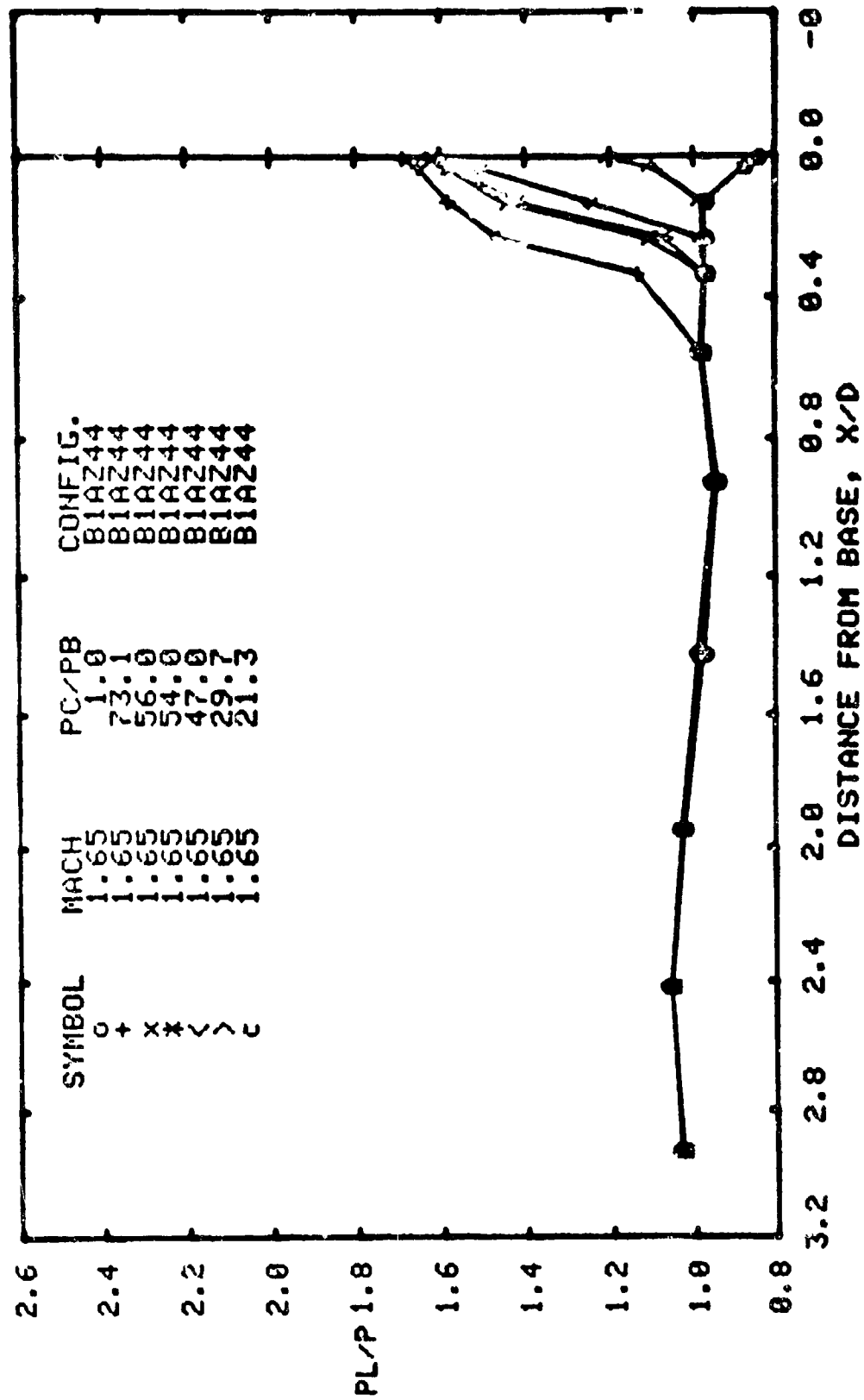
(d). M=1.0
Figure A2: cont'd



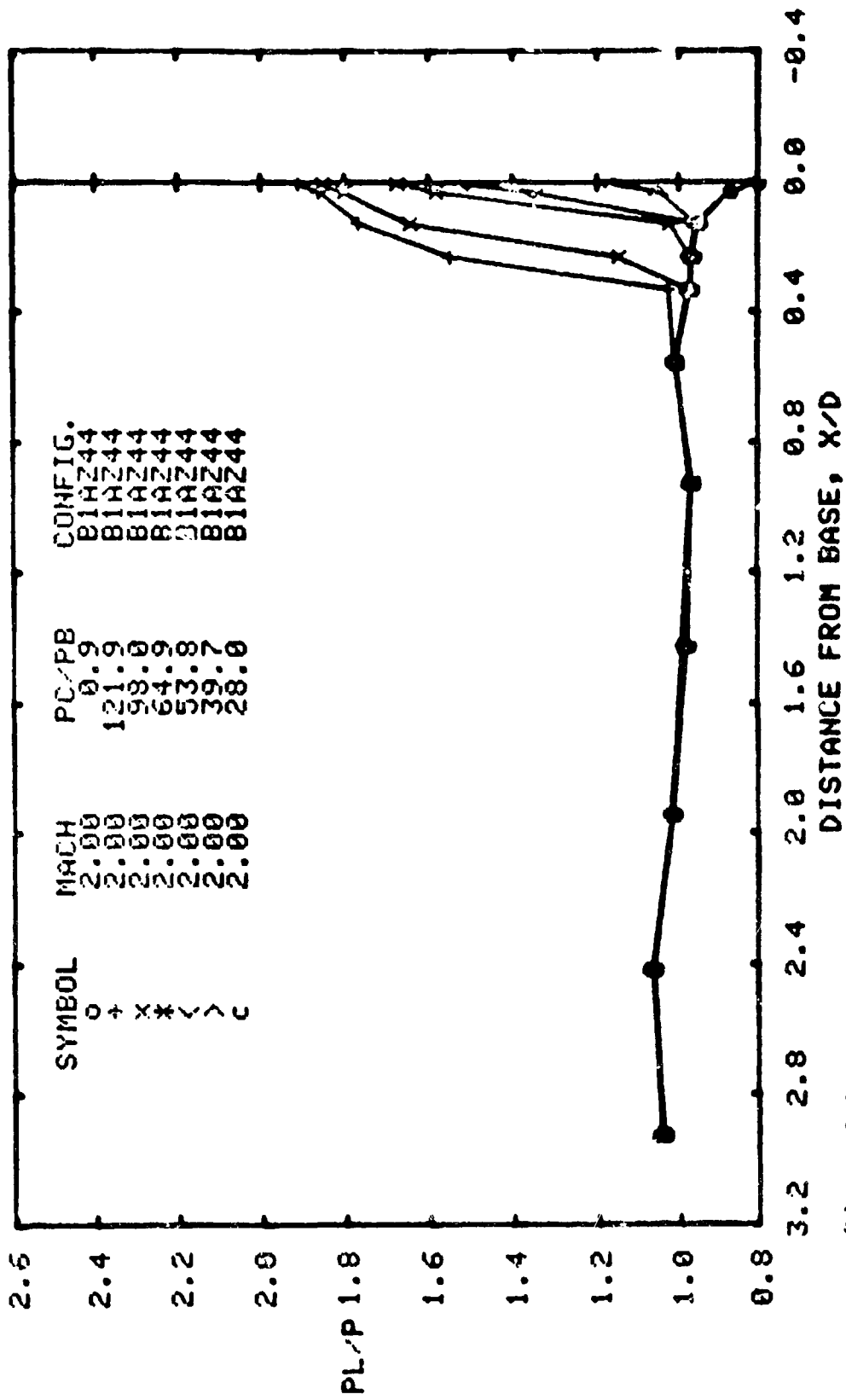
(e). M=1.1
Figure A2: cont'd



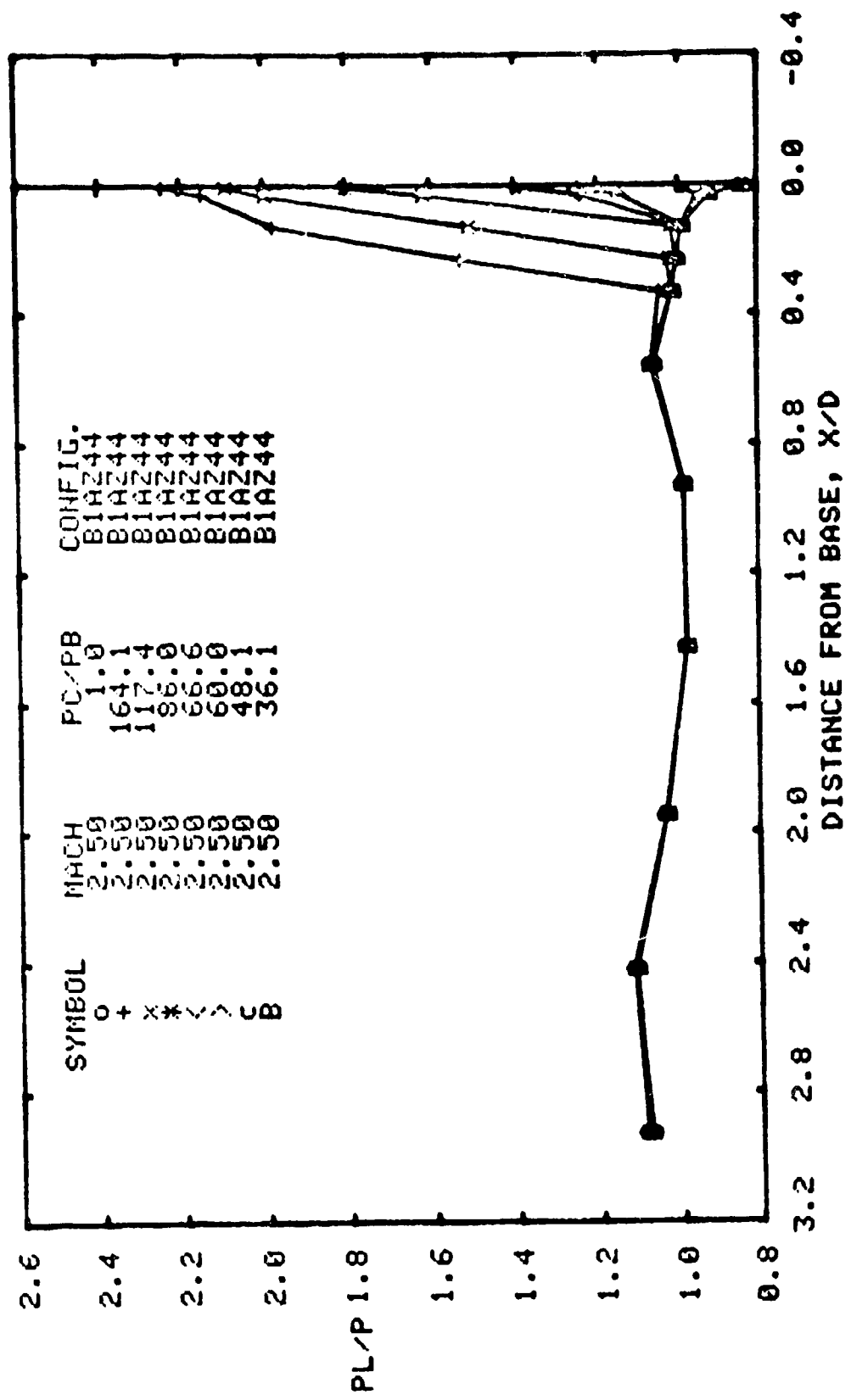
(F). M=1.25
Figure A2: cont'd



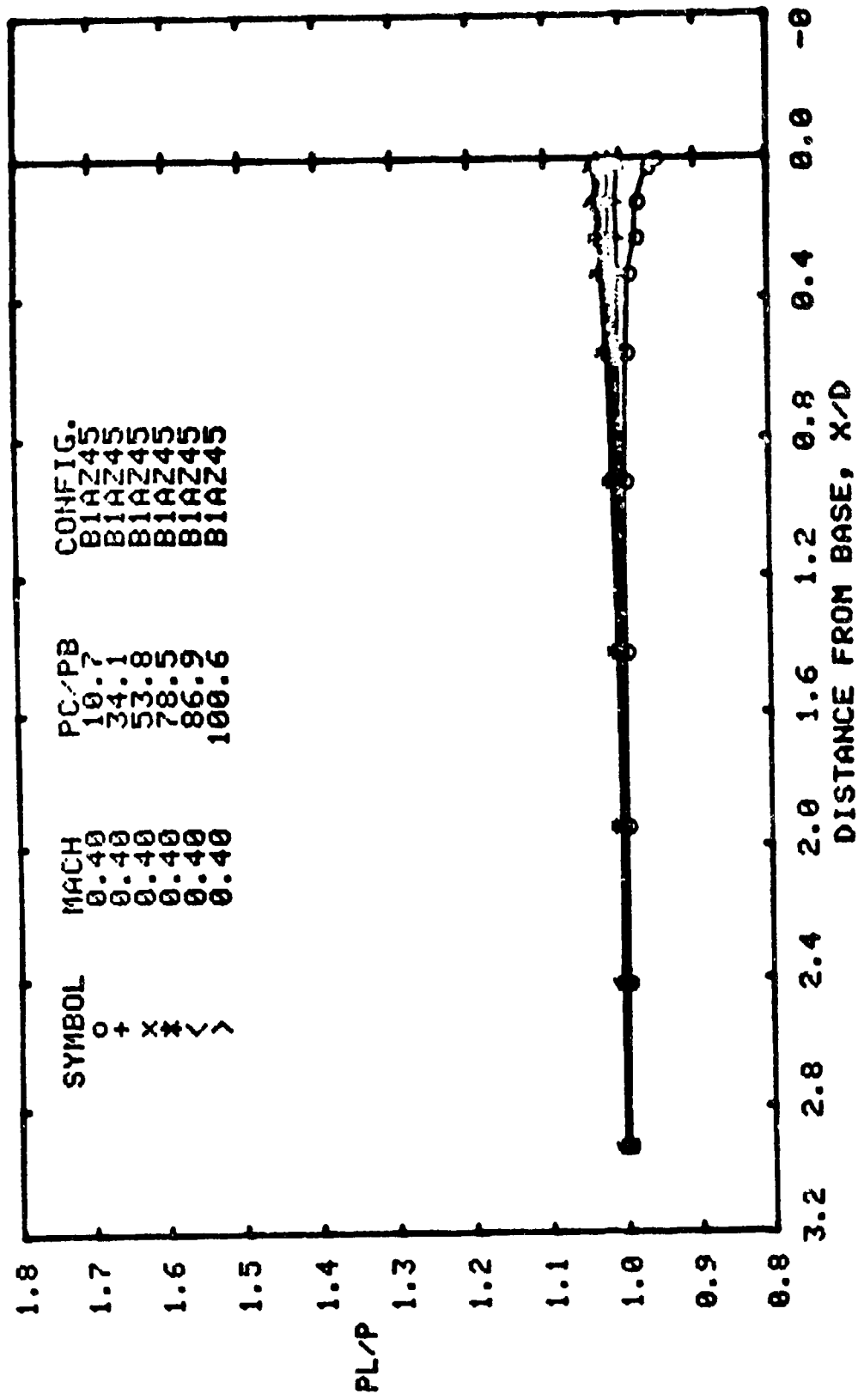
(g). M=1.65
Figure A2: cont'd



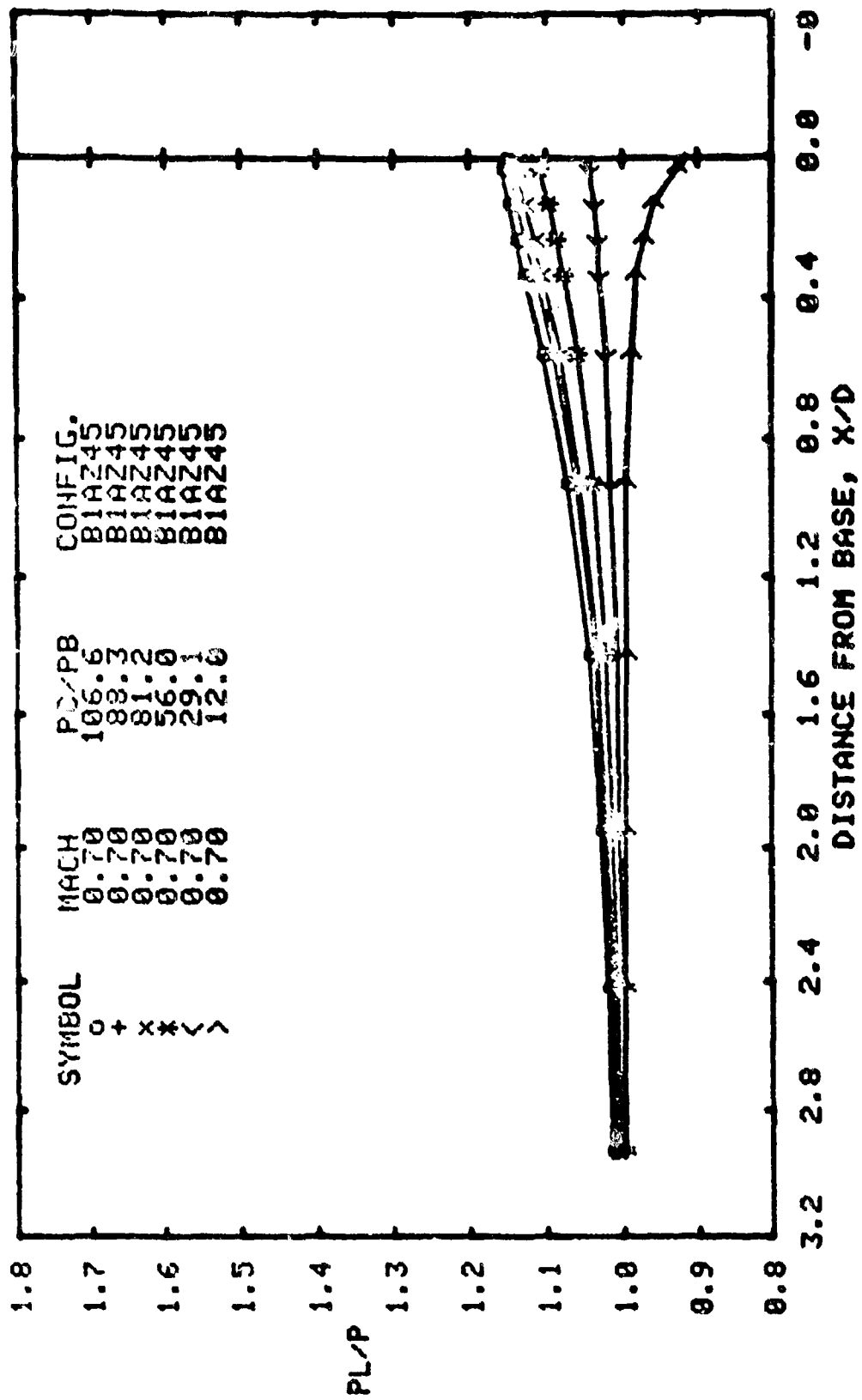
(h). M=2.0
Figure A2: cont'd



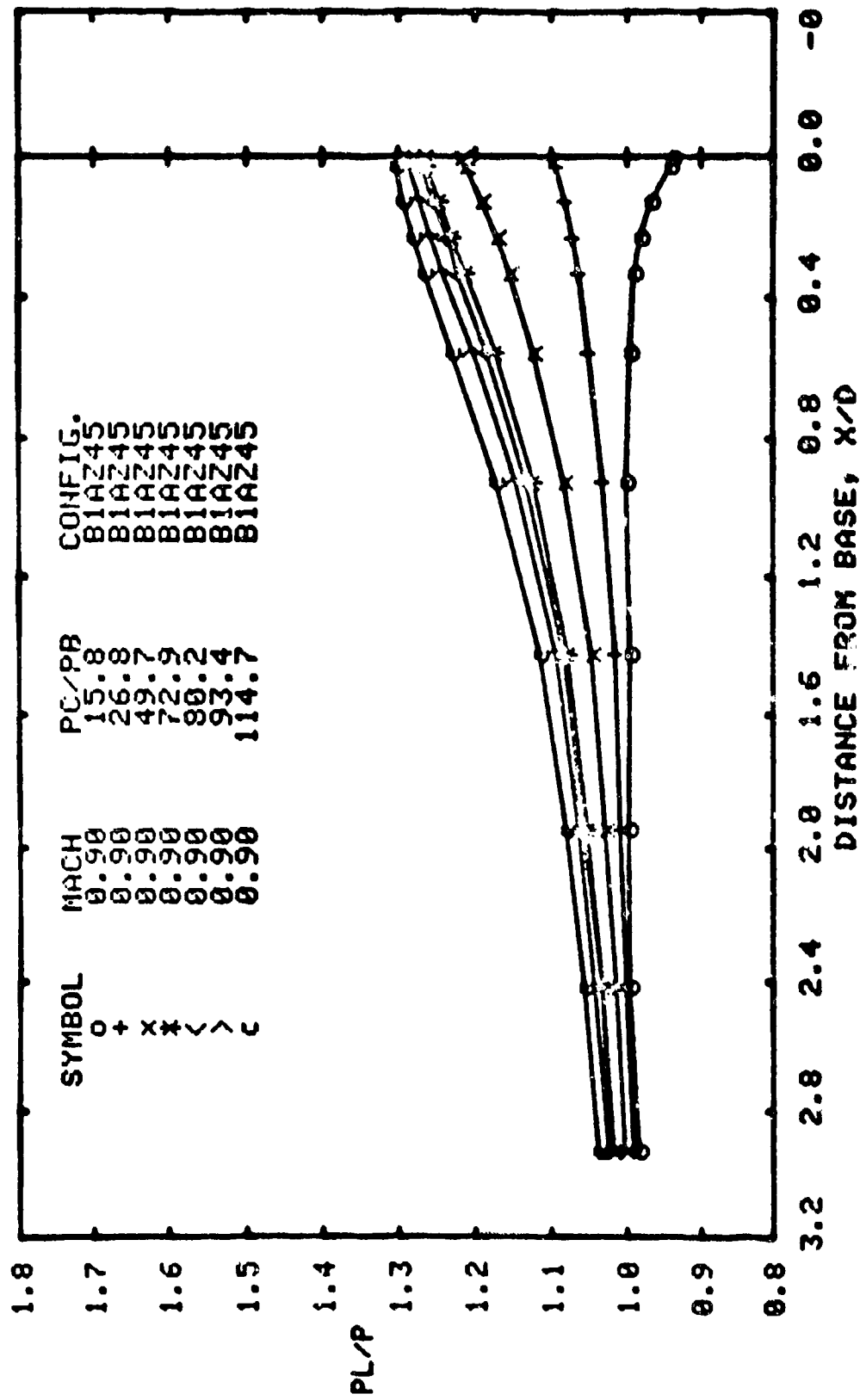
(1). M=2.5
Figure A2: concl'd.



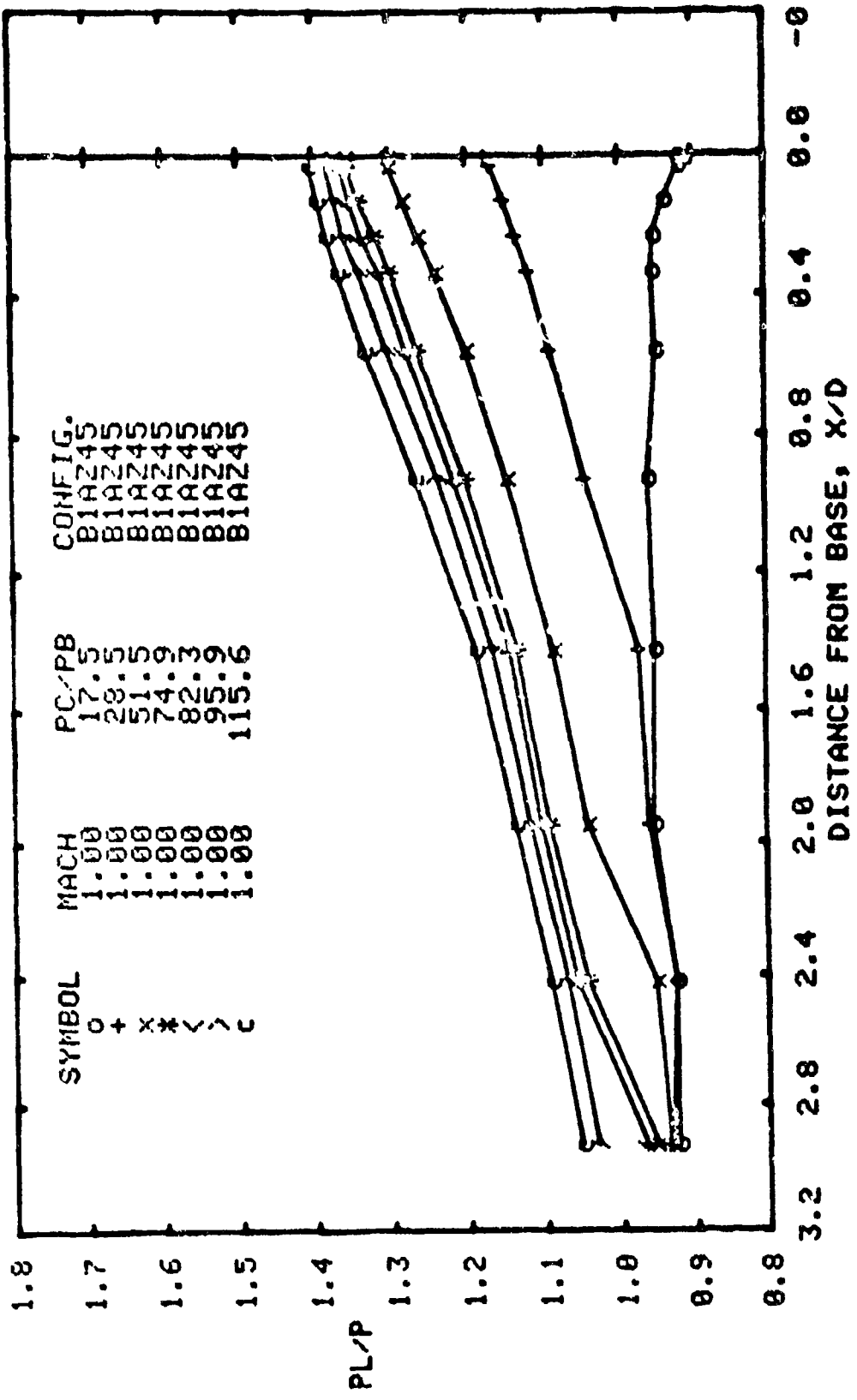
(J). M=0.4
 Figure A3: Effect of jet total pressure ratio on body pressure distribution at various free stream Mach numbers. Configuration BIAZ45: $M_j=2.4$, $\theta_n=19.35$, $D_n/D_B=0.8$.



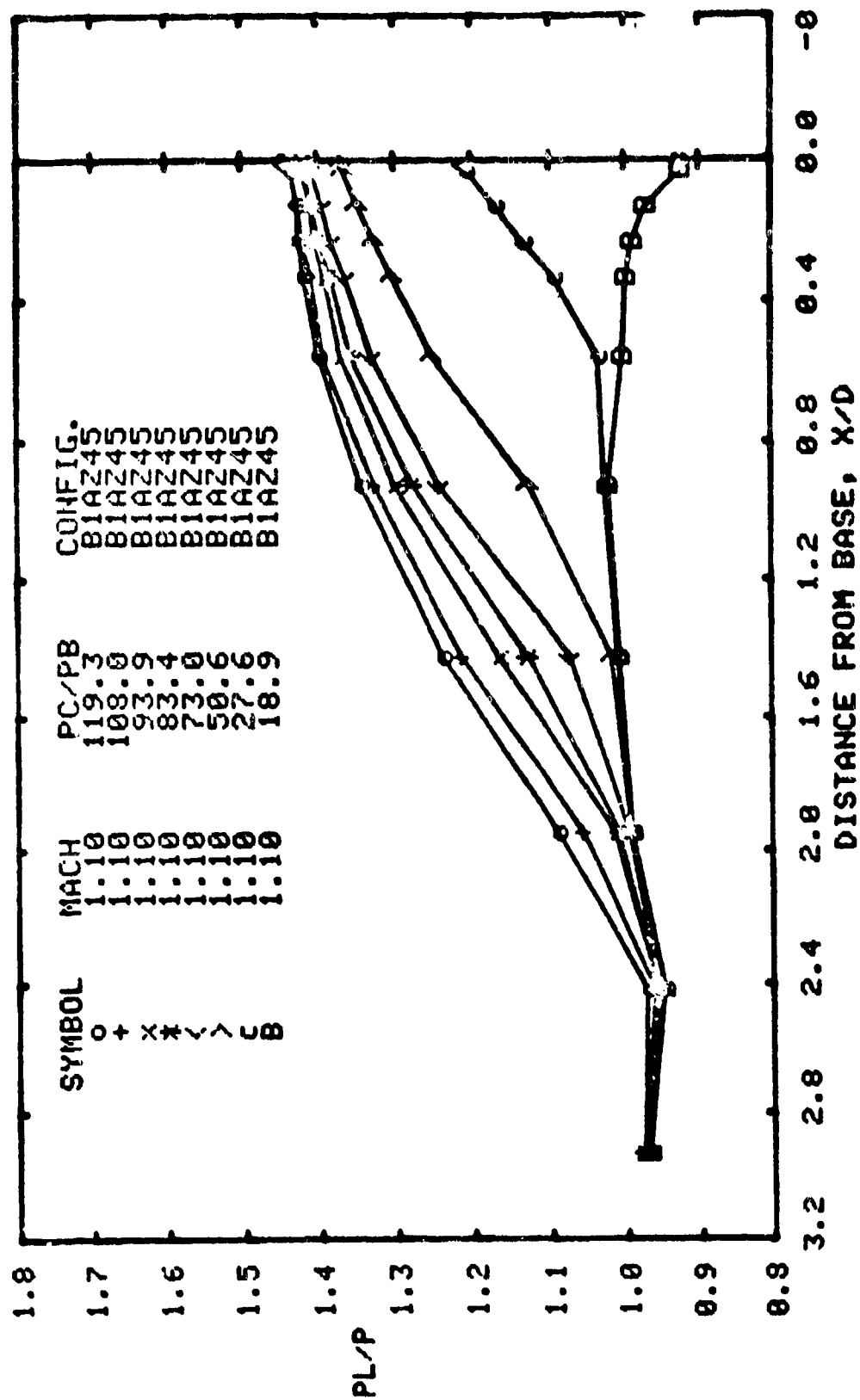
(b). M=0.7
Figure A3: cont'd



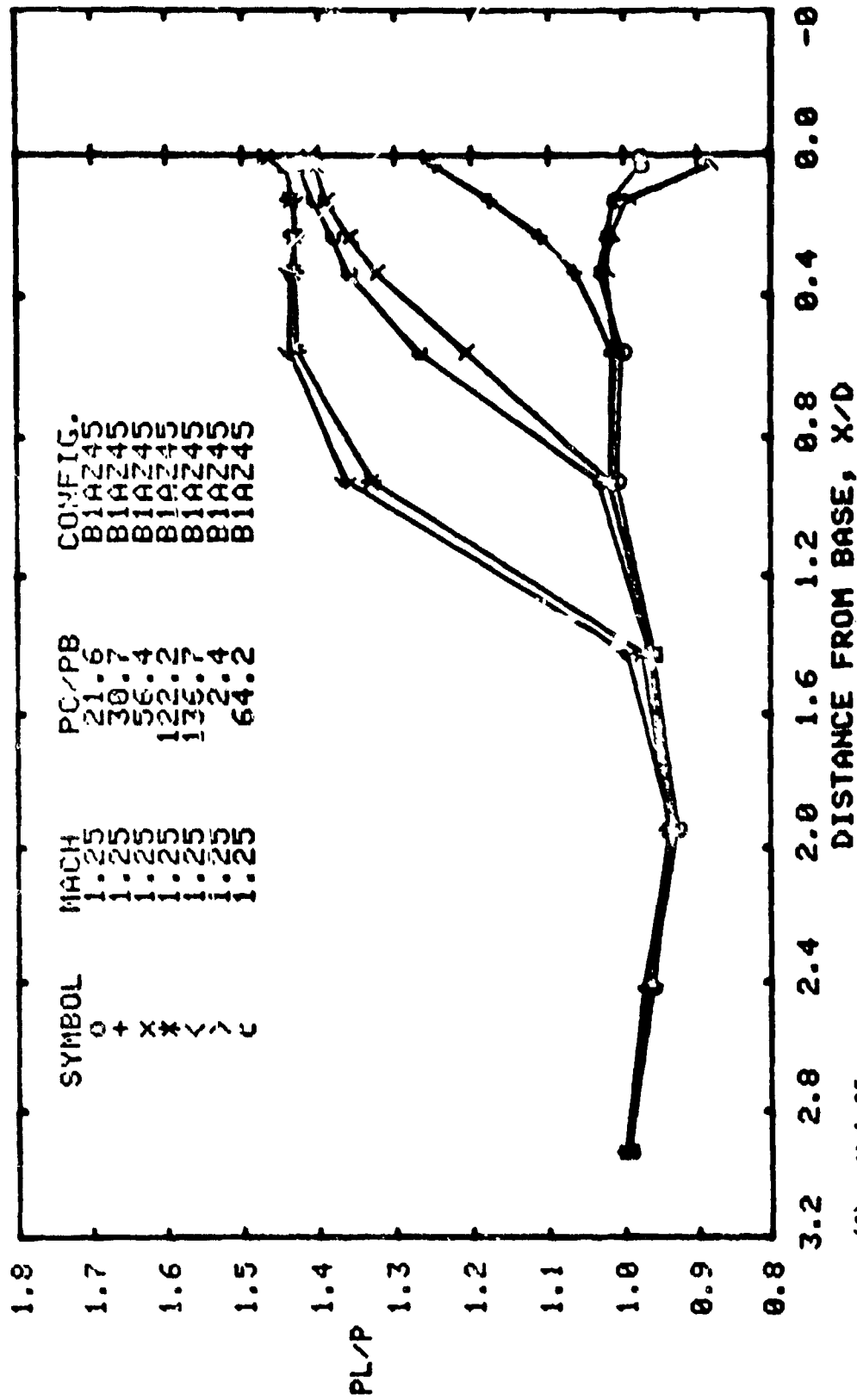
(c). $M=0.9$
Figure A3: cont'd



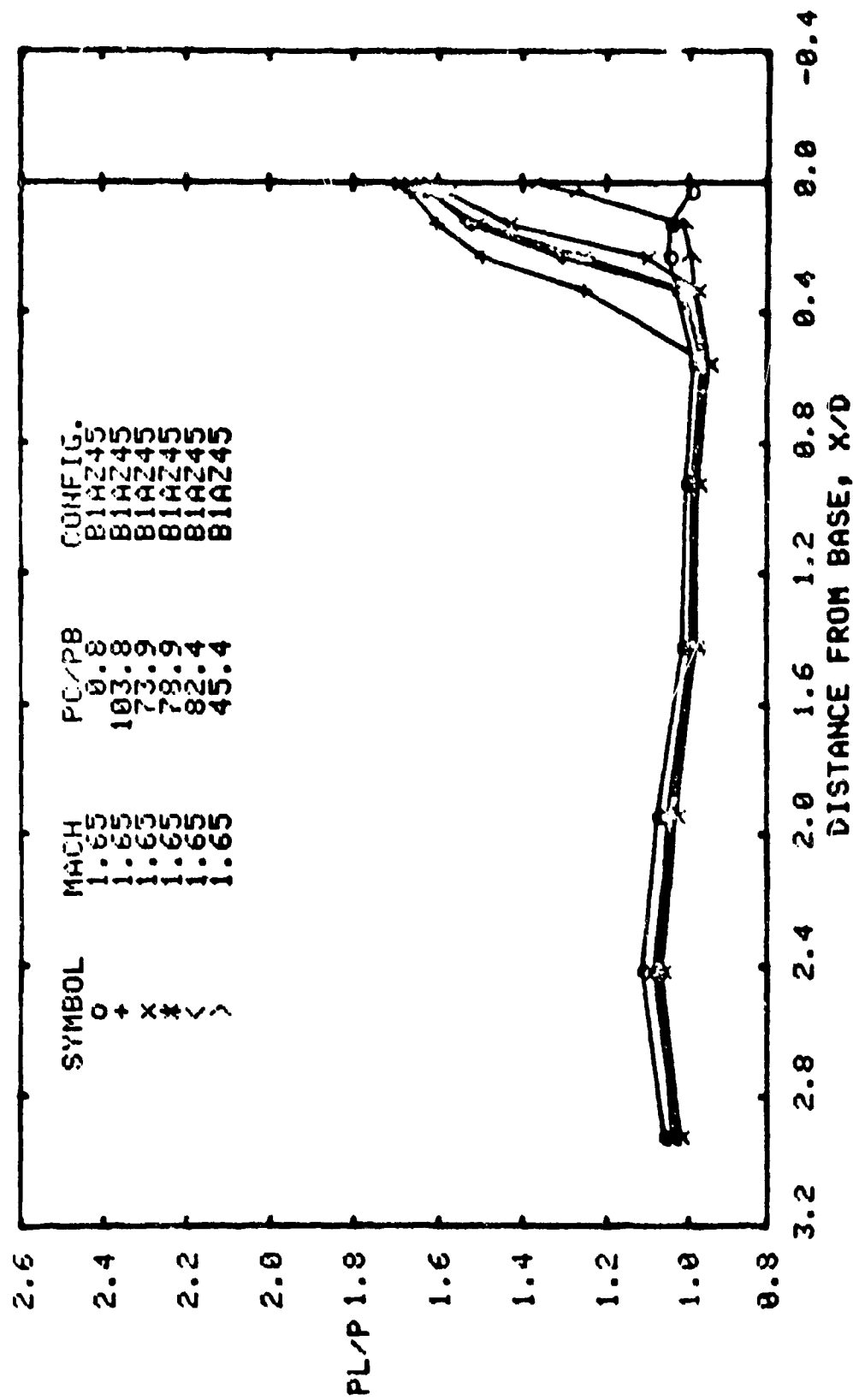
(d). M=1.0
Figure A3: cont'd



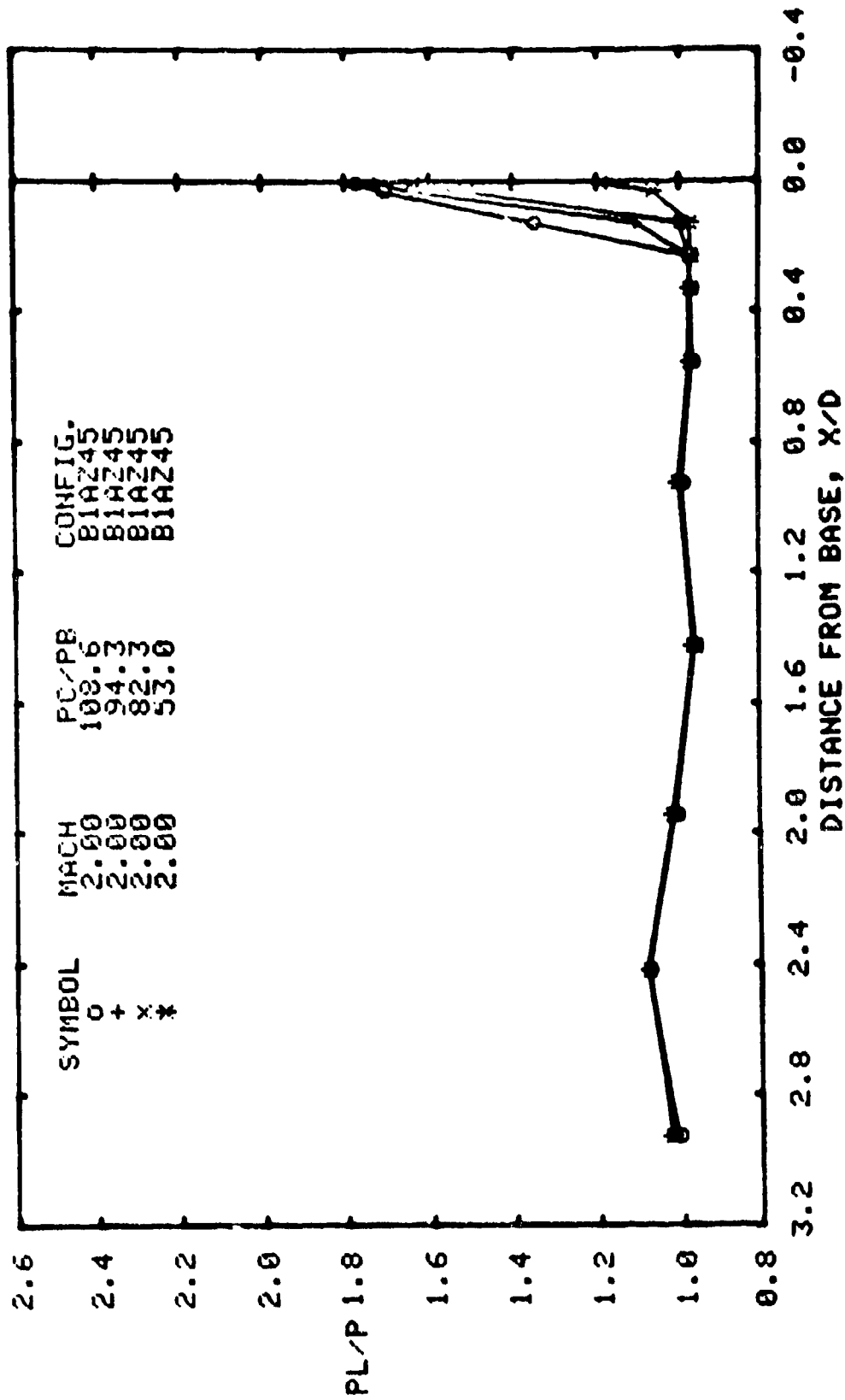
(e). M=1.1
Figure A3: cont'd



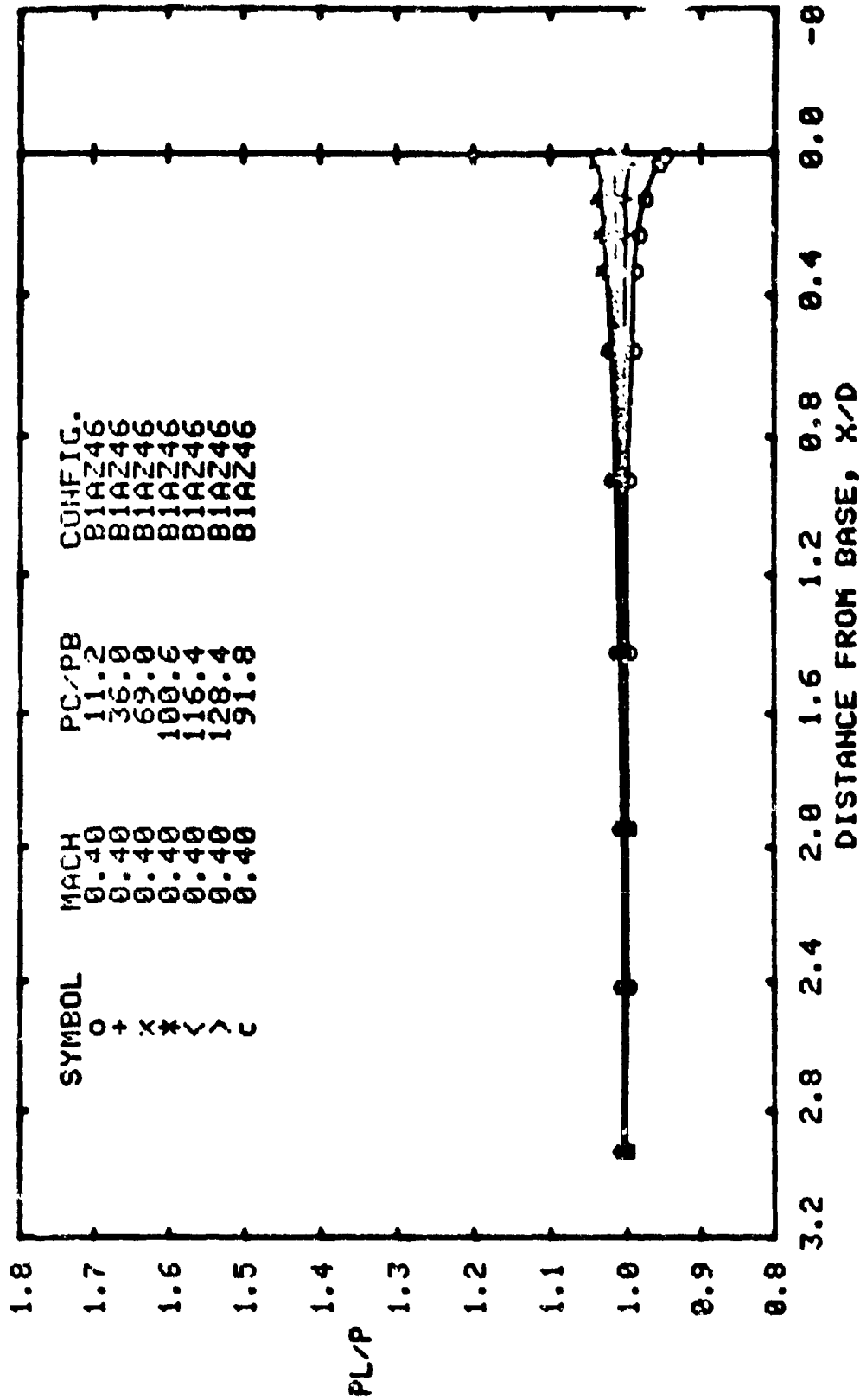
(f). M=1.25
Figure A3: cont'd



(g). M=1.65
Figure A3: cont'd

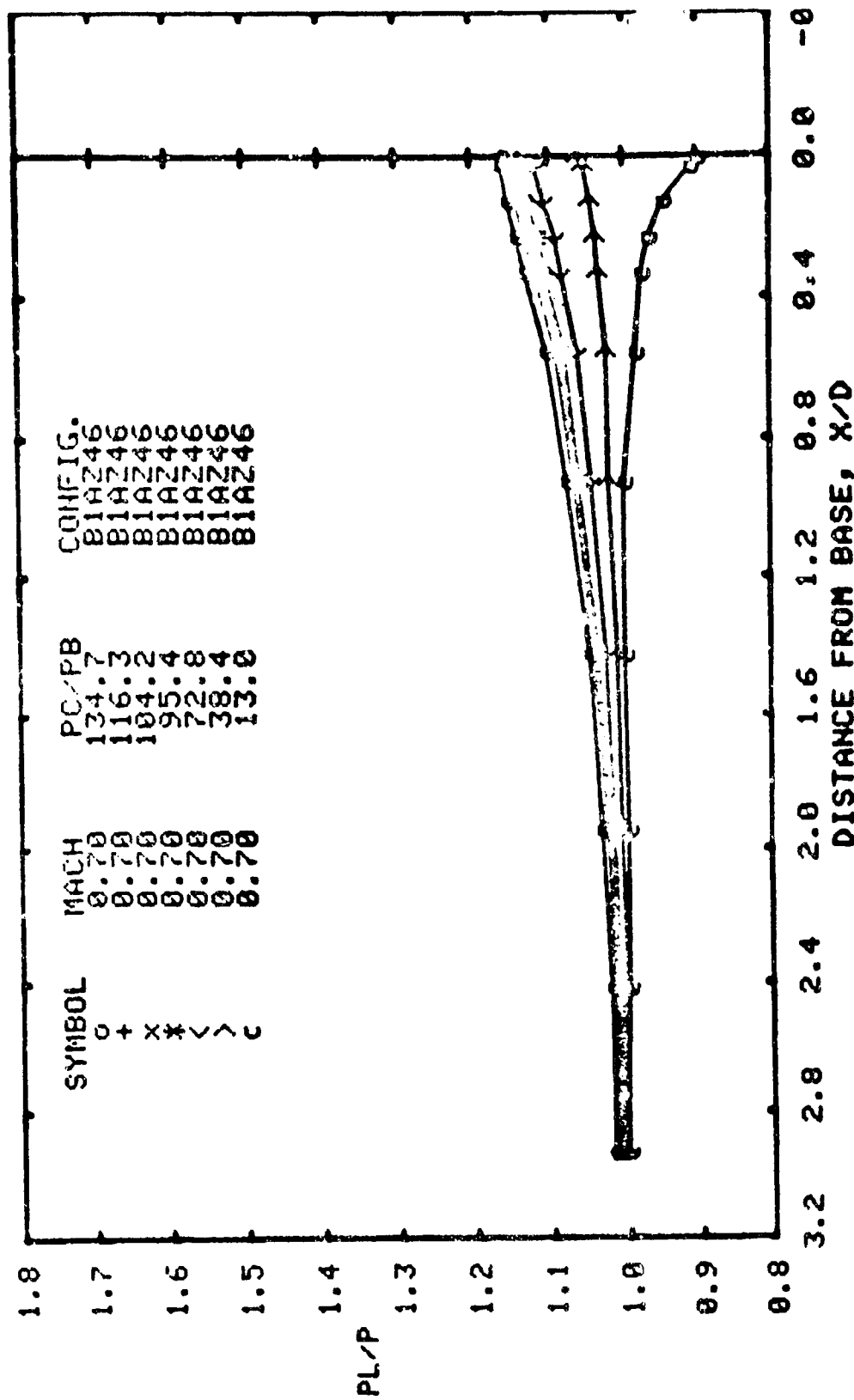


(h). M=2.0
 Figure A3: concl'd.

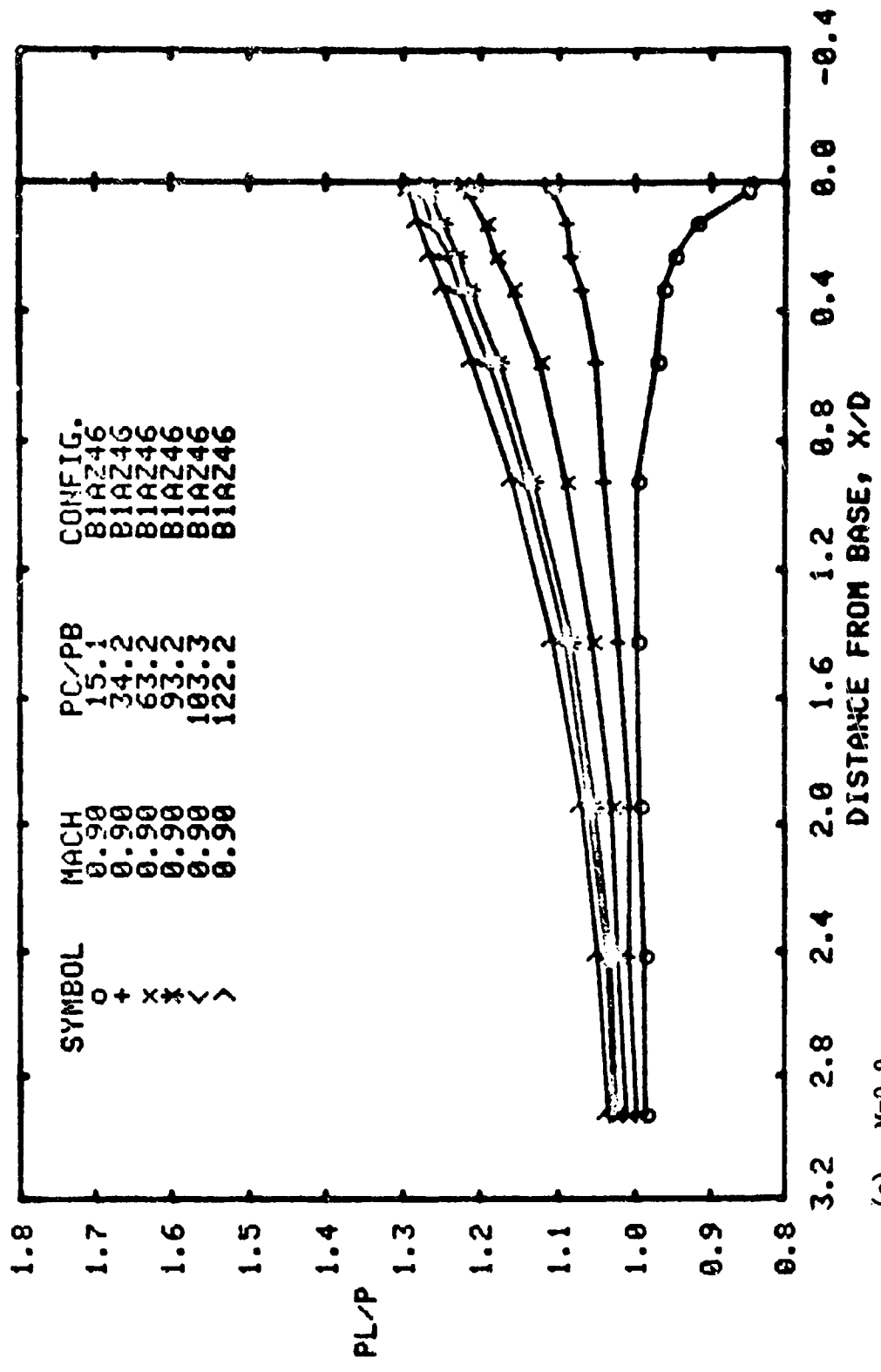


(a). $M = 0.4$

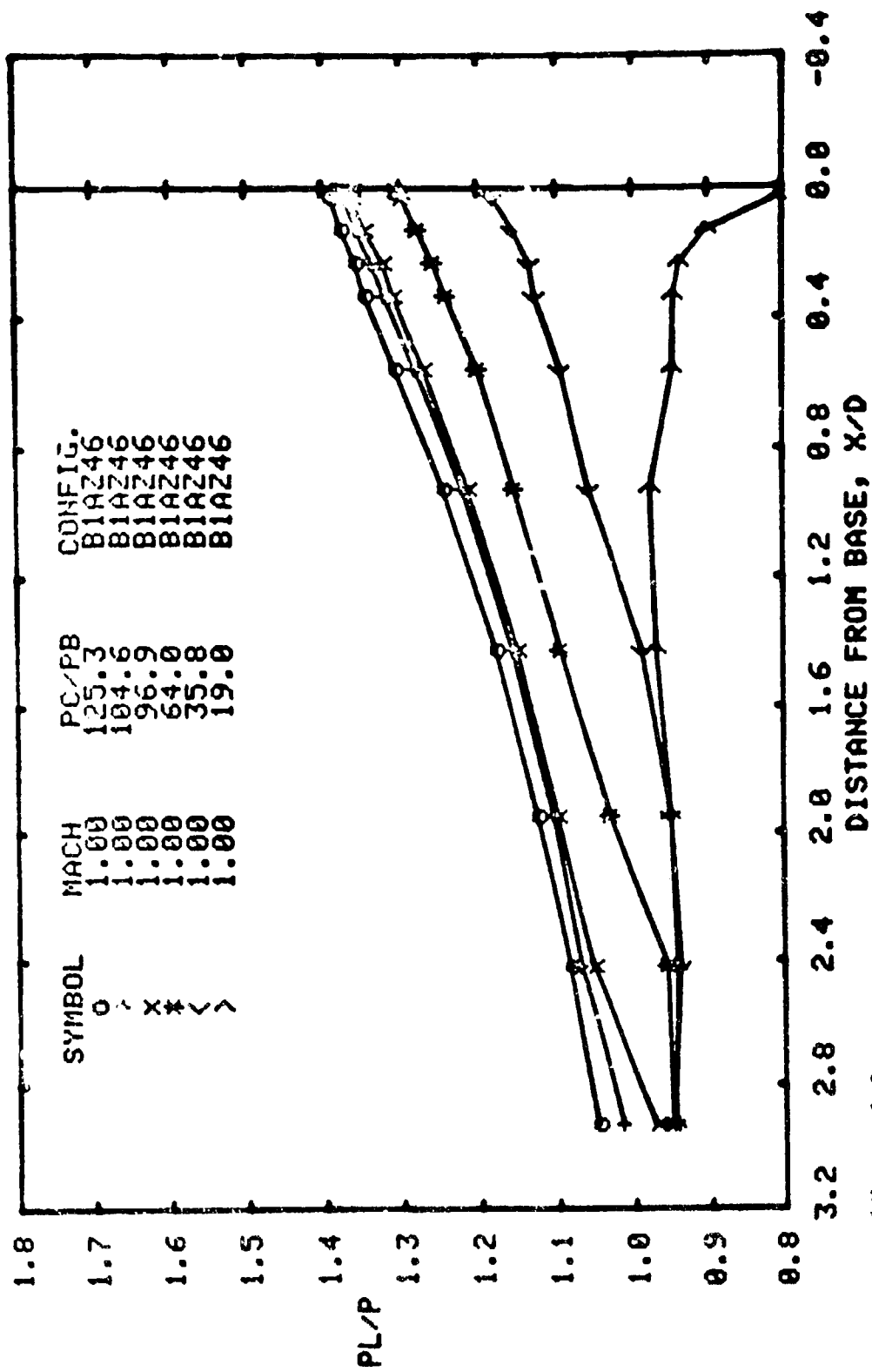
Figure A4: Effect of jet total pressure ratio on body pressure distribution at various free stream Mach numbers. Configuration B1AZ46: $M_j = 2.7$, $\theta_N = 23.3^\circ$, $D_N/D_B = 0.8$.



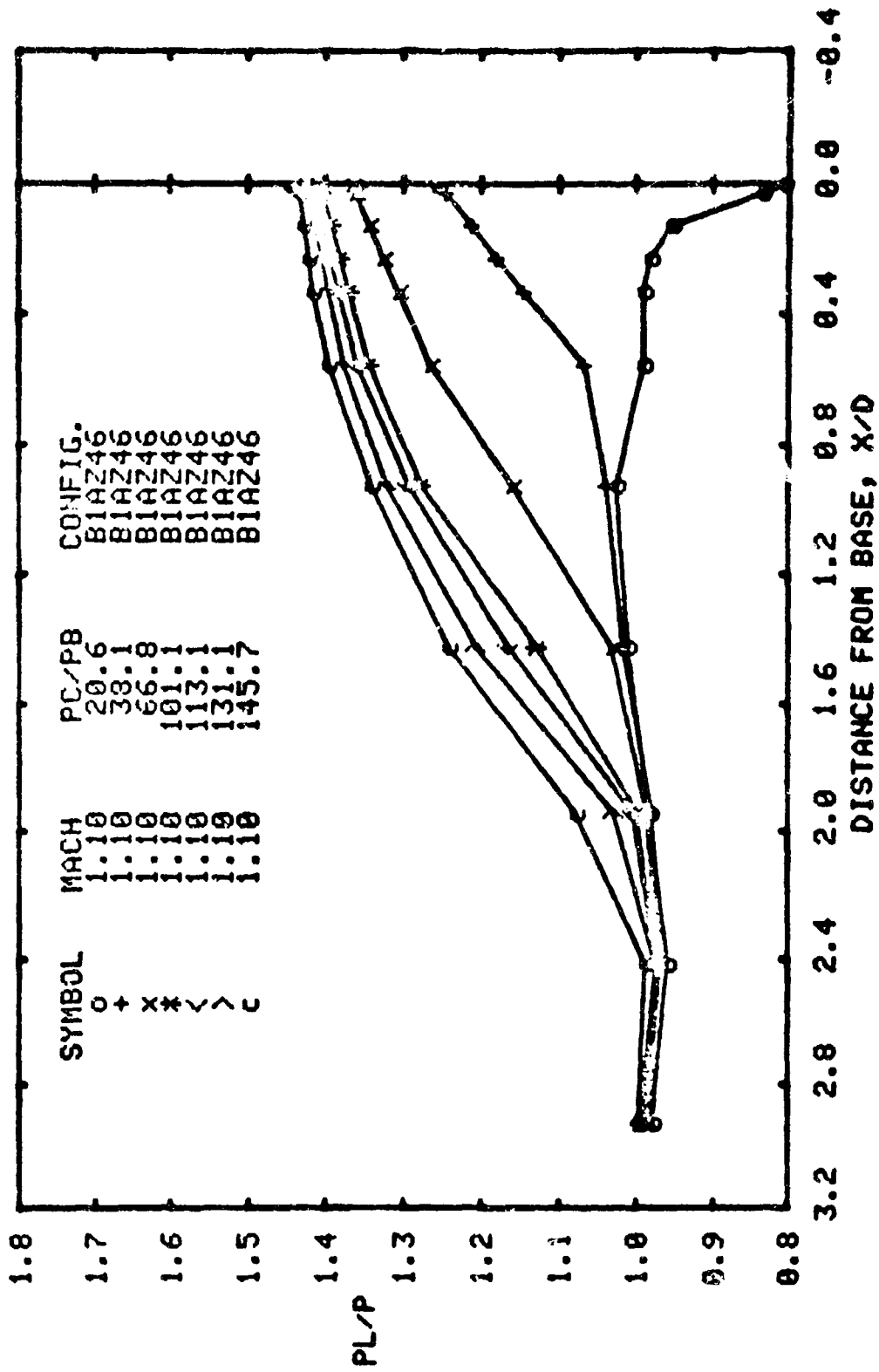
(b). M=0.7
 Figure A4: cent'd



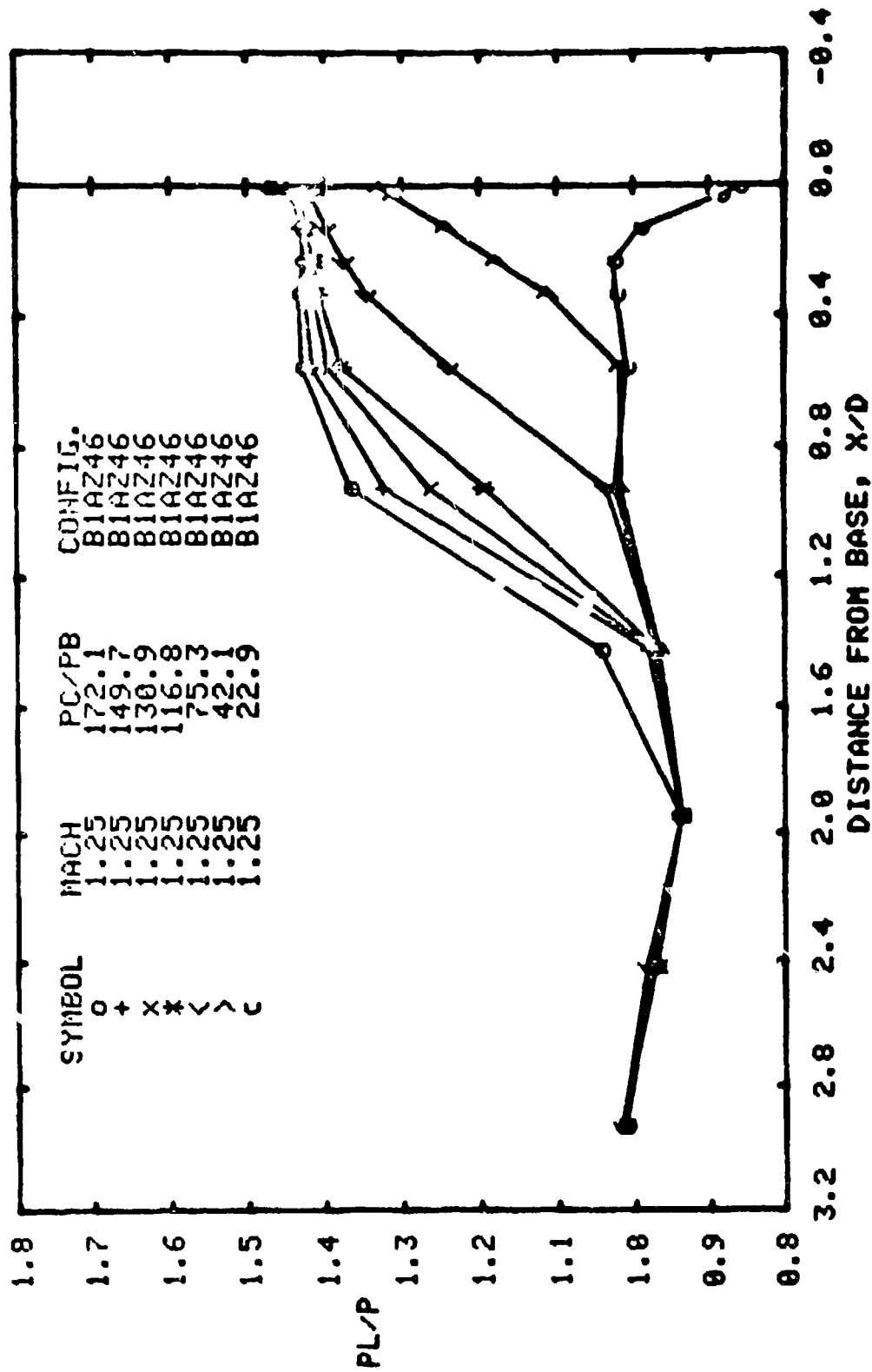
(c). M=0.9
Figure A4: cont'd



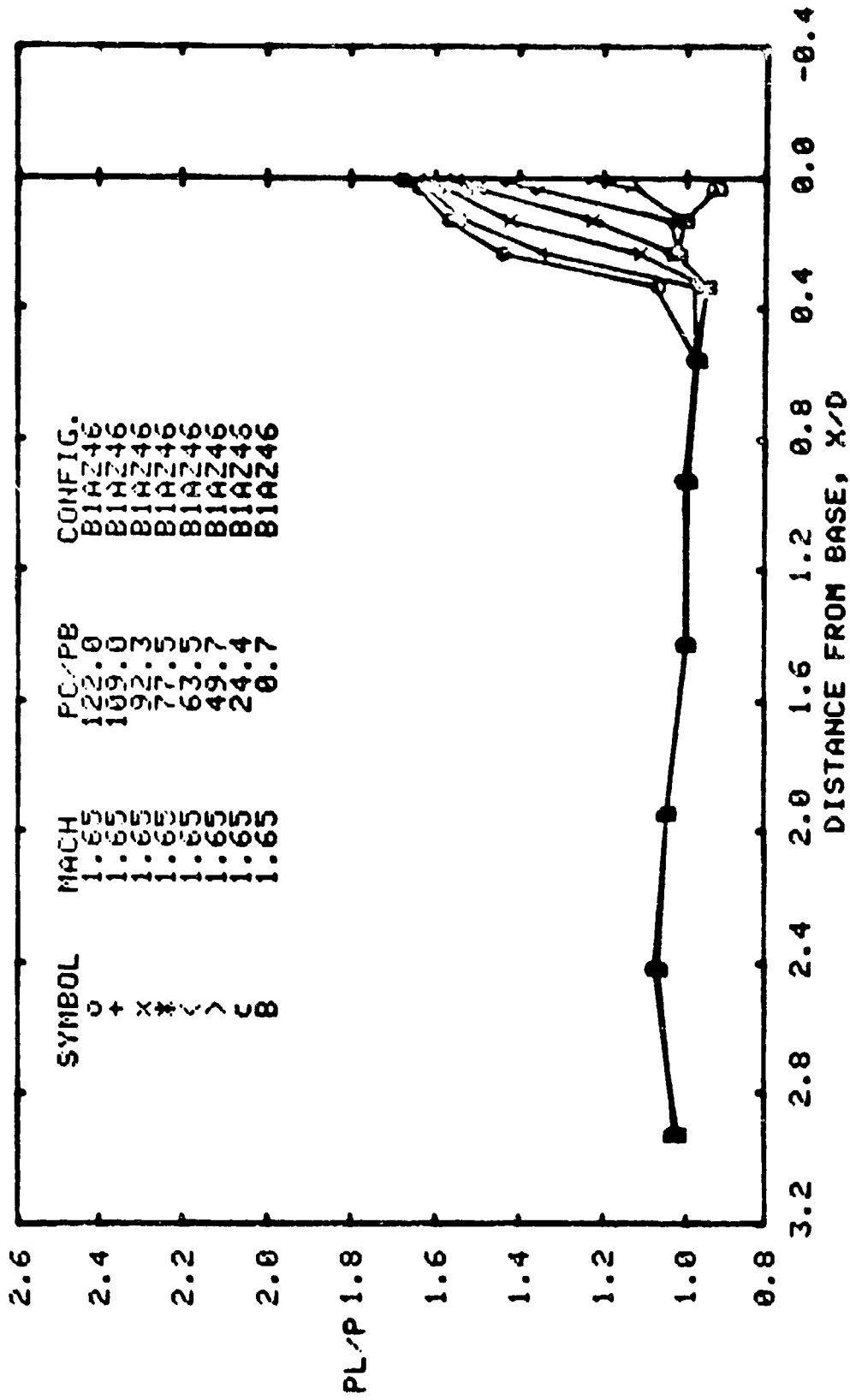
(d). M=1.0
Figure A4: cont'd



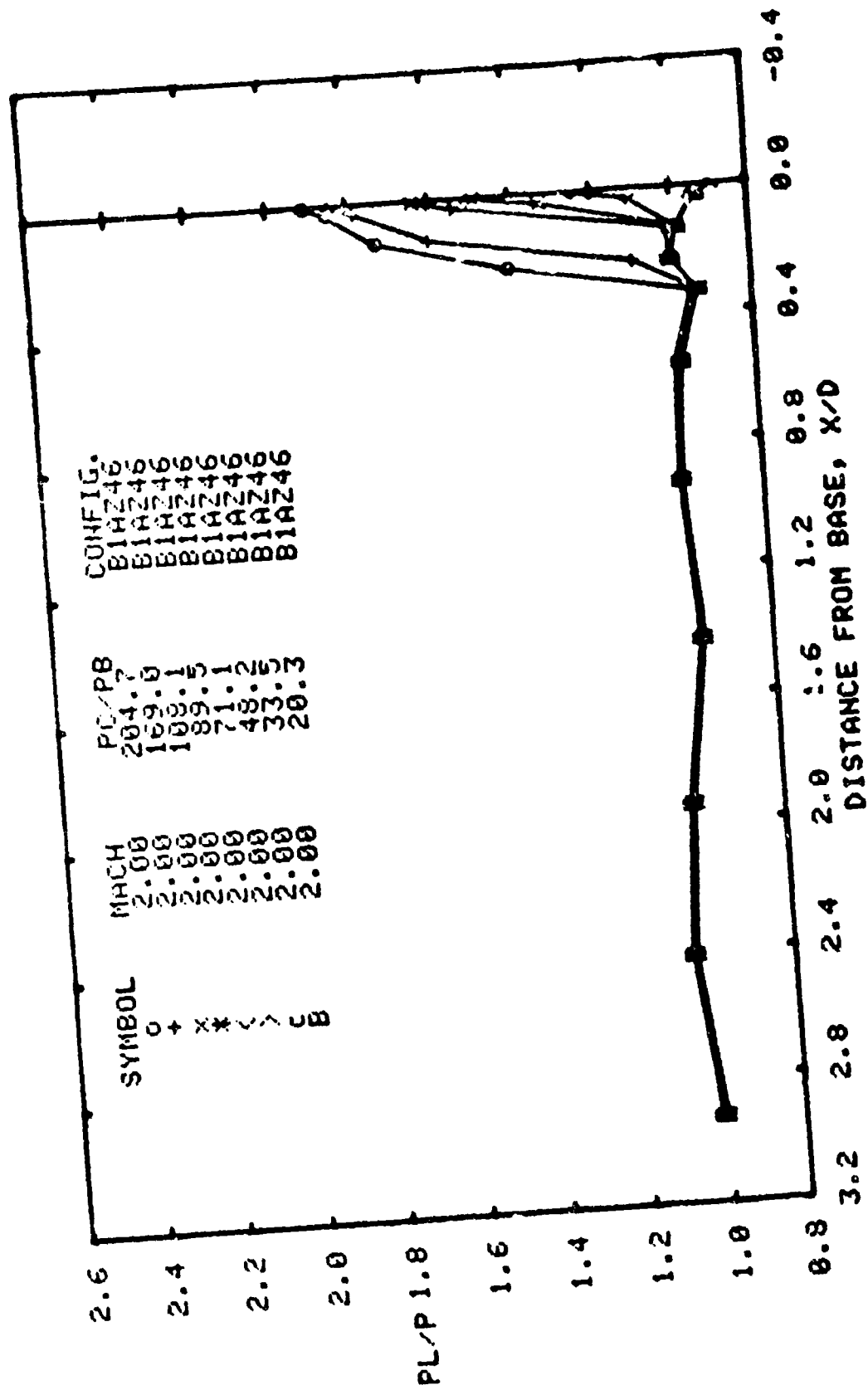
(e). M=1.1
Figure A4: cont'd



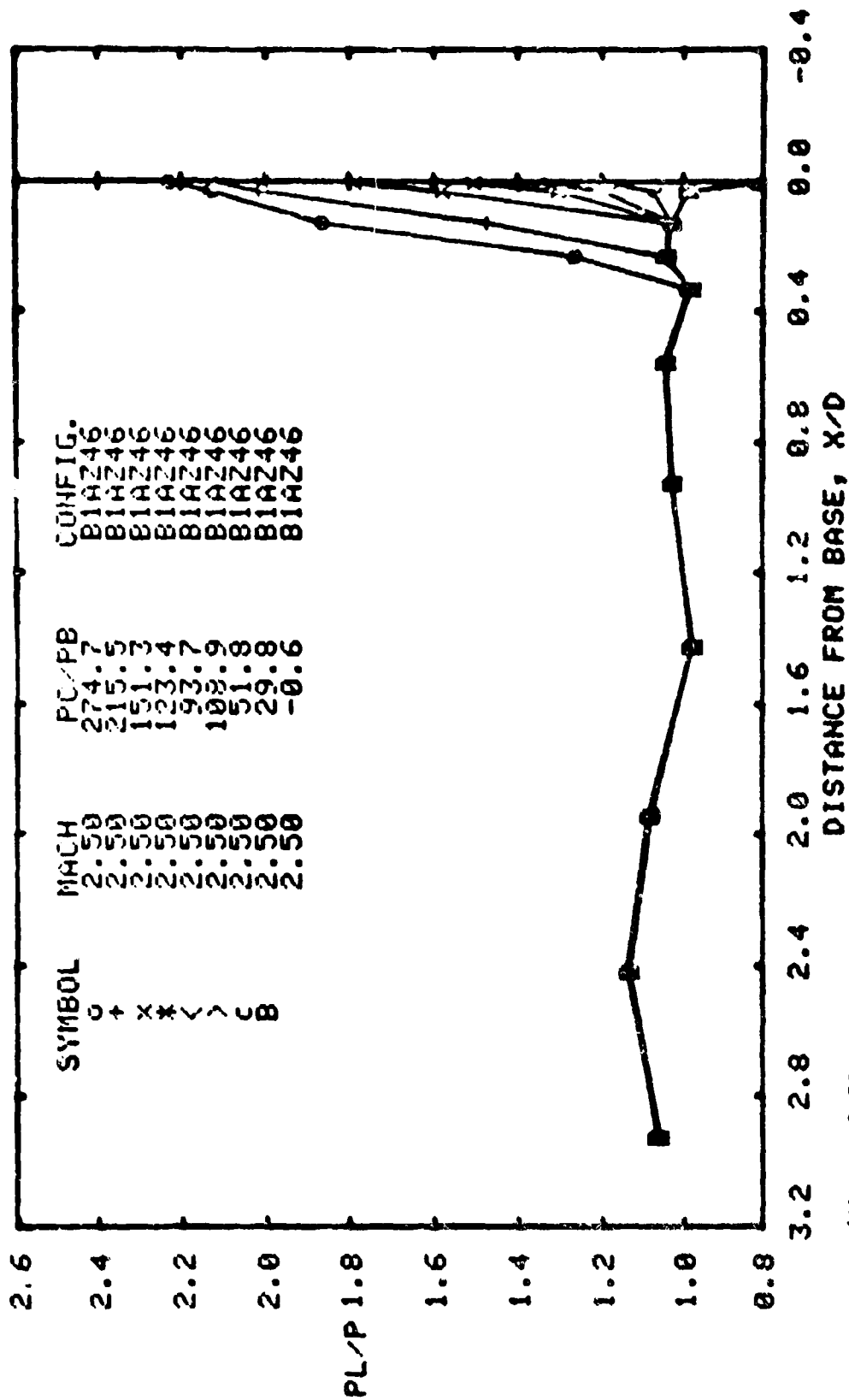
(f). M=1.25
Figure A4: cont'd



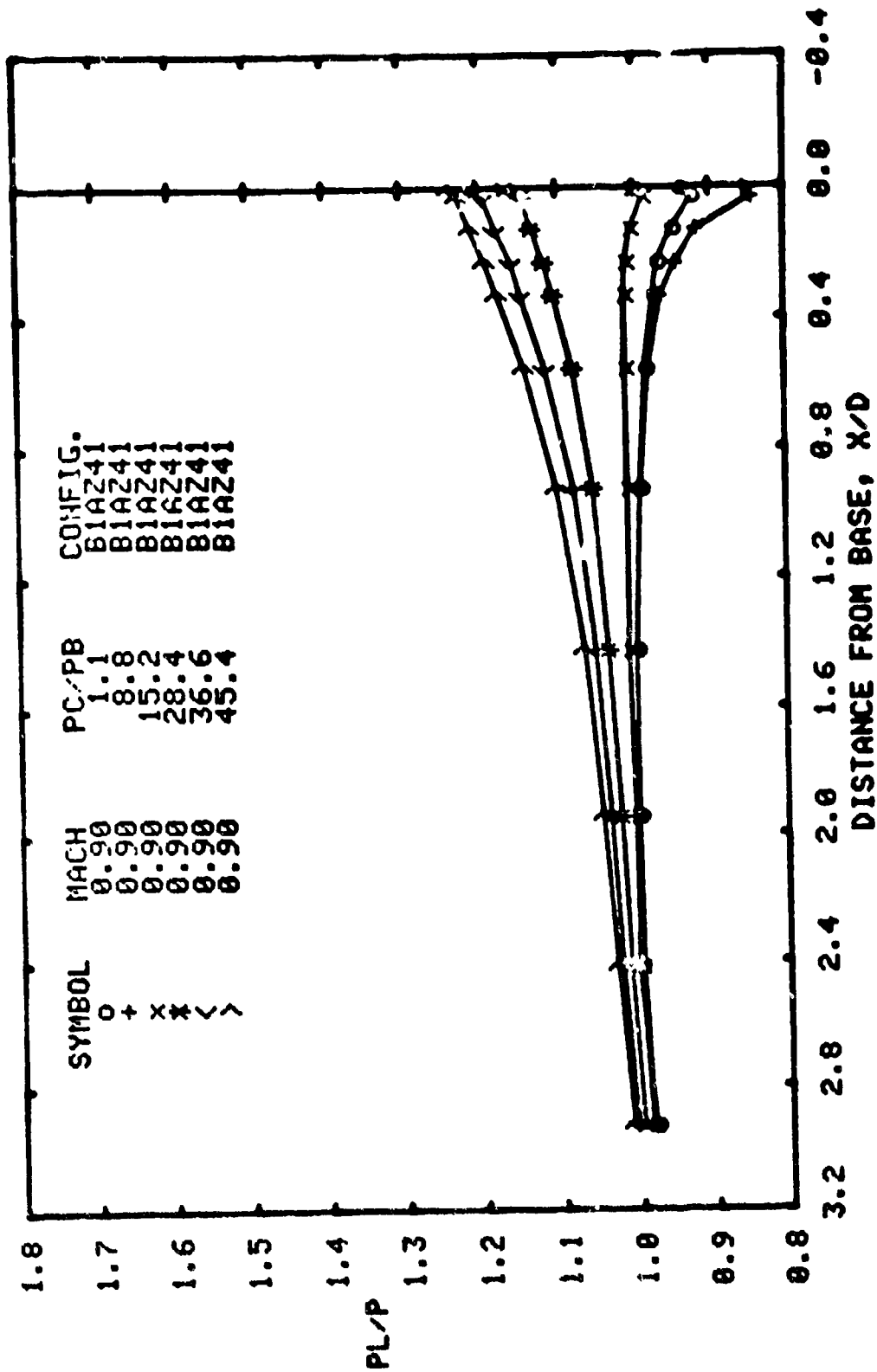
(g). M=1.65
Figure A4: cont'd



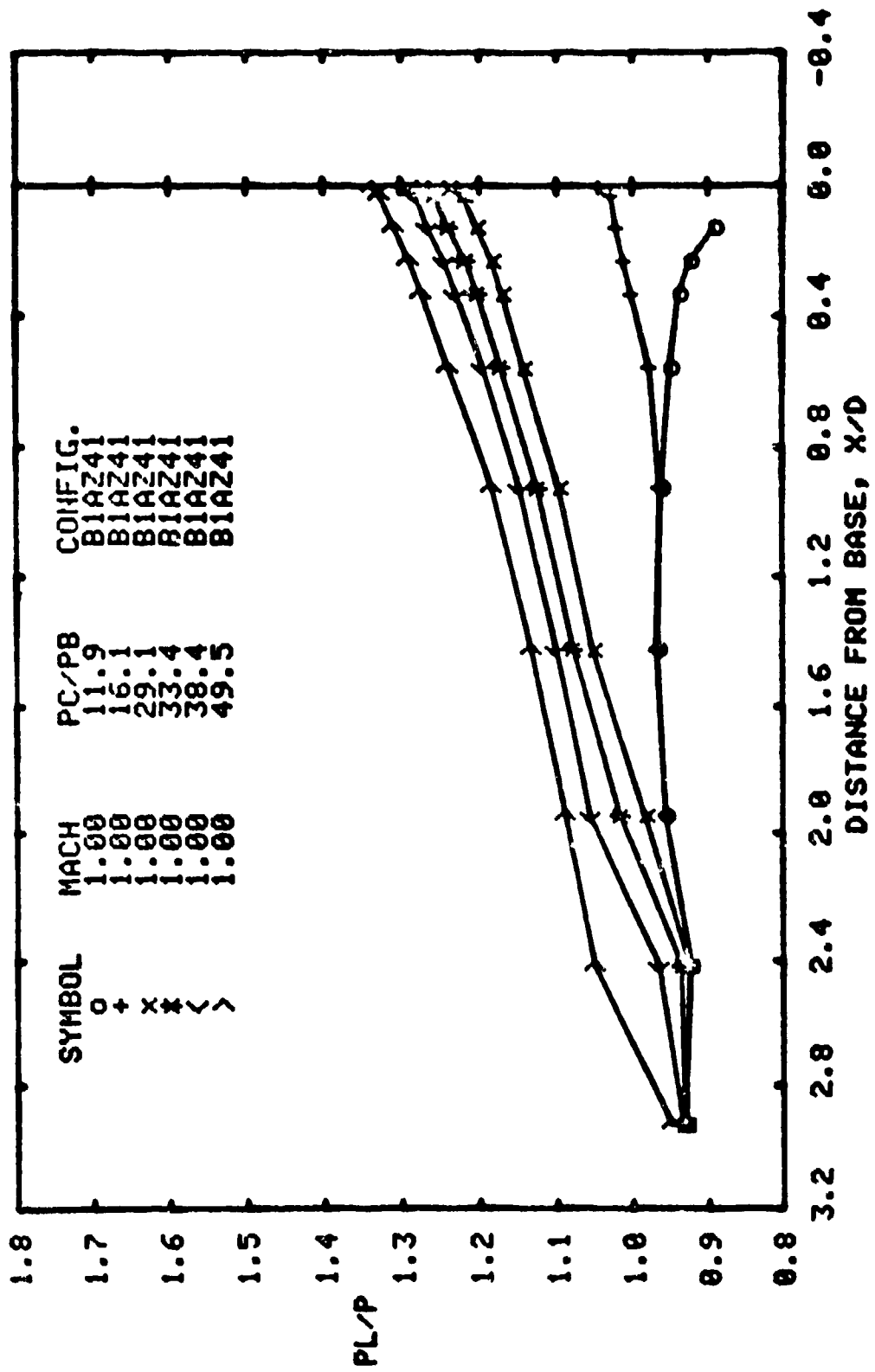
(h). M=2.0
Figure A4: cont'd



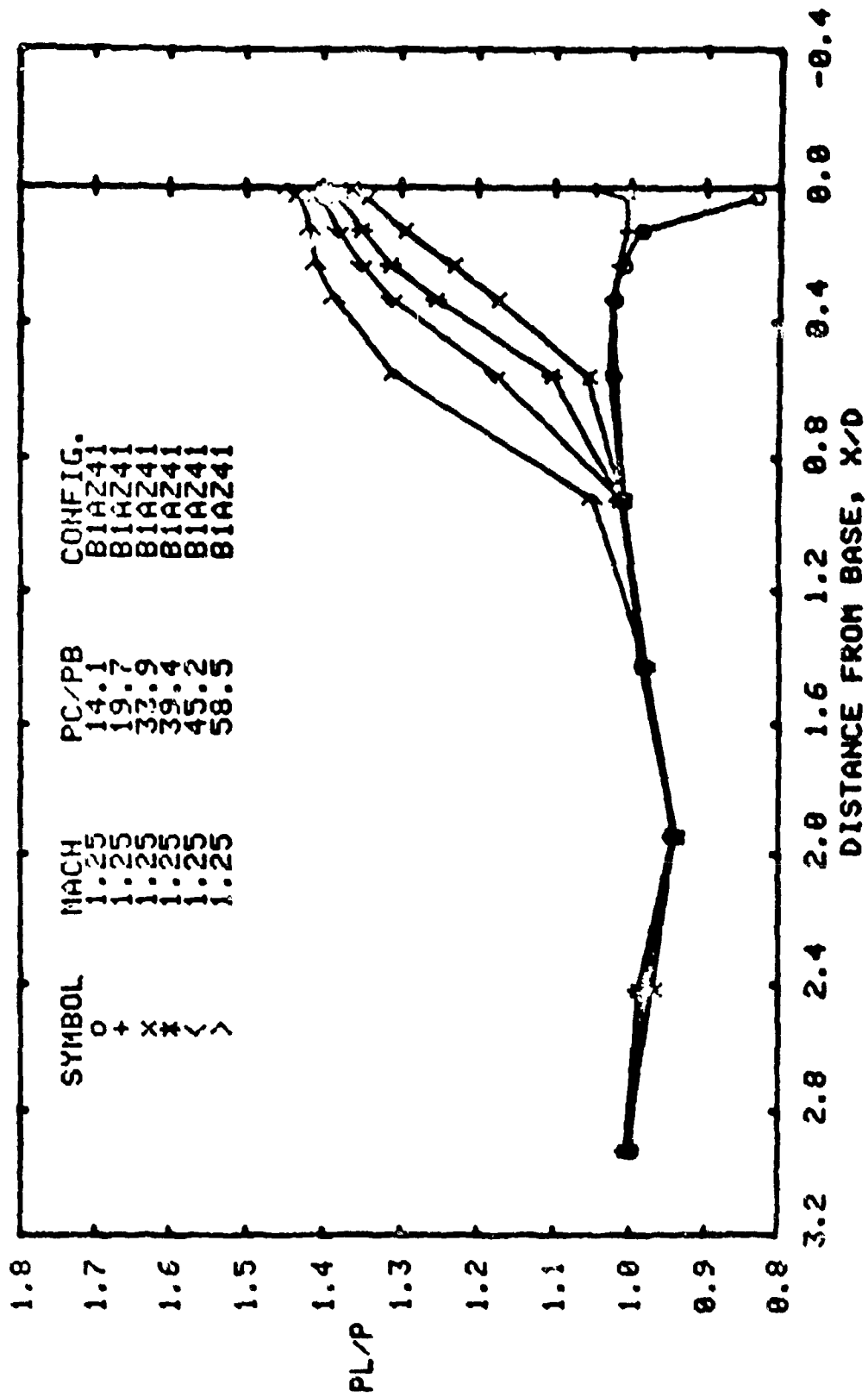
(1). M=2.50
Figure A4: concl'd.



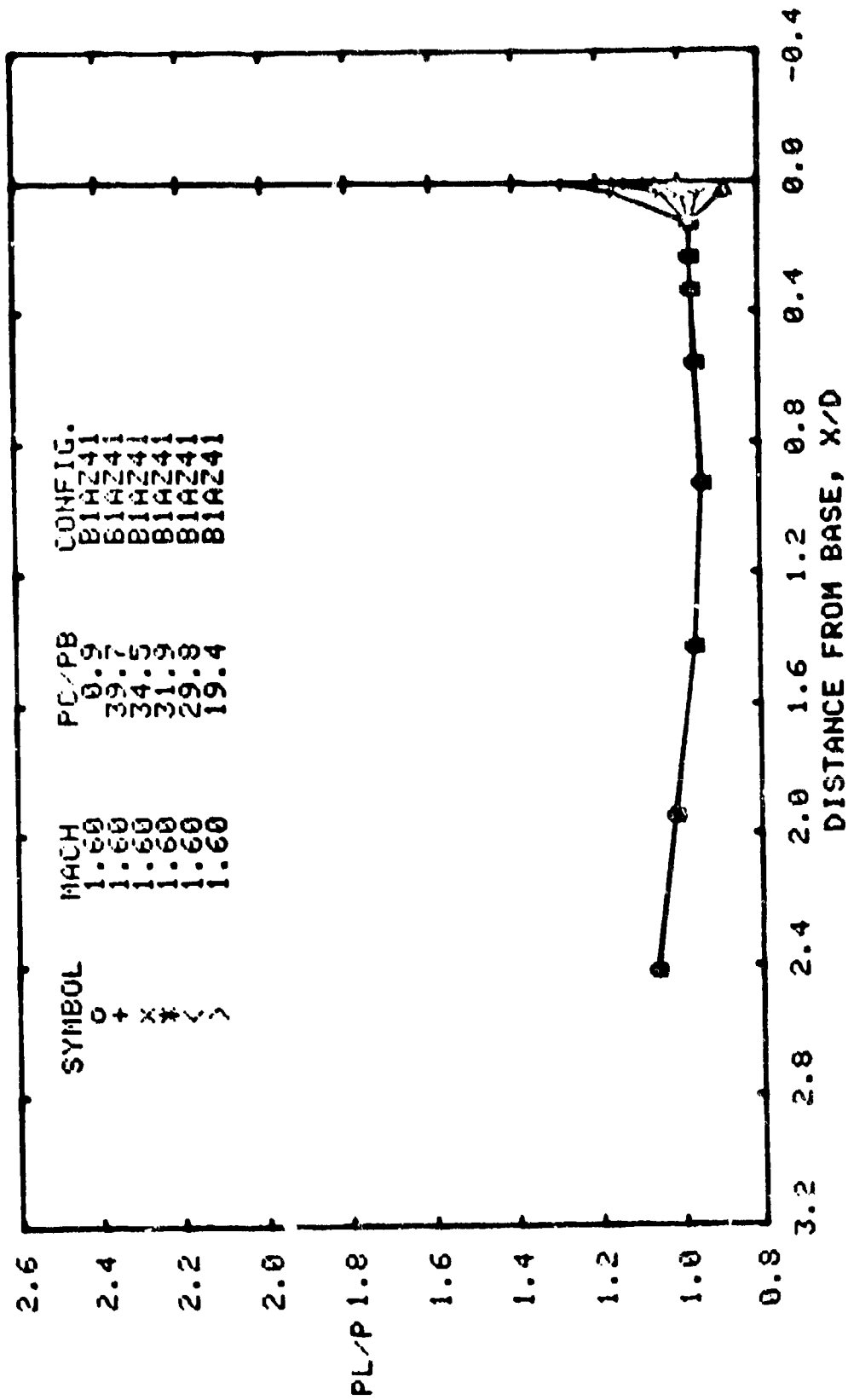
(a). $M=0.9$
 Figure A5: Effect of jet total pressure ratio on body pressure distribution at various free stream Mach numbers. Configuration BIAZ41: $M_j=1.76$, $\theta_N=3.95^\circ$, $D_N/D_B=0.8$.



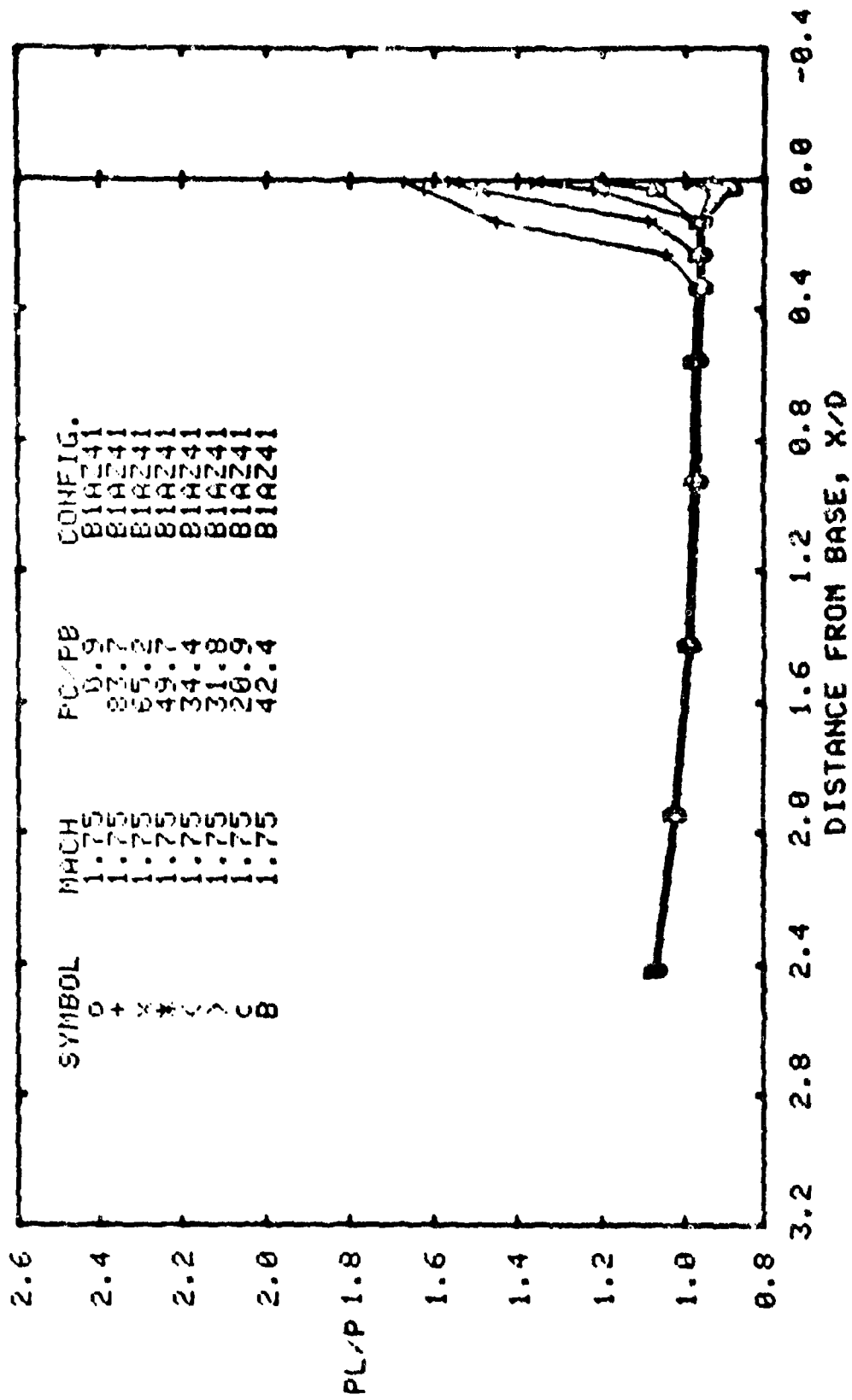
(b). M=1.0
Figure A5: cont'd



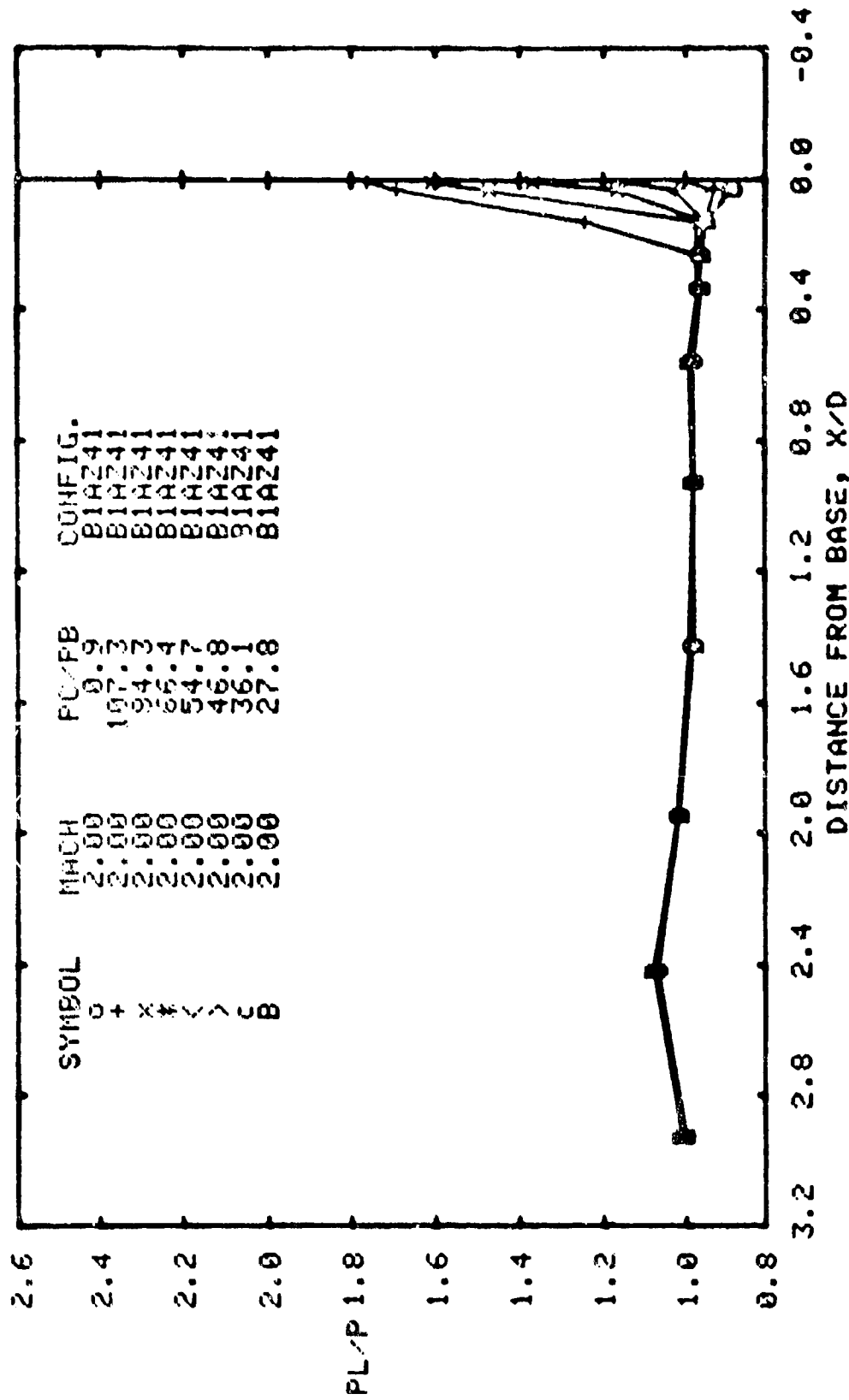
(c). M=1.25
Figure A5: cont'd



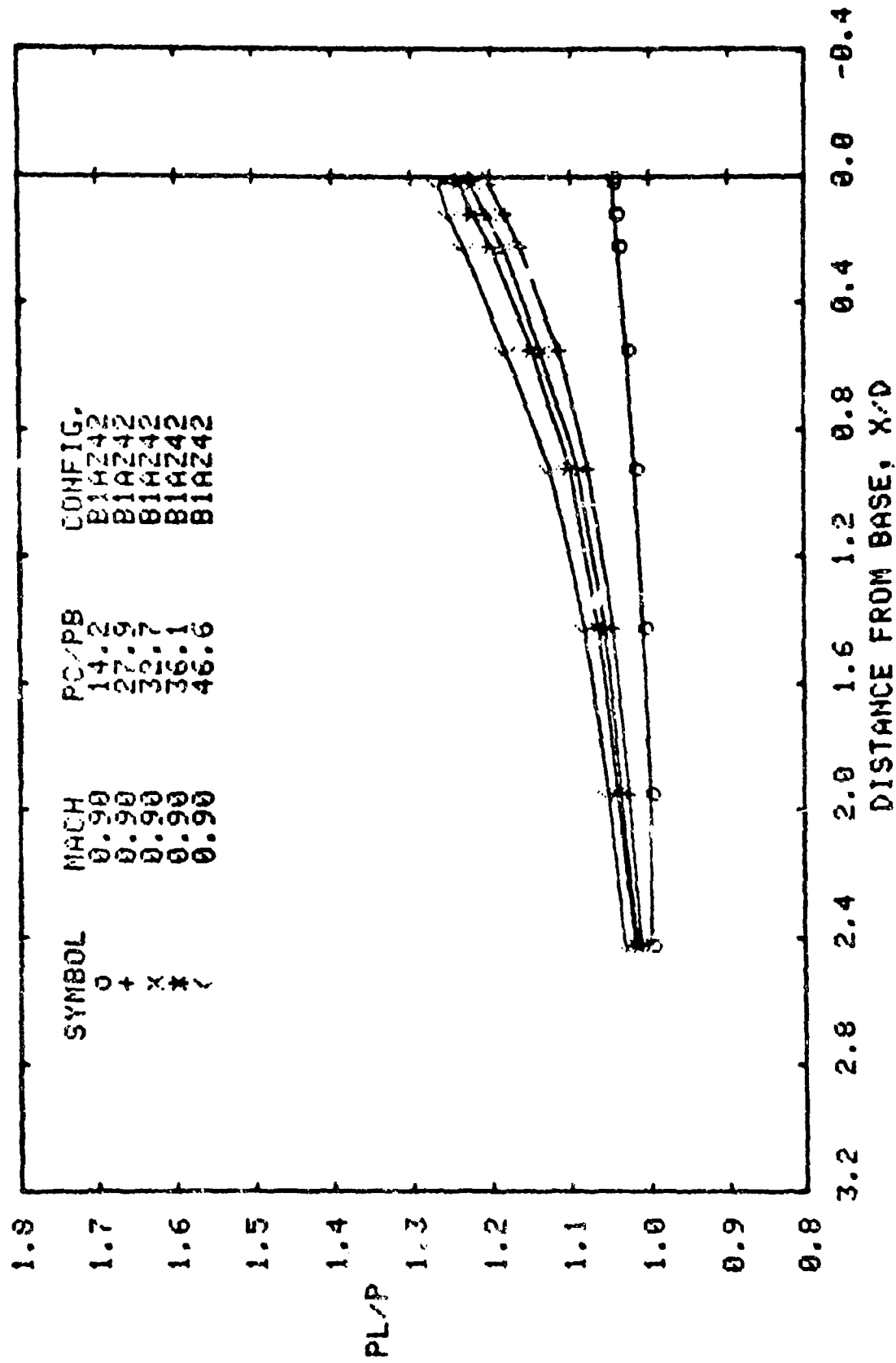
(d). M=1.6
Figure A5: cont'd



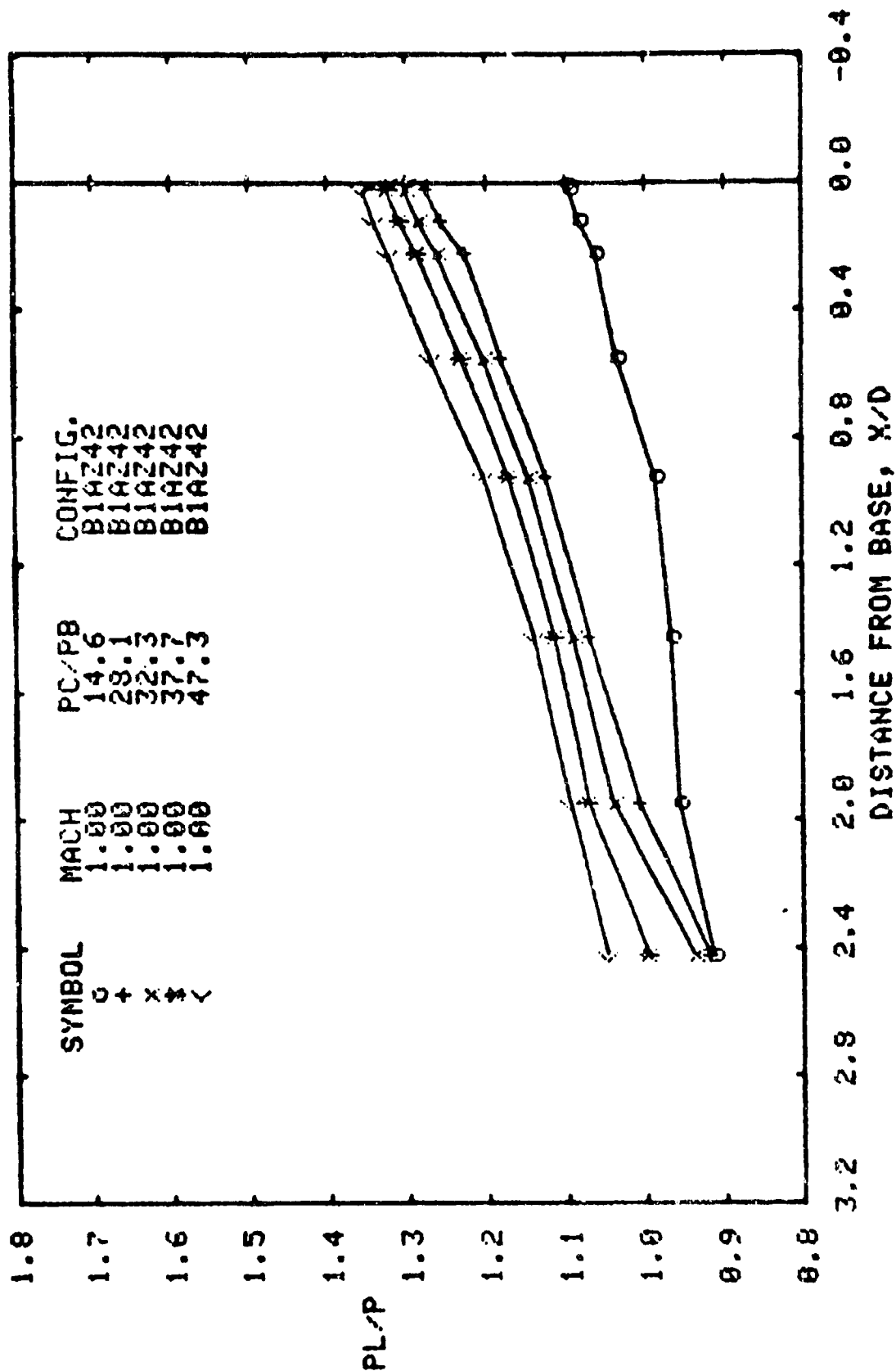
(e). M=1.75
 Figure A5: cont'd



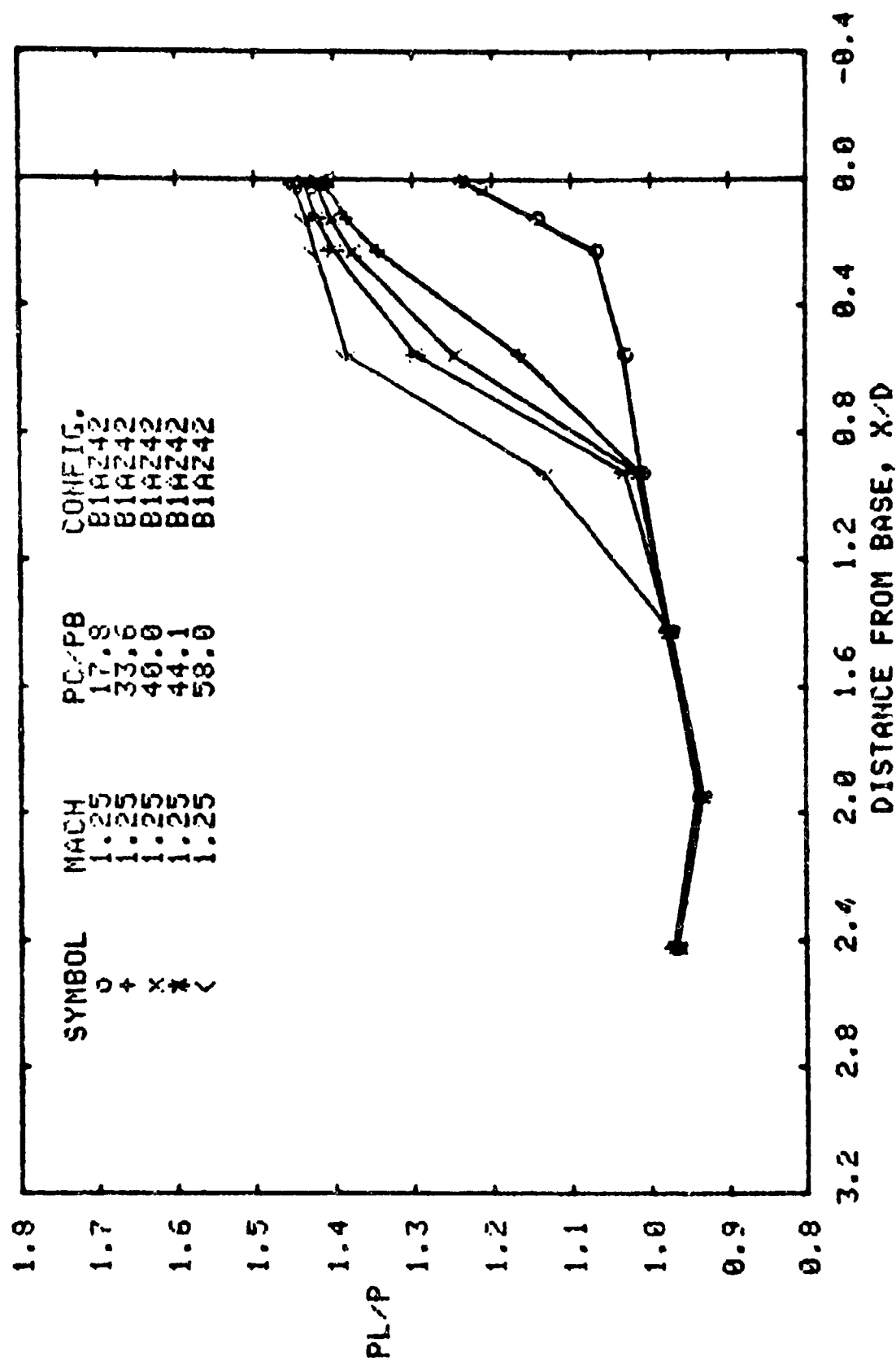
(F). M=2.0
Figure A5: concl'd.



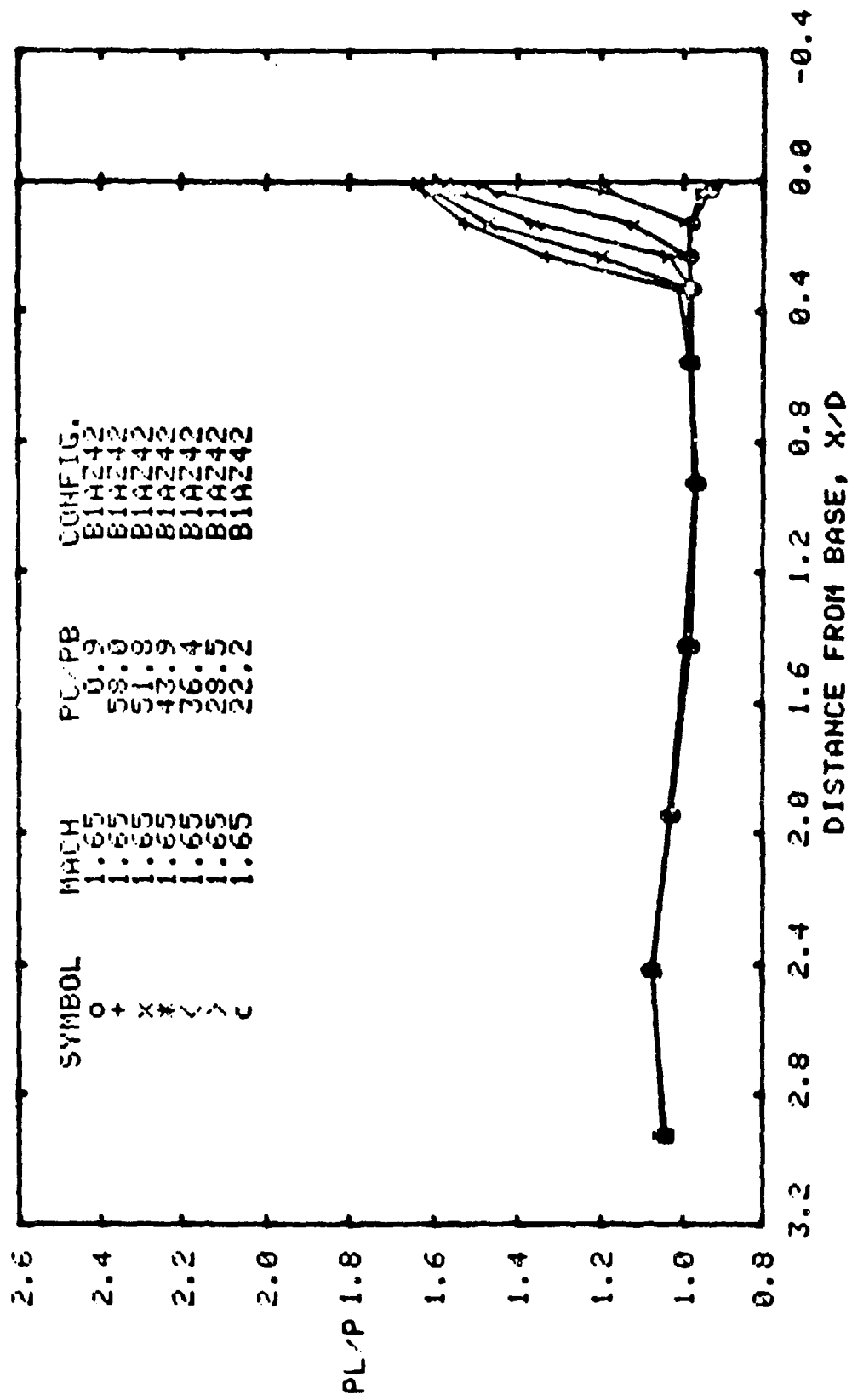
(a). $M=0.90$
 Figure A6: Effect of jet total pressure ratio on body pressure distribution at various free stream Mach numbers. Configuration BIAZ42: $M_j=1.76$, $\rho_N=3.95$, $D_N/D_B=.93$.



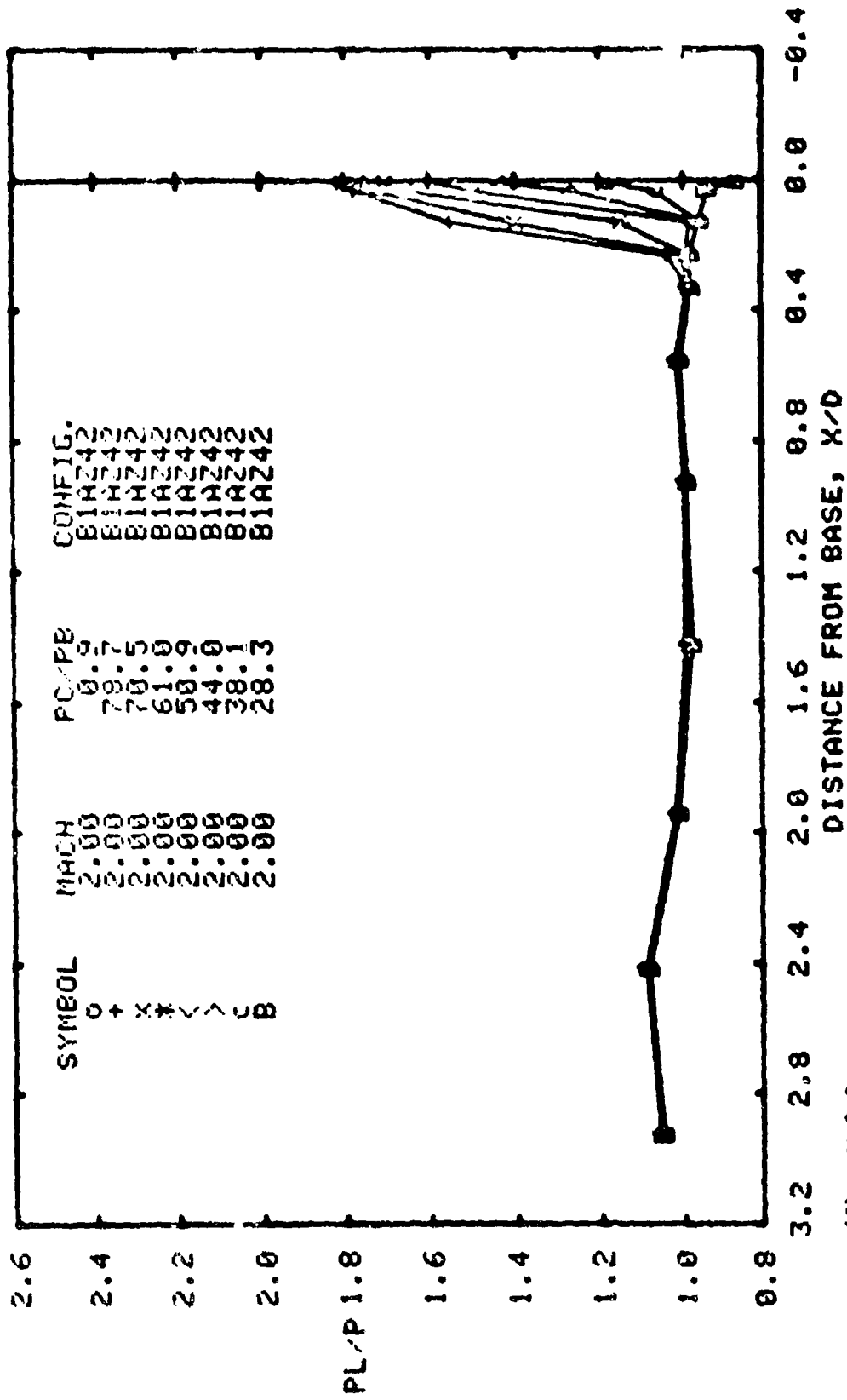
(b). M=1.00
Figure A6: cont'd.



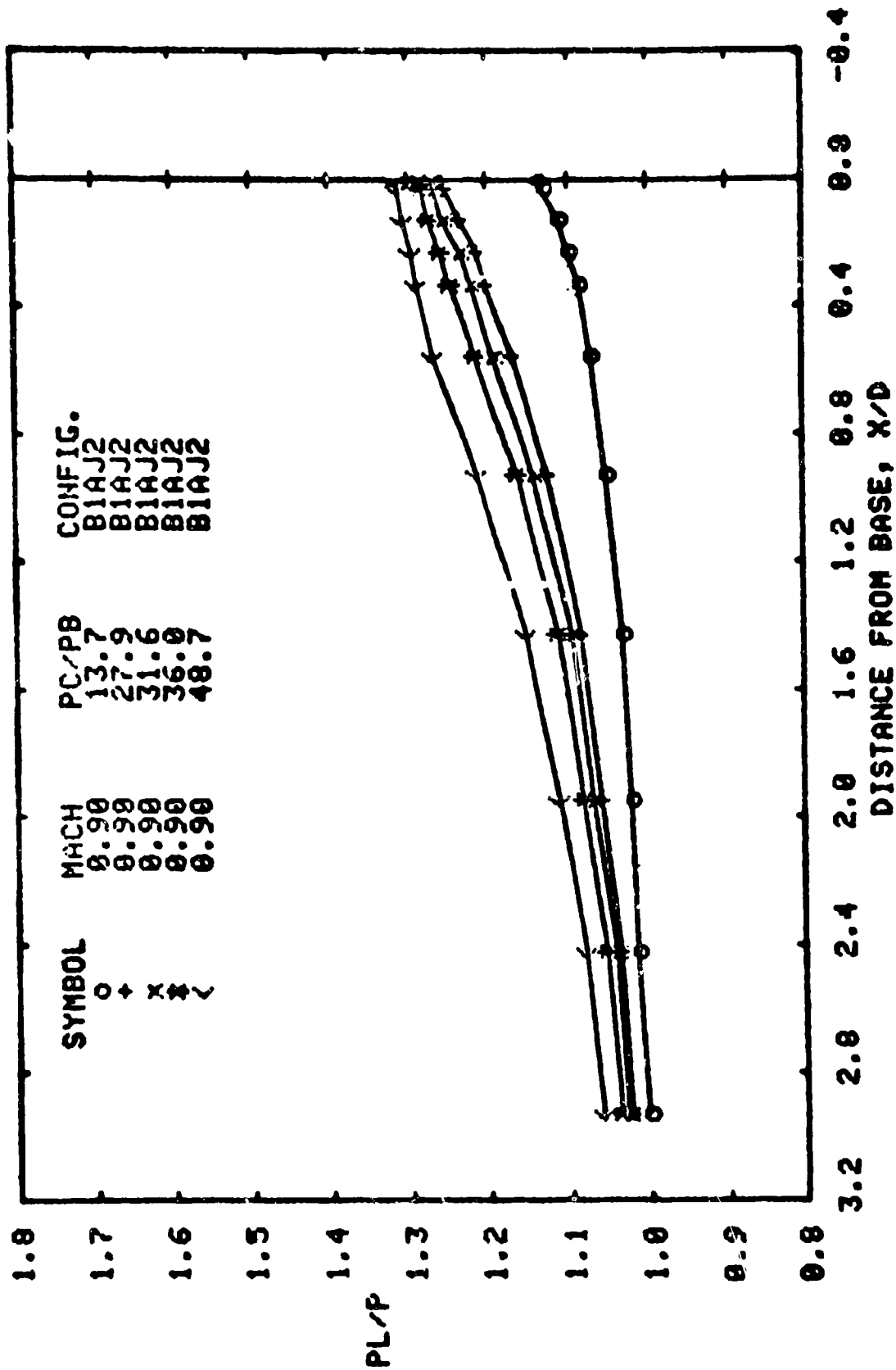
(c). M=1.25
Figure A6: cont'd.



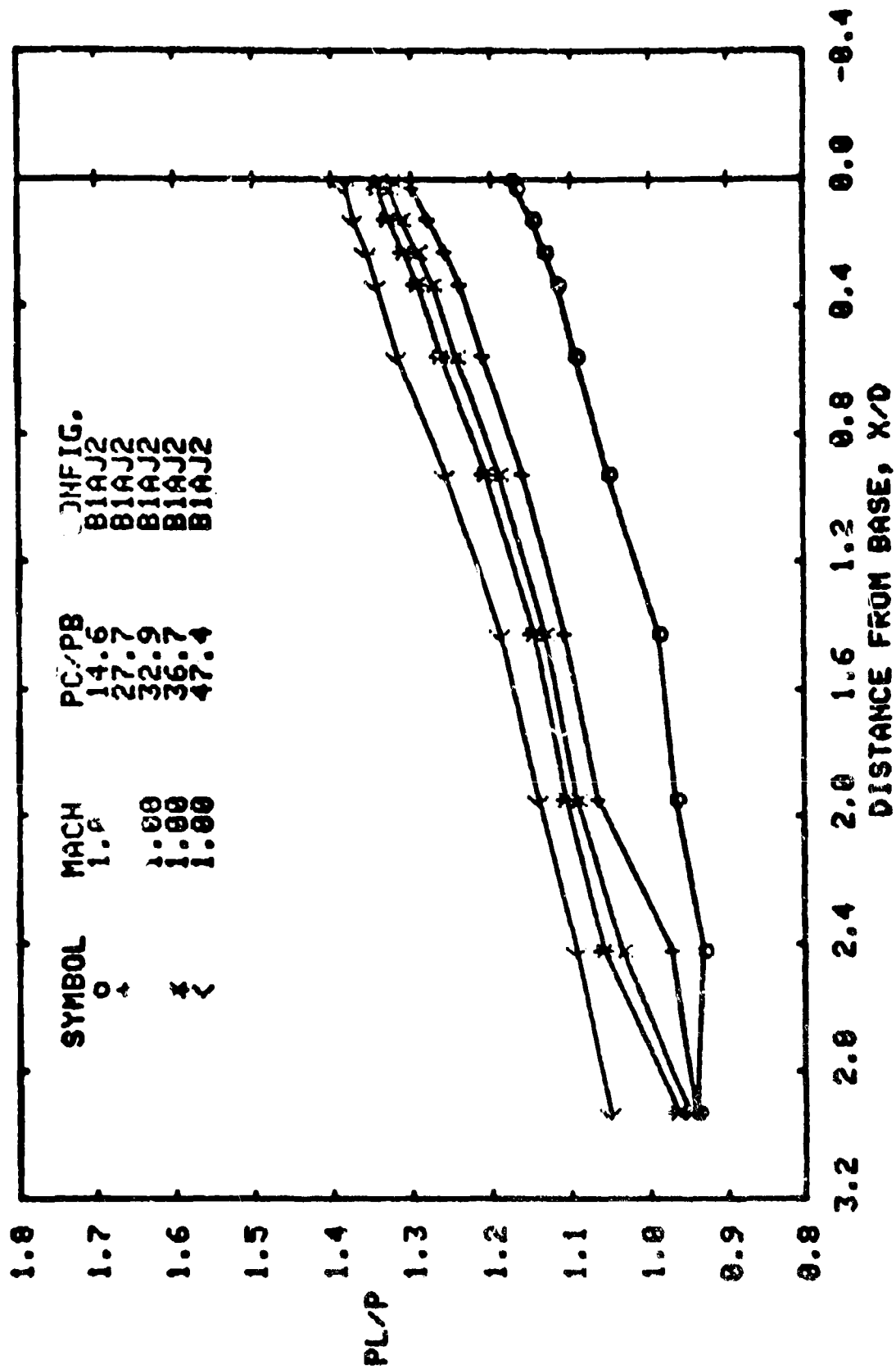
(d). M=1.65
Figure A6: cont'd



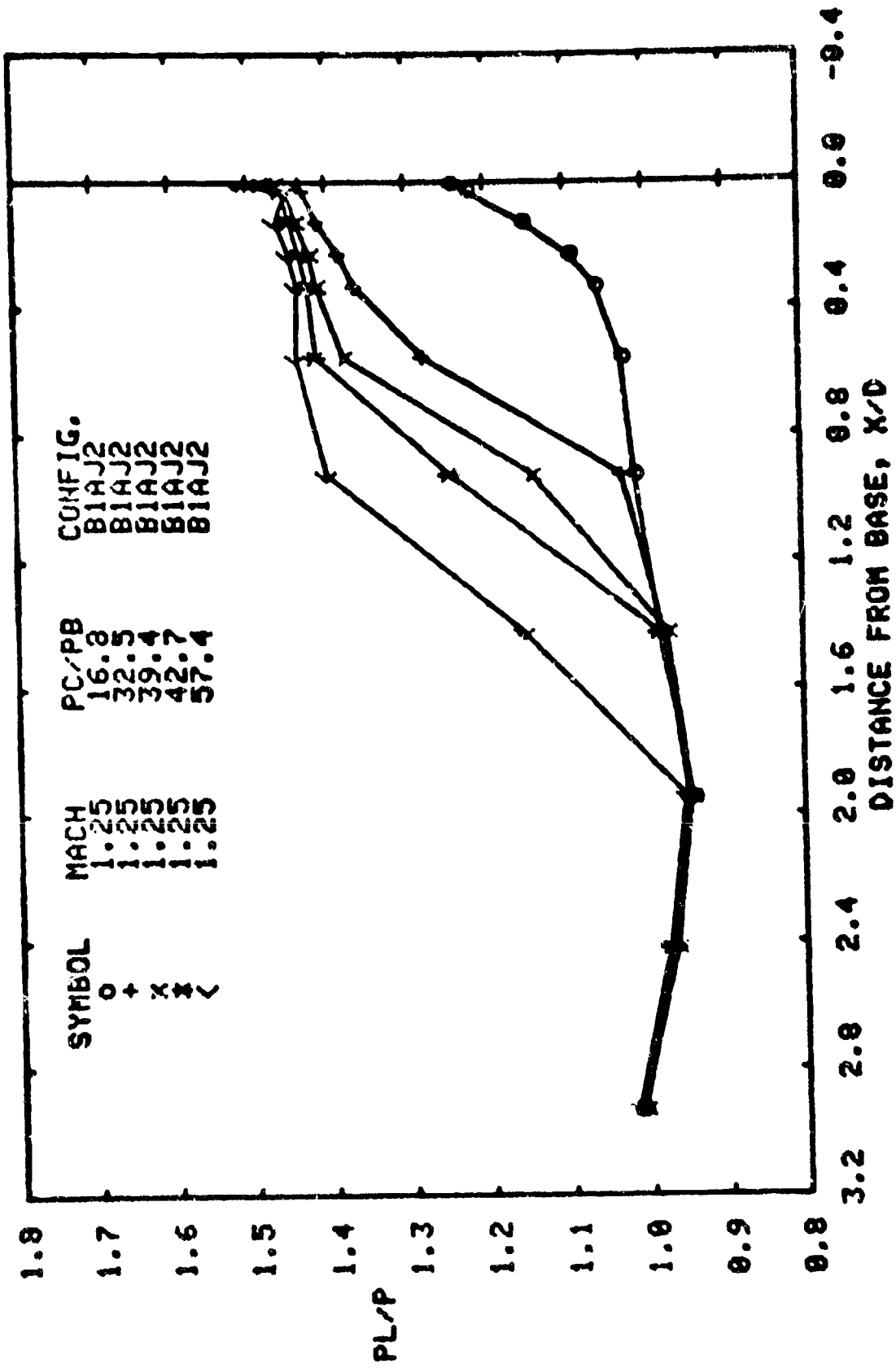
(f). M=2.0
Figure A6: concl'd.



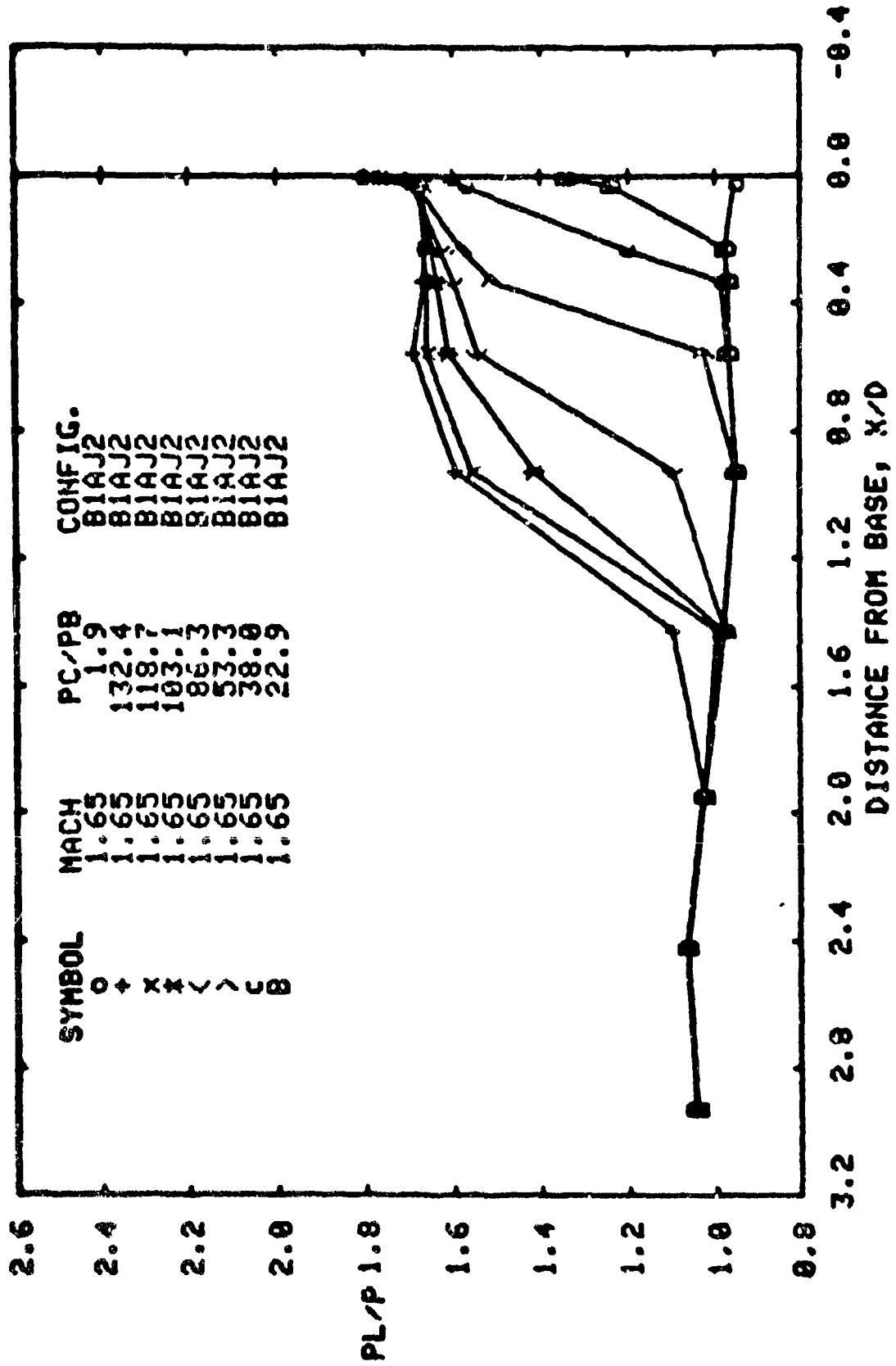
(a) M=0.9
 Figure A7: Effect of normal jet simulator pressure ratio on body pressure distribution at various free stream Mach numbers. Configuration B1AJ2.



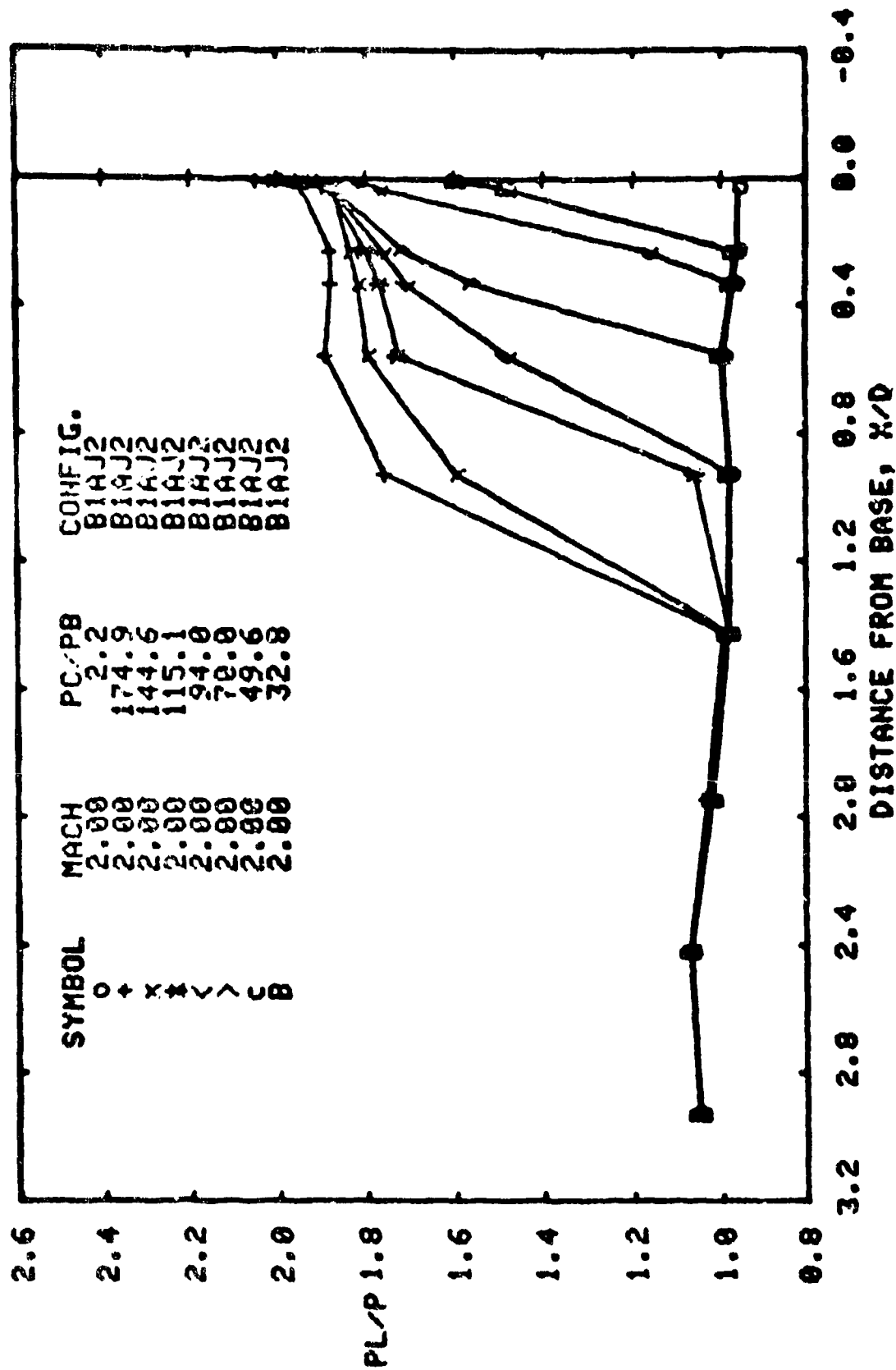
(b). M=1.0
Figure A7: cont'd.



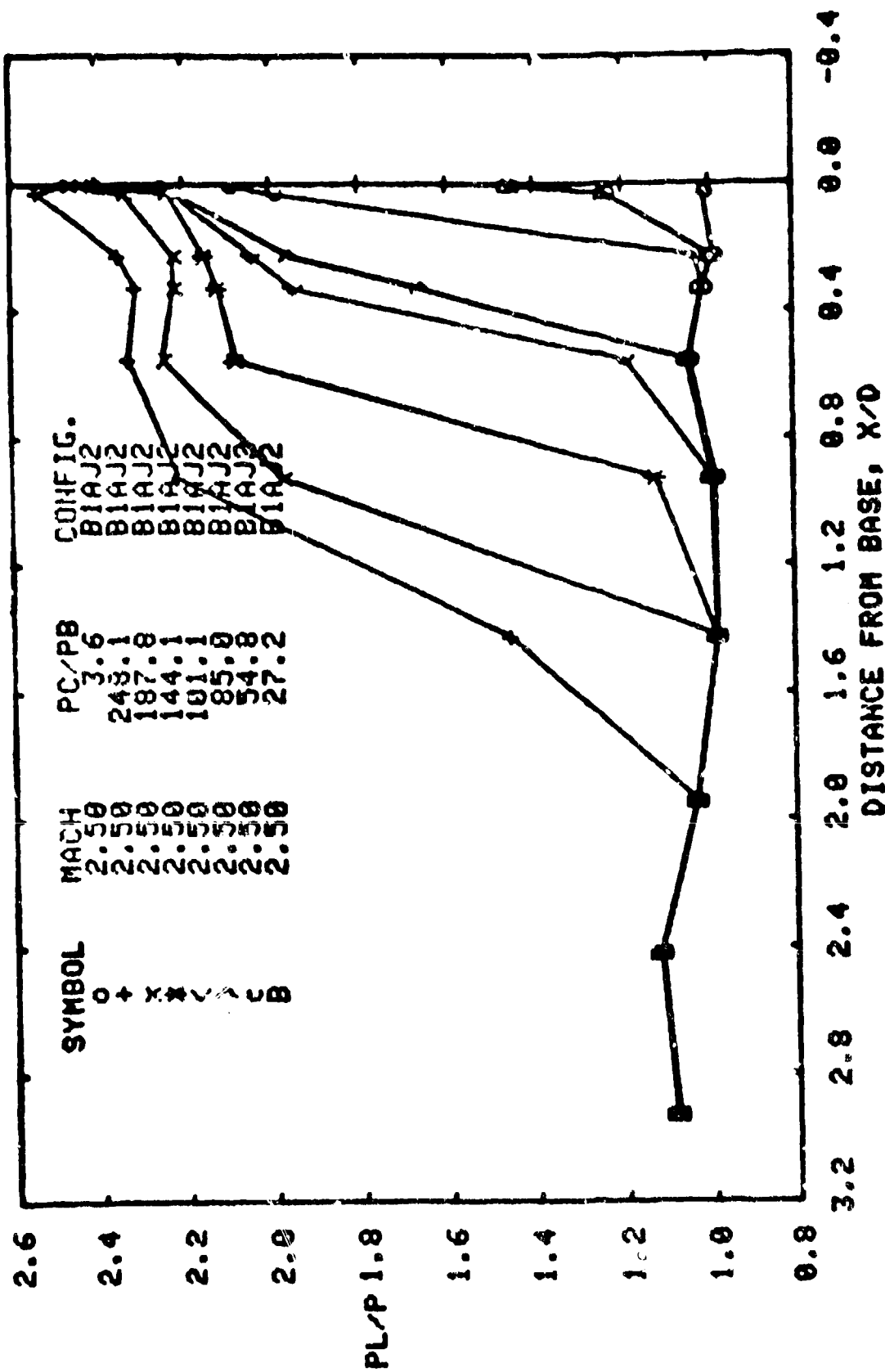
(c). $M=1.25$
 Figure A7: cont'd.



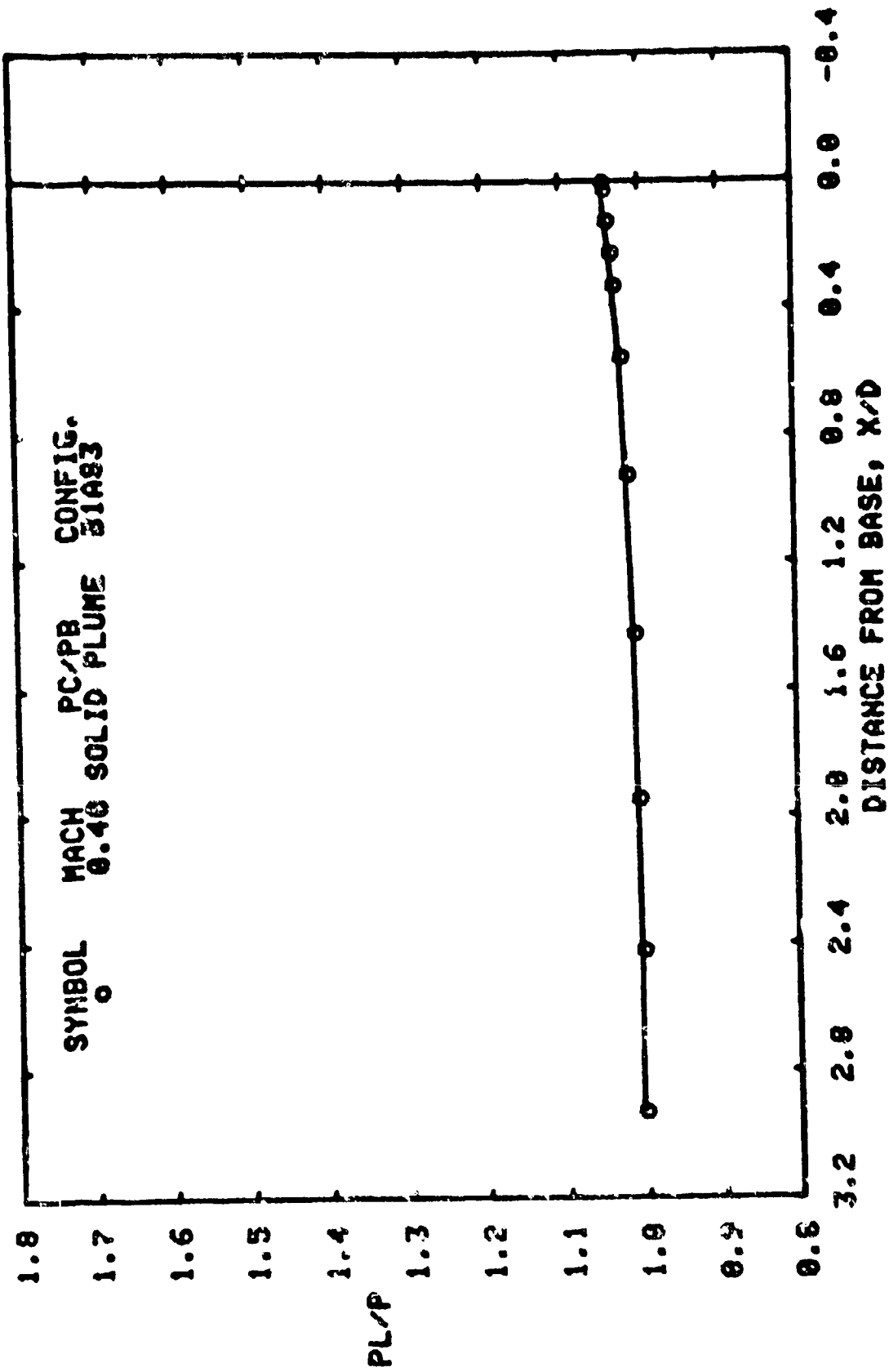
(d). M=1.65
Figure A7: cont'd.



(e). M=2.0
Figure A7: cont'd.

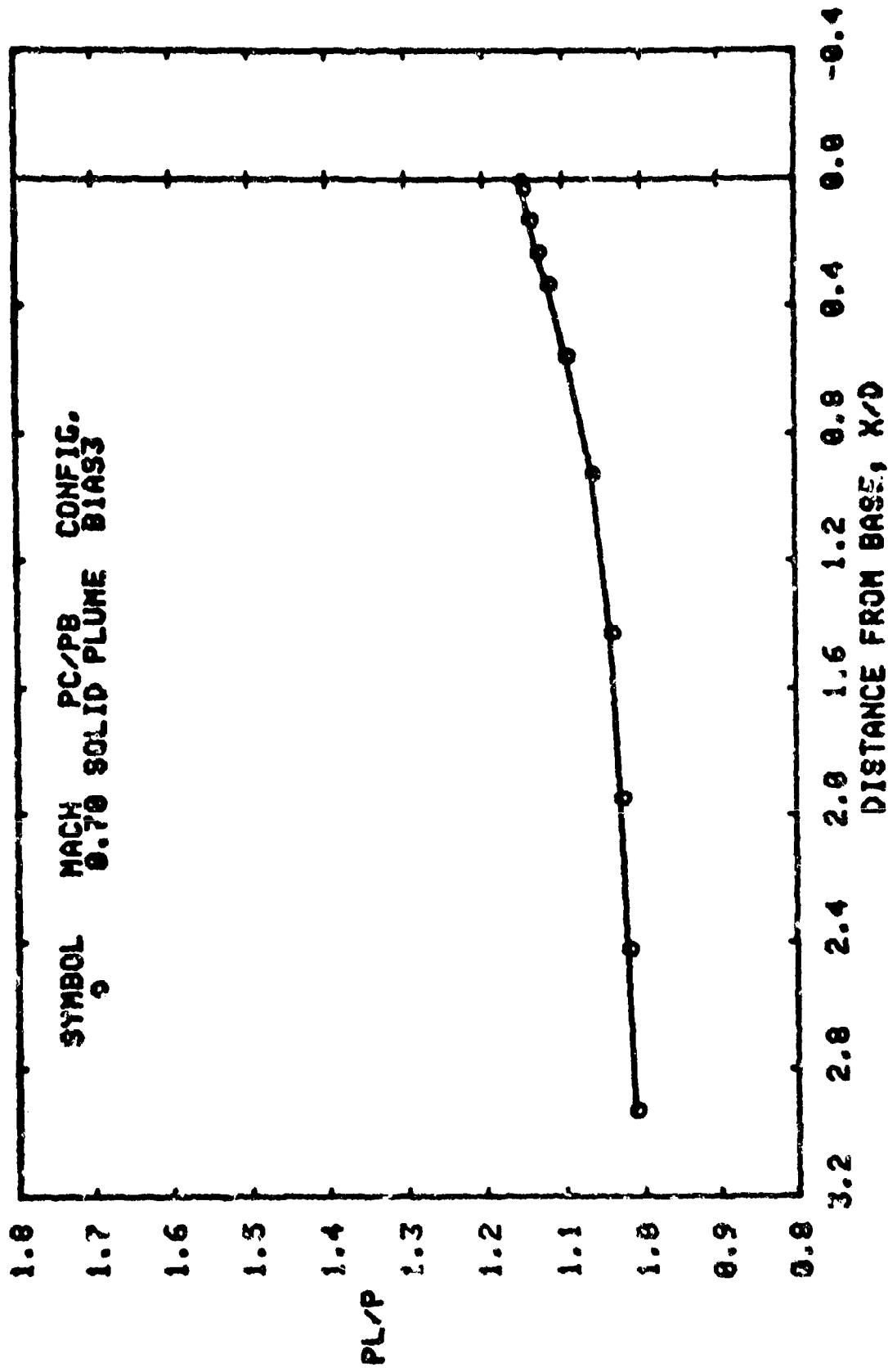


(f). M=2.50
 Figure A7: concl'd.

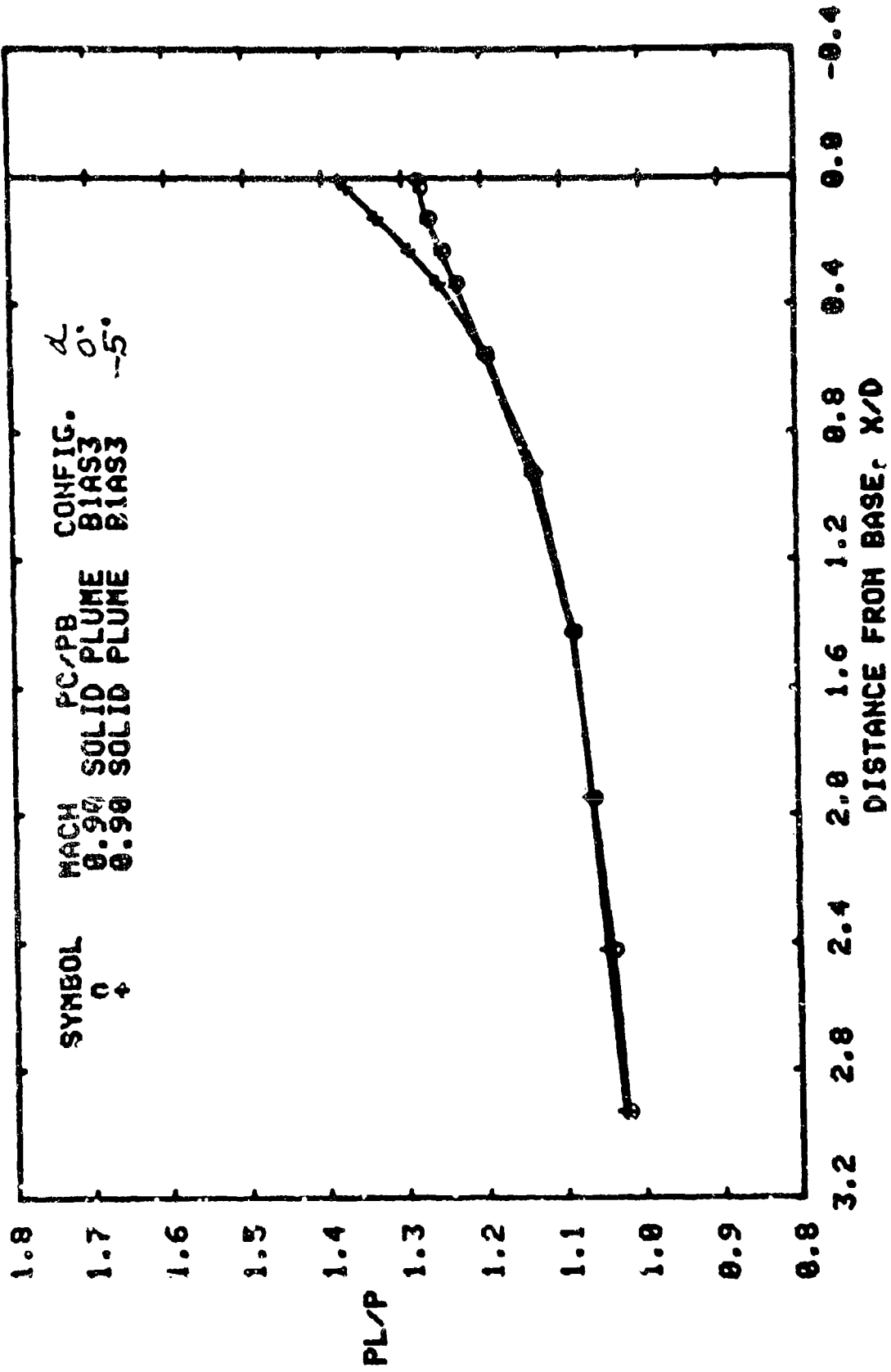


(a). M=0.40

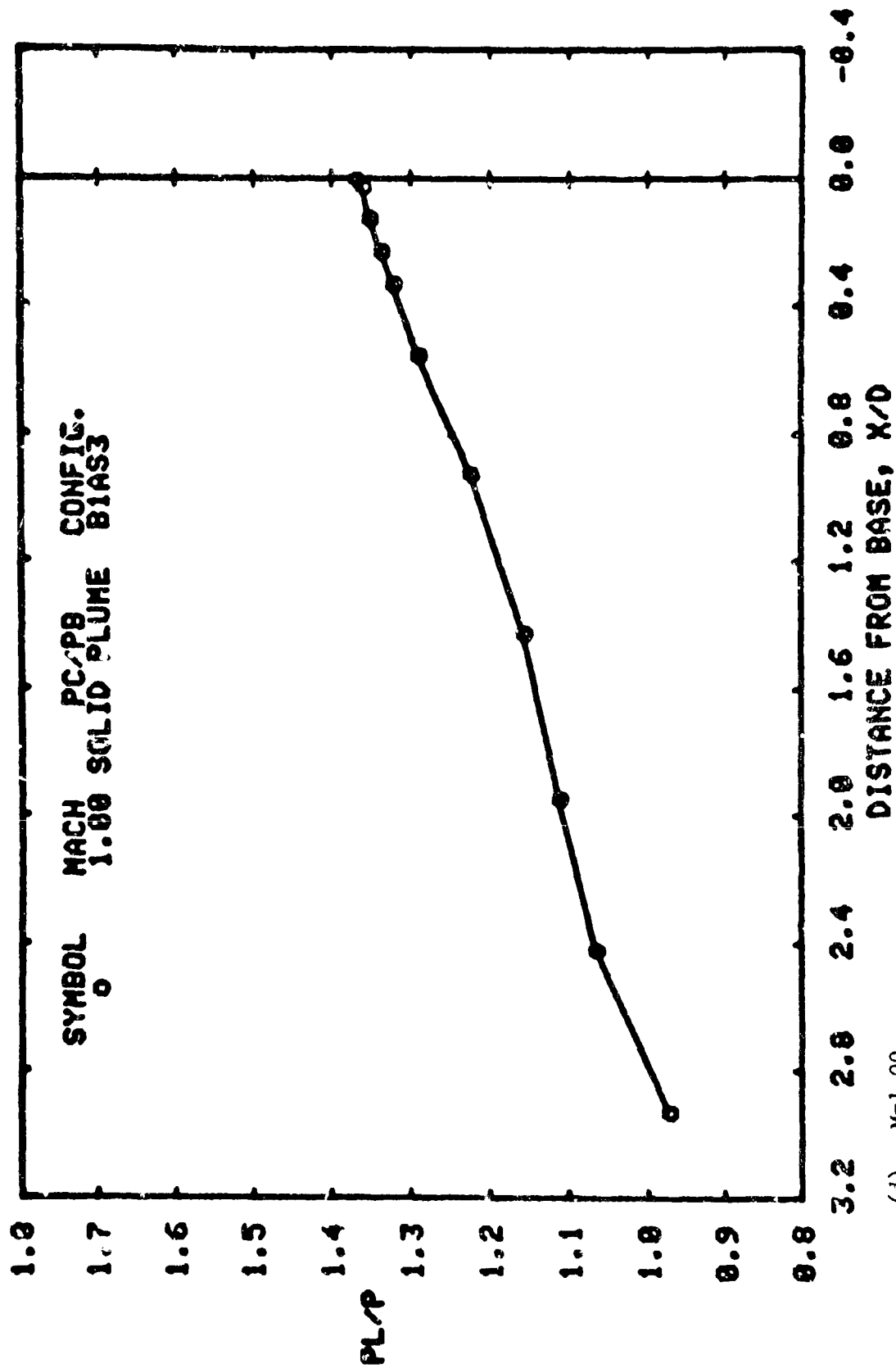
Figure A8: Effect of solid plume simulator on body pressure distribution. Configuration B1A83.



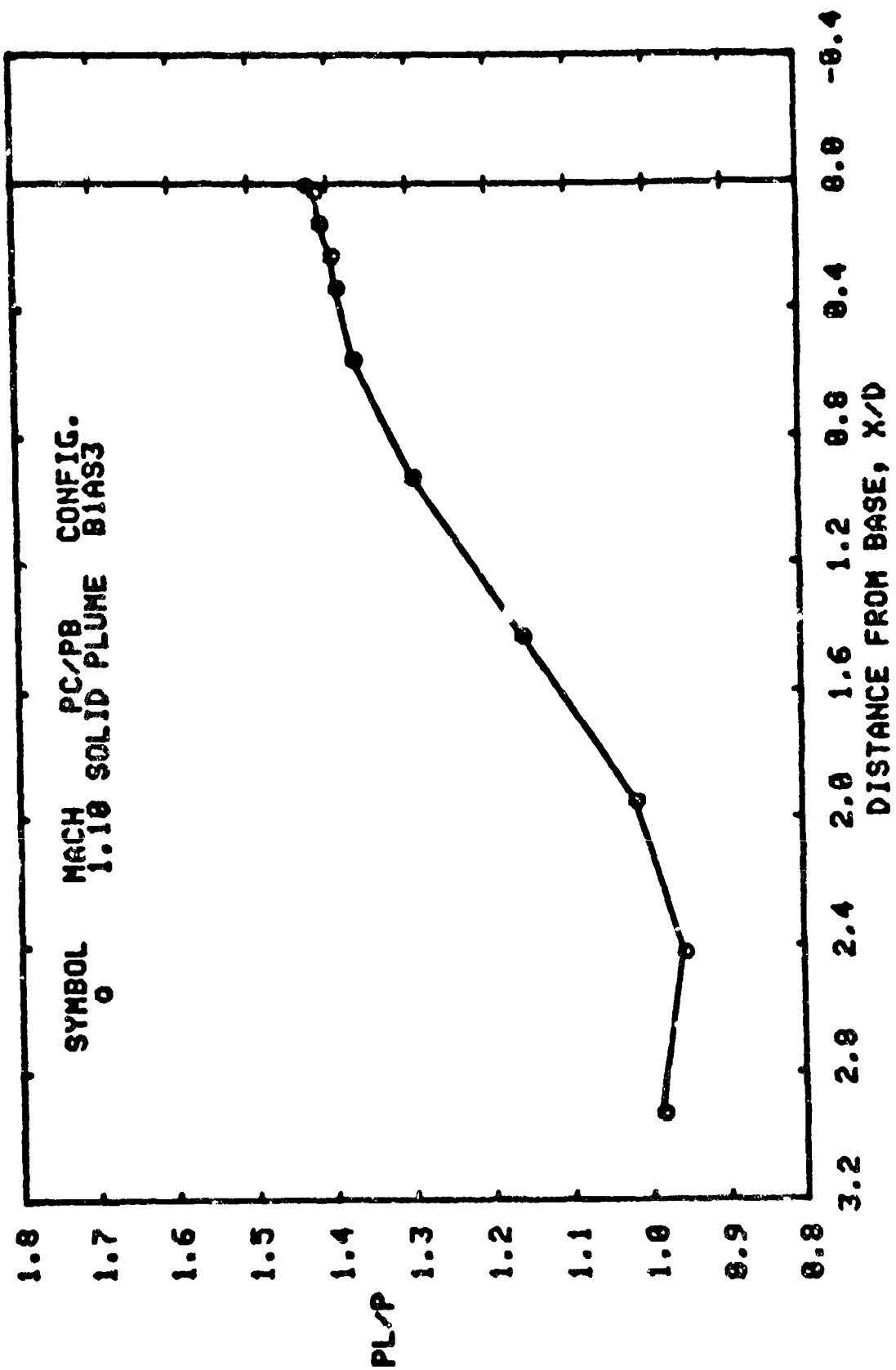
(b). $M=0.90$
 Figure A8: cont'd.



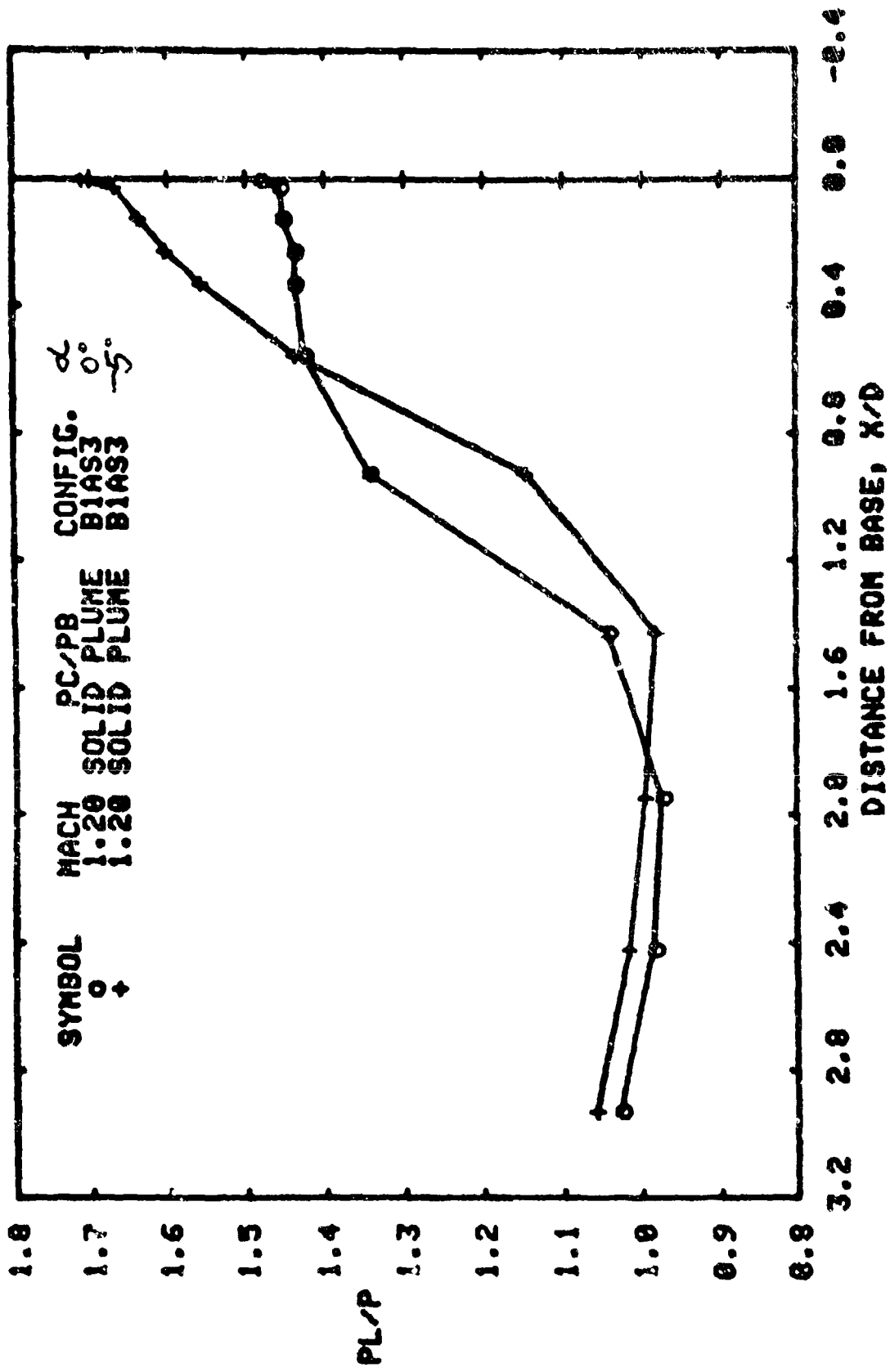
(c). M=0.90
Figure A8: cont'd.



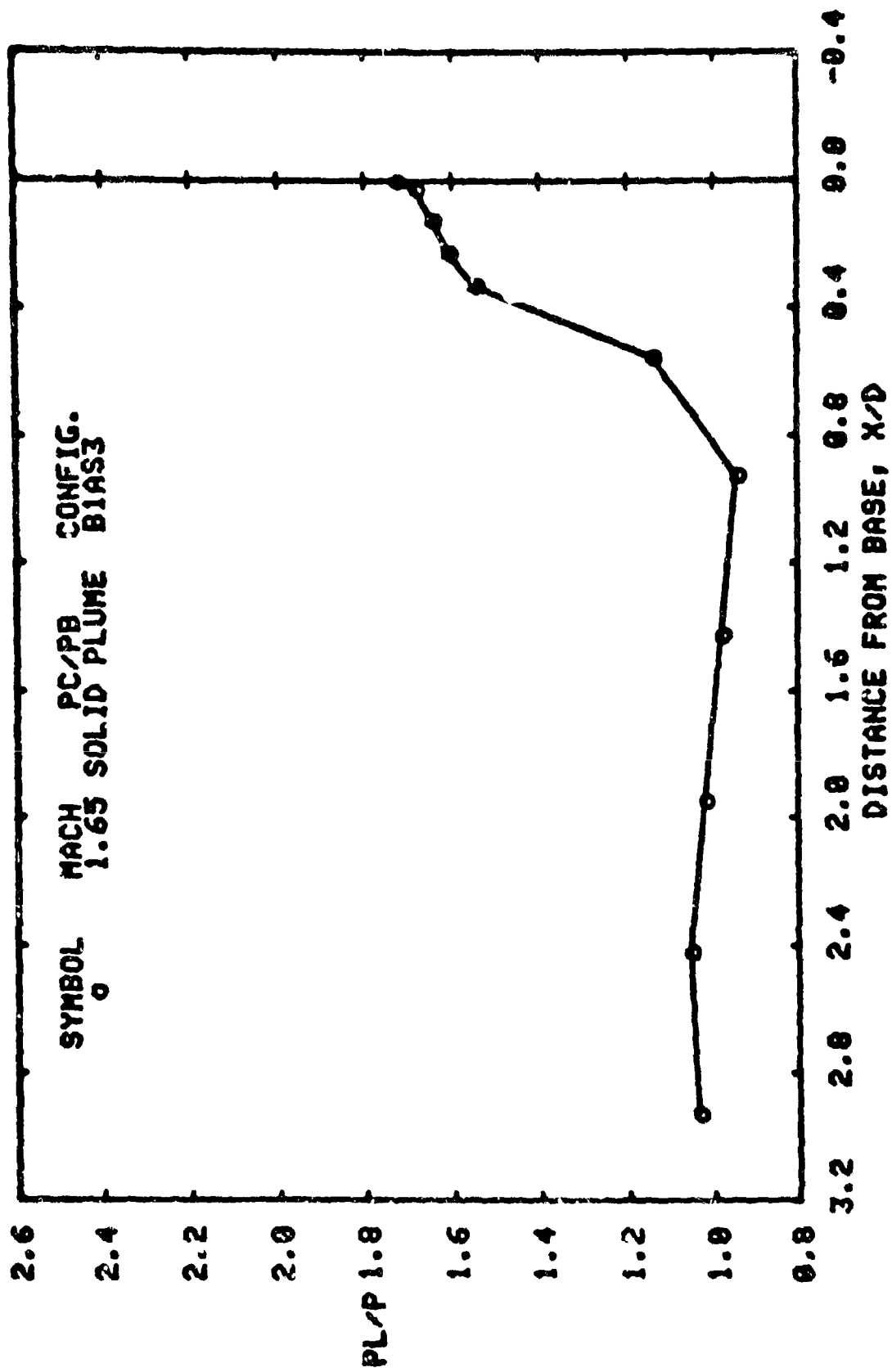
(d). M=1.00
Figure A8: cont'd.



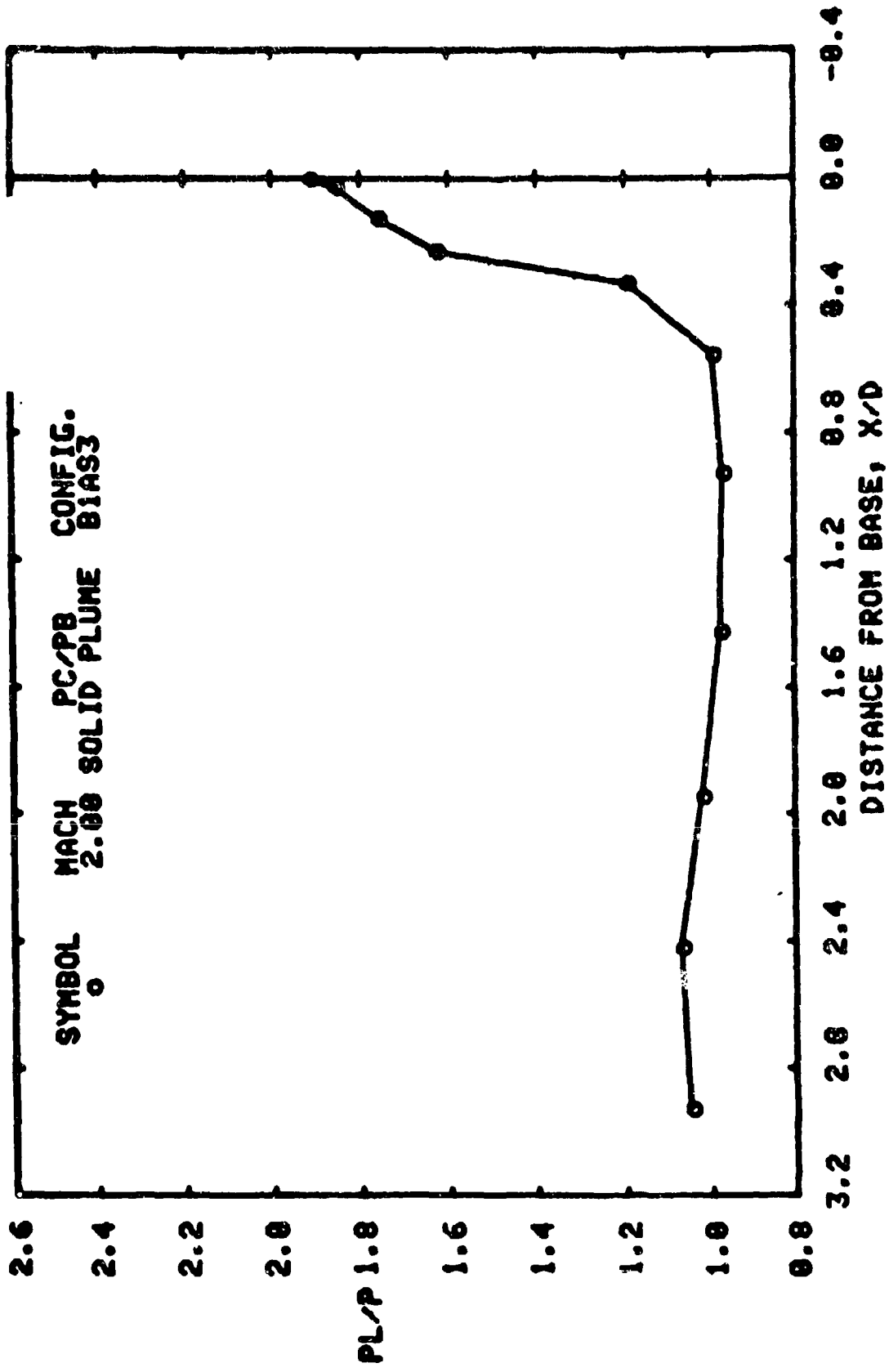
(0), $M=1.10$



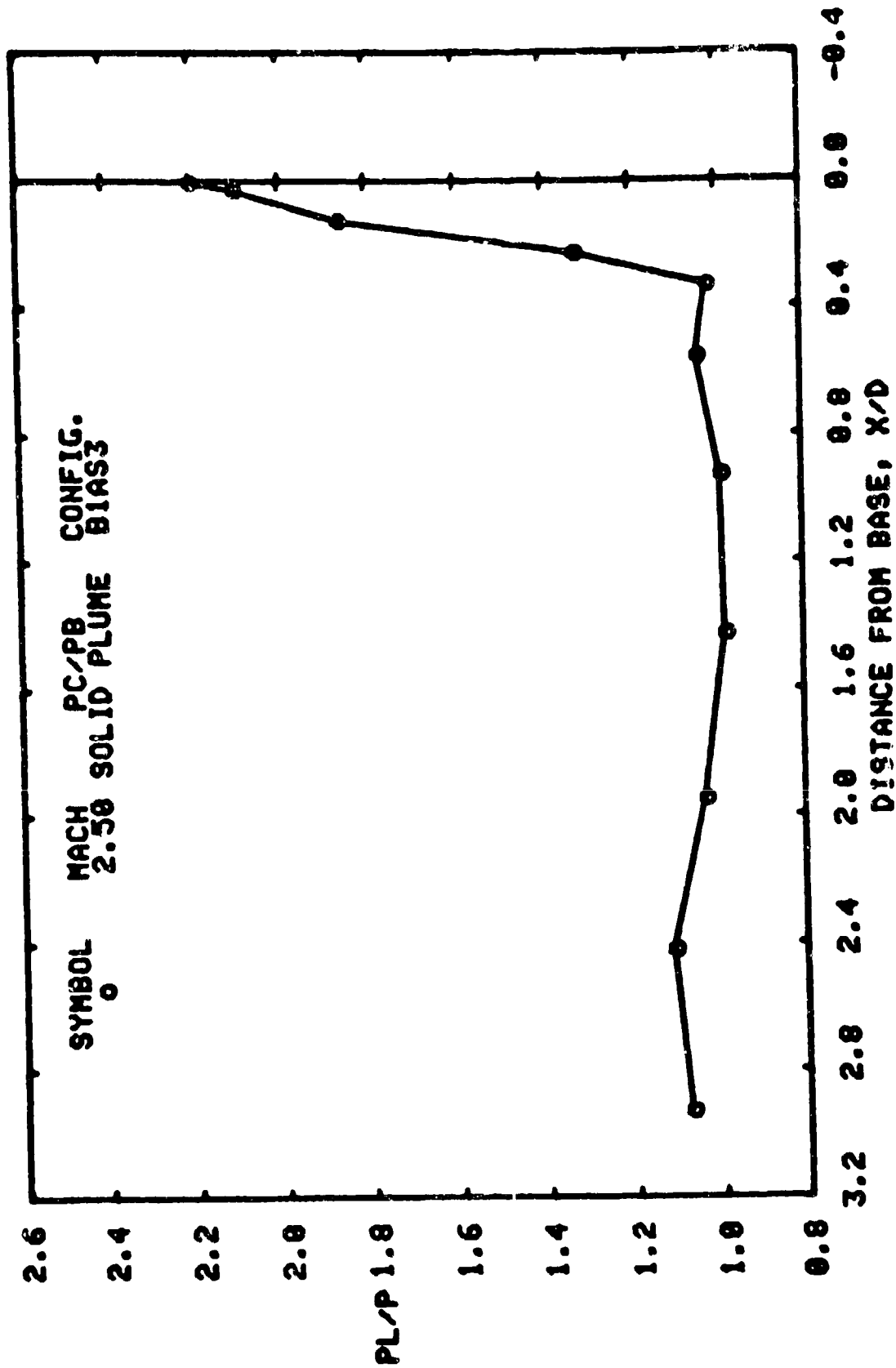
(f). M=1.20
Figure A8: cont'd.



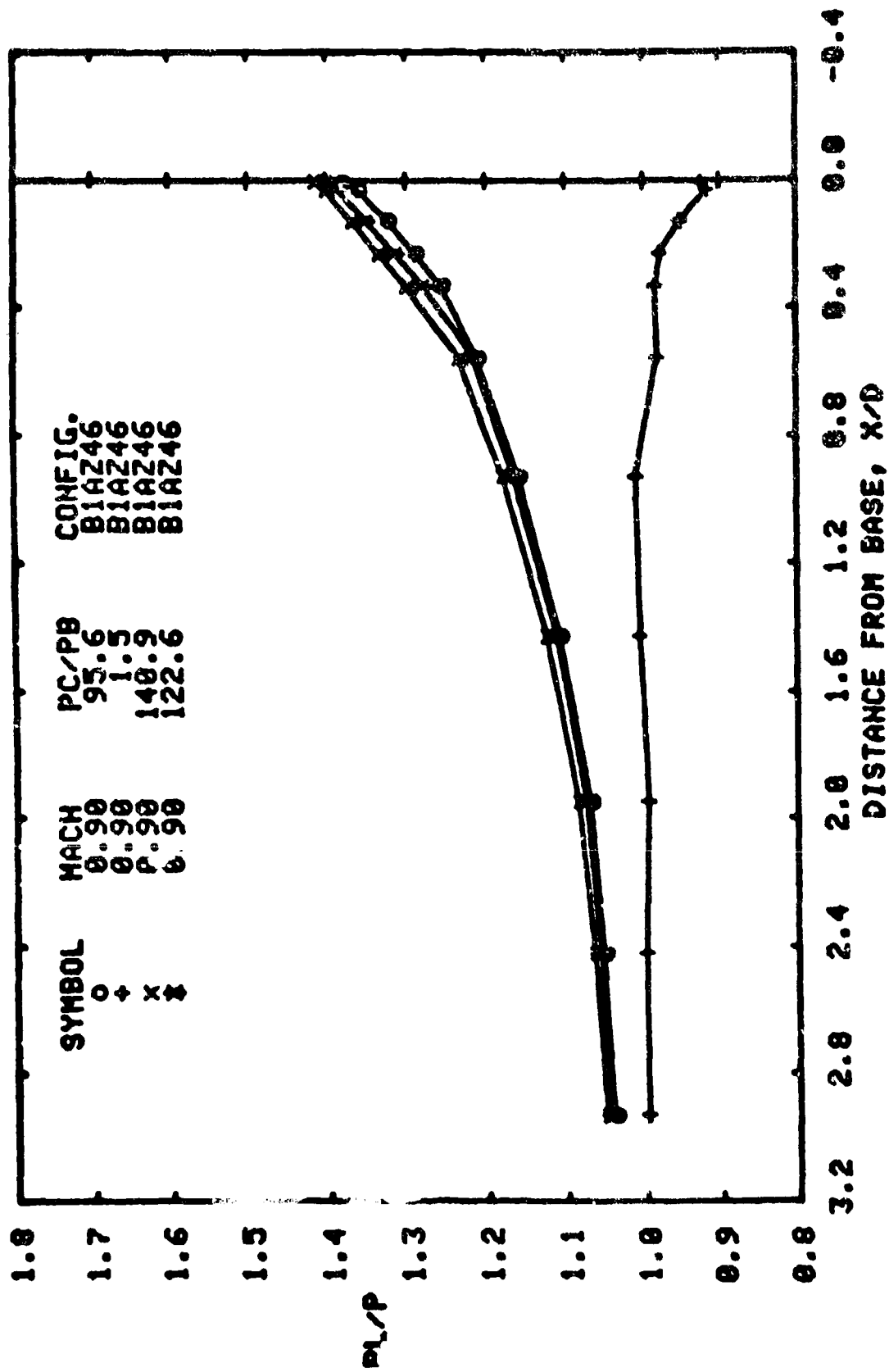
(8). M=1.65
 Figure A8: cont'd.



(h). M=2.0
Figure A8: cont'd.

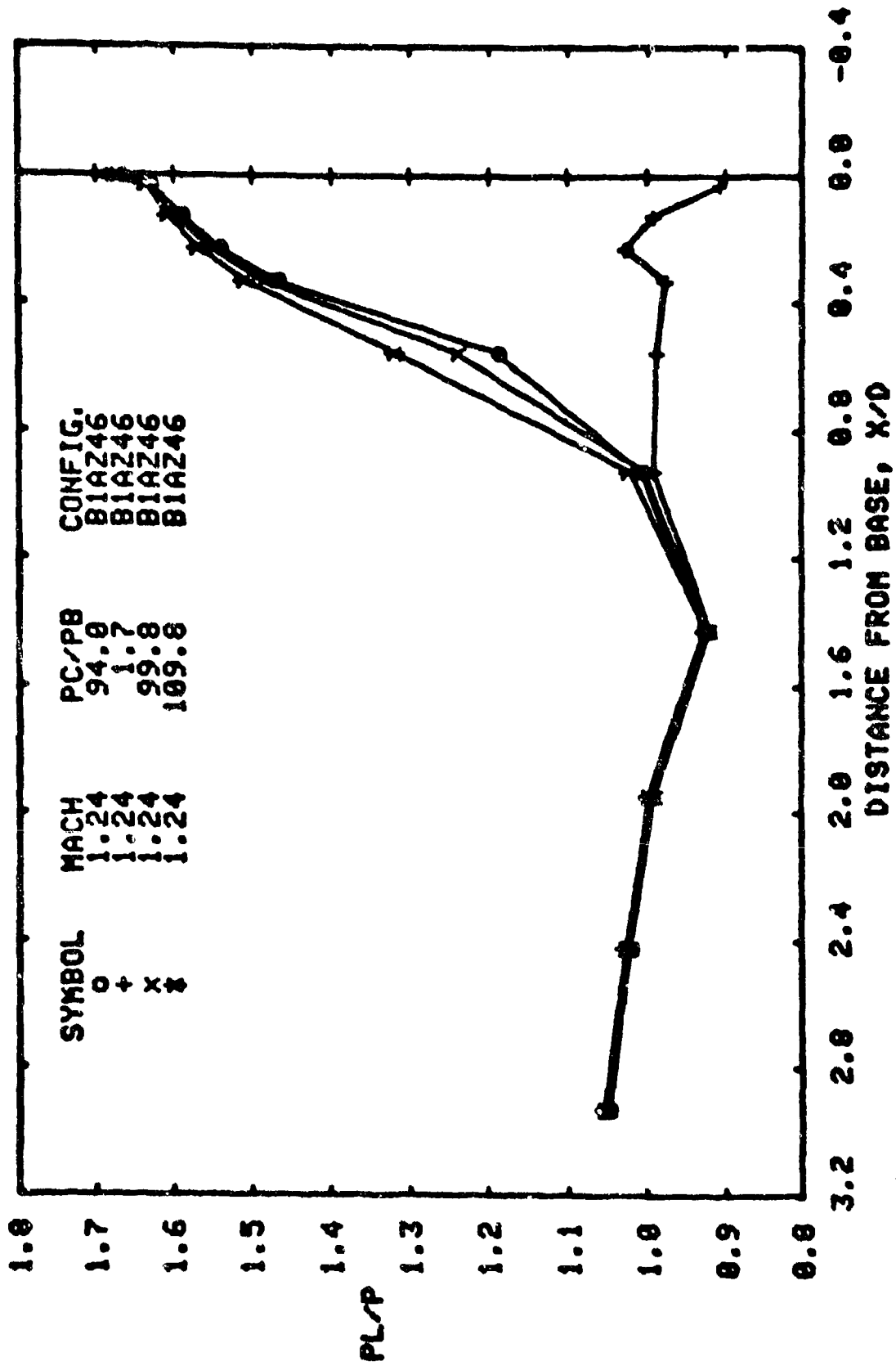


(1). M=2.5
 Figure A8: concl'd.



(a). $M=0.90$

Figure A9: Effect of jet total pressure on body pressure distribution at an angle of attack of -5° . Configuration BIAZ46: $M_j=2.7$, $\mu_N=23.3$, $D_N/D_B=0.8$.



(b). M=1.25
Figure A9: cont'd.

BLANK PAGE

DISTRIBUTION

No. of
Copies

Office of Secretary of Defense OUSDRE/TWP/Land Warfare, Rm 3E1025 The Pentagon Washington, D.C. 20301 Attn: Dr. James Richardson	1
Commander U.S. Army Materiel Development and Readiness Command 5001 Eisenhower Ave. Alexandria, Virginia 22333 Attn: DRCIRD-1, Bob Schleger DRCDL	1 1
Commander U.S. Army Research and Development Command Dover, New Jersey 07801 Attn: DRDAR-LCA-F, A. Loeb	1
Director U.S. Army Aeromechanics Laboratory Ames Research Center Moffett Field, California 94035 Attn: Dr. Irving C. Statler, Mail Stop 215-1	1
Weapons Systems Concepts Team Aberdeen Proving Ground, Maryland 21010 Attn: Mr. Miles Miller, DRDAR-ACW	1
Commanding Officer Air Force Armament Laboratory Eglin Air Force Base, Florida 32542 Attn: Mr. C. Butler Mr. E. Howard Dr. D. Daniel	1 1 1
Arnold Engineering and Development Center Arnold Air Force Station, Tennessee 37389 Attn: Library Mr. R.C. Bauer	1 1
Air Force Flight Dynamics Laboratory Wright-Patterson Air Force Base, Ohio 45433 Attn: FDCC, Mr. Val Dahlem	1

DISTRIBUTION (Continued)

	No. of Copies
Commanding Officer U.S. Naval Surface Weapons Center White Oak Silver Spring, Maryland 20910 Attn: B. Piper, W-A21	1
F. Moore	1
Library	
U.S. Army Armament Research and Development Command Ballistic Research Laboratories Aberdeen Proving Ground, Maryland 21005 Attn: Dr. Charles Murphy	1
NASA-Langley Research Center Hampton, Virginia 23665 Attn: Mr. Bill Corlett	1
Mr. Peter Covell	1
Mr. Charles Jackson	1
Library	1
Commanding Officer and Director Naval Ship Research and Development Center Carderock, Maryland 20007 Attn: Aerodynamic Laboratory	1
NASA-Ames Research Center Moffett Field, California 94035 Attn: Library	1
NASA-Lew Research Center Cleveland, Ohio 44135 Attn: Library	1
NASA-Marshall Space Flight Center Marshall Space Flight Center, Alabama 35812 Attn: Dr. W. Dahm	1
Mr. J. Sims	1
Library	1
U.S. Air Force Academy USAF Academy, Colorado 80840 Attn: DFAN Capt. Brilliant	1
Philco Corporation Aeronutronic Division Ford Road Newport Beach, California 92663 Attn: Technical Information Services-Acquisitions Mr. Fred Hayes	1

DISTRIBUTION (Continued)

	No. of Copies
Rockwell International Columbus Aircraft Division 4300 East Fifth Avenue Columbus, Ohio 43216 Attn: Mr. Fred Hessman	1
Sandia Corporation Sandia Base Division 9322 Box 5800 Albuquerque, New Mexico 87115 Attn: Mr. W. Curry	1
Purdue University Lafayette, Indiana 47907 Attn: Dr. J. Hoffman, Propulsion Center	1
University of Tennessee Space Institute Tullahoma, Tennessee 37388 Attn: Dr. J.M. Wu	1
University of Alabama Department of Aerospace Engineering University, Alabama 35468 Attn: Dr. J.O. Doughty Dr. E. Bailey	1 1
Jet Propulsion Laboratory California Institute of Technology 4800 Oak Grove Drive Pasadena, California 91109 Attn: Mr. Robert Martin	1
Commander U.S. Naval Ordnance Station Indian Head, Maryland 20640 Attn: Mr. N. Seiden	1
Commander U.S. Naval Weapons Laboratory Code 3243 China Lake, California 93555 Attn: Mr. Ray Smith	1
Arvin Calspan Advanced Technology Center P.O. Box 400 Buffalo, New York 14225 Attn: Mr. C.F. Reid	1

DISTRIBUTION (Continued)

	No. of Copies
Commander Naval Ship Research and Development Center Bethesda, Maryland 20034 Attn: Mr. Dale Chaddock	1
University of Missouri at Columbia Department of Mechanical Engineering Columbia, Missouri 65201 Attn: Dr. D.E. Wollersheim	1
University of Illinois College of Engineering Urbana, Illinois 61801 Attn: Dr. A.L. Addy	1
Dr. H.H. Korst	1
Dr. R.A. White	1
Engineering Library	1
Johns Hopkins University Applied Physics Laboratory Silver Spring, Maryland 20910 Attn: Dr. L. Cronvich	1
Mr. Gordon Dugger	1
Mr. Tisserand	1
University of Notre Dame Department of Aerospace Engineering Notre Dame, Indiana 46556 Attn: Dr. T.J. Mueller	1
Naval Ordnance Systems Command Washington, D.C. 20360 Attn: Mr. Lionel Pasiuk, ORD-035A	6
For transmittal to:	
TTCP	
Boeing Company P.O. Box 3707 Seattle, Washington 98124 Attn: Library Unit Chief	1
Mr. R.J. Dixon	1
Mr. H.L. Giles	1
Convair, A Division of General Dynamics Corporation Pomona, California 91776 Attn: Division Library	1
Nielson Engineering and Research, Inc. 850 Maude Avenue Mountain View, California 94040 Attn: Dr. J.N. Nielson	1

DISTRIBUTION (Continued)

	No. of Copies
Hughes Aircraft Company Florence Avenue at Teale Street Culver City, California 90230 Attn: Documents Group Technical Library	1
Ling-Temco-Vought Aerospace Corp. Vought Aeronautics Division Box 5907 Dallas, Texas 75222 Attn: Dr. R. James, Unit 2-53330	1
New Technology, Inc. 4811 Bradford Blvd. Huntsville, Alabama 35806 Attn: J.H. Henderson R. Singellton	2 1
Lockheed Missiles & Space Company Huntsville Research & Engineering Center 4800 Bradford Blvd. Huntsville, AL 35806	1
Lockheed Aircraft Corporation Missile and Space Division P.O. Box 504 Sunnyvale, California Attn: Technical Information Center	1
The Martin-Marietta Corporation Orlando Division Orlando, Florida 32804 Attn: Gene Aeillo	1
Hughes Aircraft Company Bldg. CP-13 Canoga Park, California 91304 Attn: Dave Carlson, Mail Station T-94	1
McDonnell-Douglas Company West 5301 Bolsa Avenue Huntington Beach, California 92646 Attn: Library A3-328	1
McDonnell-Douglas Corporation P.O. Box 516 St. Louis, Missouri 63166	1
Northrop Corporation Electro-Mechanical Division 500 East Orangethrope Y20 Anaheim, California 92801 Attn: Mr. E. Clark	1

DISTRIBUTION (Continued)

	No. of Copies
Emerson Electric Company 8100 Florissant St. Louis, Missouri 73136 Attn: Mr. Robert Bauman	1
Commander U.S. Army Missile Command Redstone Arsenal, Alabama 35898 Attn: DRSMI-FR, Mr. Strickland	1
-LP, Mr. Voigt	1
-R, Dr. McCorkle	1
-RD	3
-RKD, Mr. Deep	1
-RDK, Mr. Landingham	20
Mr. Brazzel	1
Mr. Burt	1
Mr. Pettis	1
Mr. Martin	1
Dr. Walker	1
Mr. Dahlke	1
-RBD	3
-RPR	15
-RPT(Record Copy)	1
DRCPM-RSES, Mr. Sullivan	1

*Model tests
Technical papers
get from*

2/14 19/2

Control chart